Experimental methods in solid state physics

Organisation

Priv.-Doz. Dr. Carsten Busse
II. Physikalisches Institut
Room 227
e-mail: busse@ph2.uni-koeln.de
phone: 3570

Website: http://www.ph2.uni-koeln.de/489.html
Homepage II. Physik -> Lehre -> Vorlesungen & Skripte -> Experimental Methods

Script: User name: Experimental, password: Methods

Examination? Please ask

Motivation

The principle of science, the definition almost, is the following: 'The test of all knowledge is experiment'. Experiment is the sole judge of scientific 'truth.'. . . Experiment itself. . Gives us hints. . But also needed is 'imagination' to create from these hints the great generalizations - to guess at the wonderful, simple, but very strange patterns beneath them all. And then to experiment to check again, whether we have made the right guess.

This imagination process is so difficult, that there is a division of labor in physics: there are theoretical physicists who imagine, deduce and guess at new laws, but do not experiment; and then there are experimental physicists who experiment, imagine, deduce and guess.“

Richard Feynman, Lectures on Physics

Outline

1. **Structure of solids (crystal structure)**
2. **Electronic structure (band structure, core levels)**
3. **Magnetism (individual mag. moments, magnetic structure, mag. dynamics)**
4. **extreme conditions: high pressure, low temperature, high magnetic fields, ultra high vacuum**

Ewald-Konstruktion

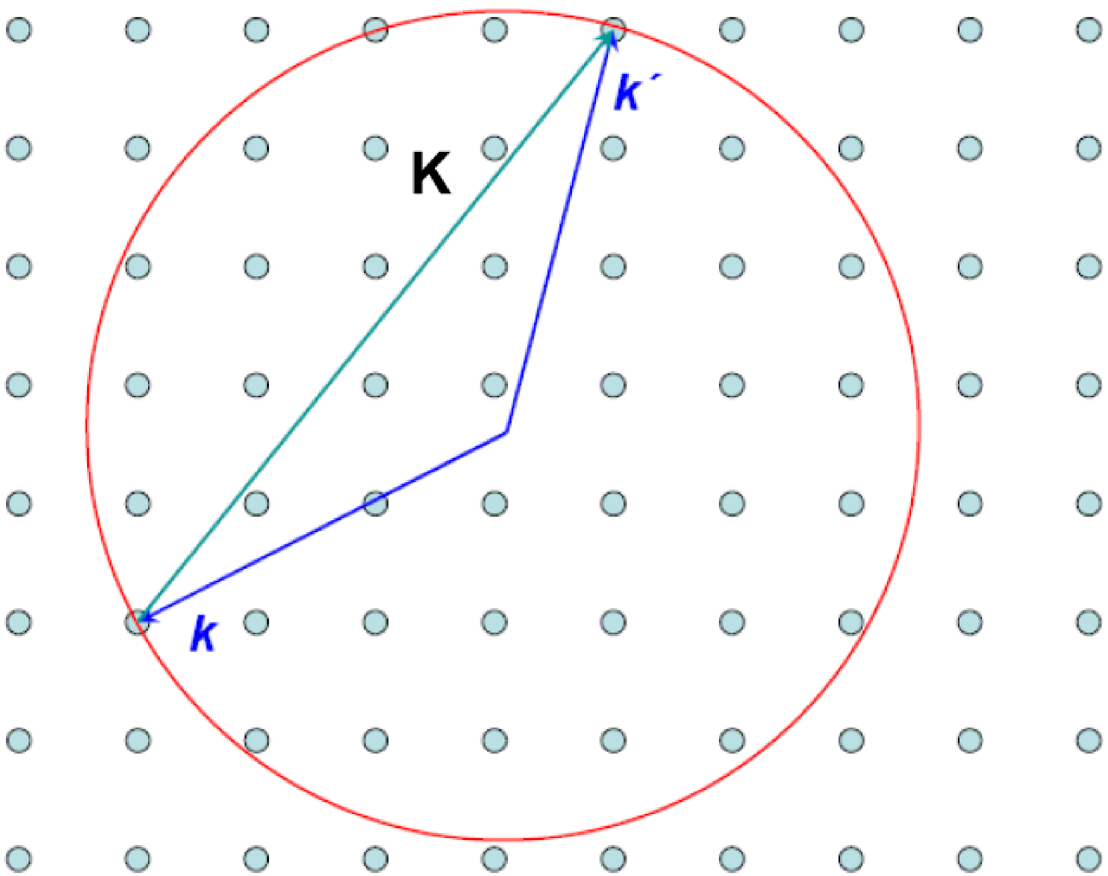

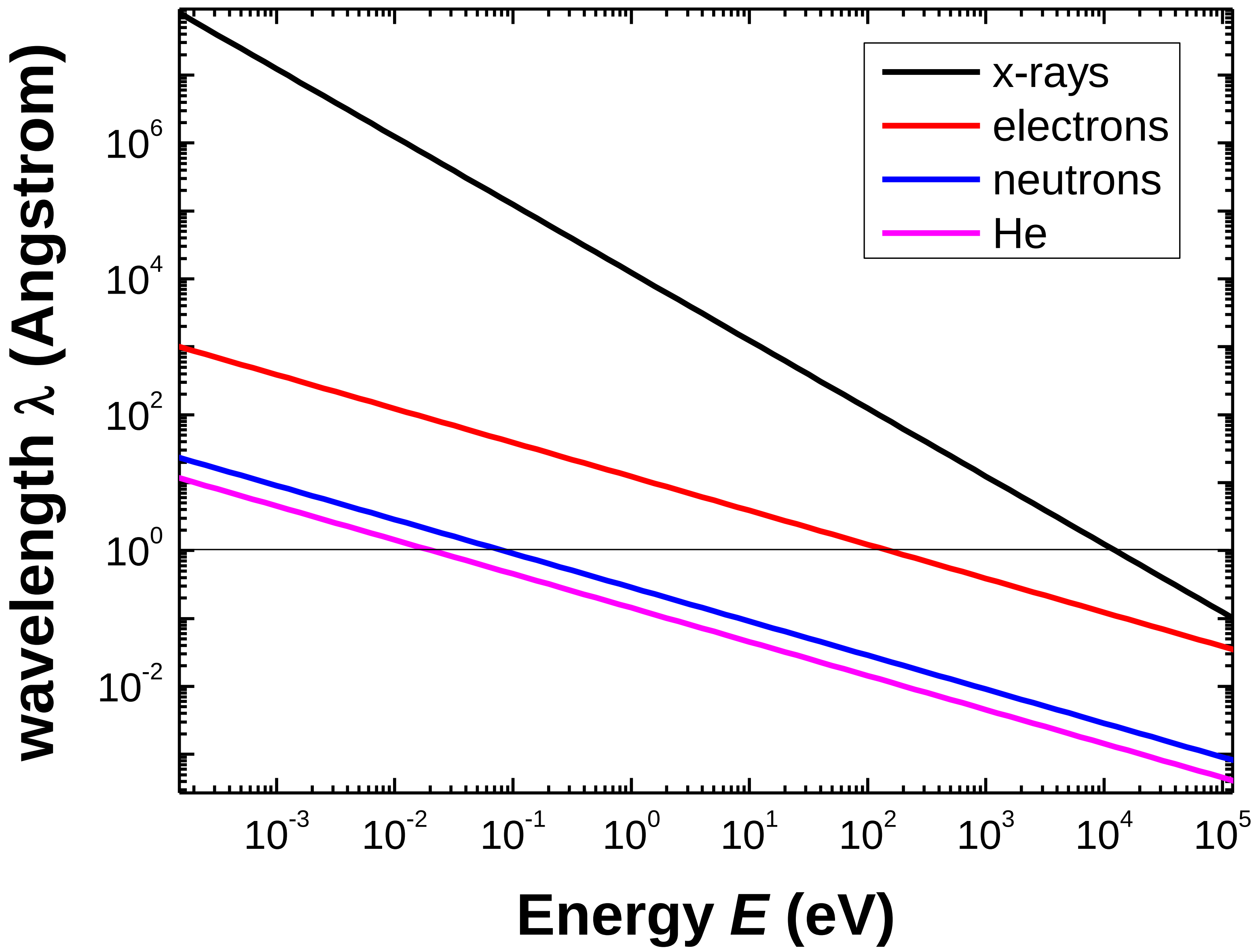

x-rays
electrons
neutrons
He
wavelength λ (Angstrom)
10^{6}
10^{4}
10^{2}
10^{0}
10^{-2}
10^{-3}
10^{-2}
10^{-1}
10^{0}
10^{1}
10^{2}
10^{3}
10^{4}
10^{5}
Energy *E* (eV)

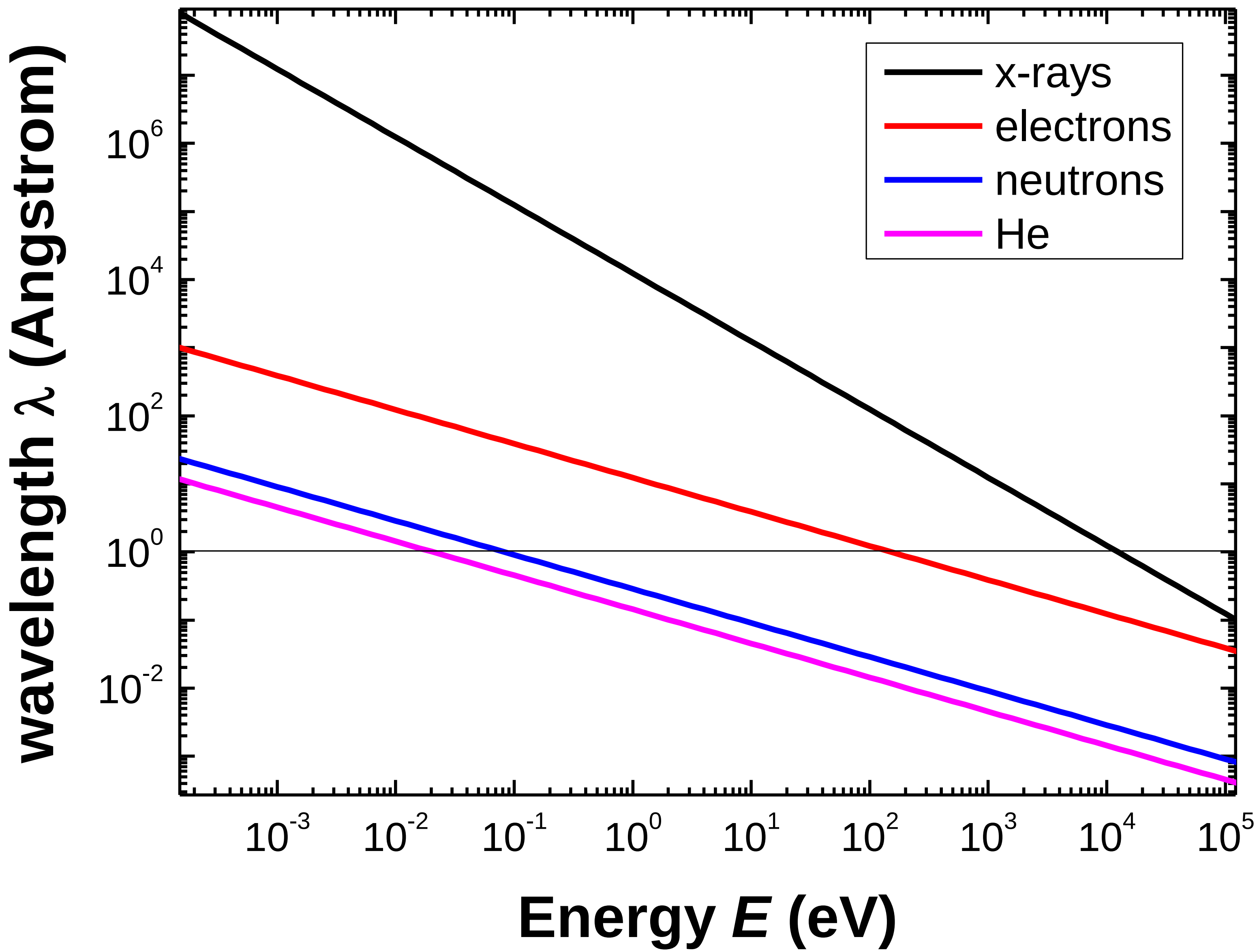

x-rays
electrons
neutrons
He
wavelength λ (Angstrom)
Energy E (eV)
10^6
10^4
10^2
10^0
10^-2
10^-3
10^-2
10^-1
10^0
10^1
10^2
10^3
10^4
10^5

The Universal Curve for the Electron Mean Free Path

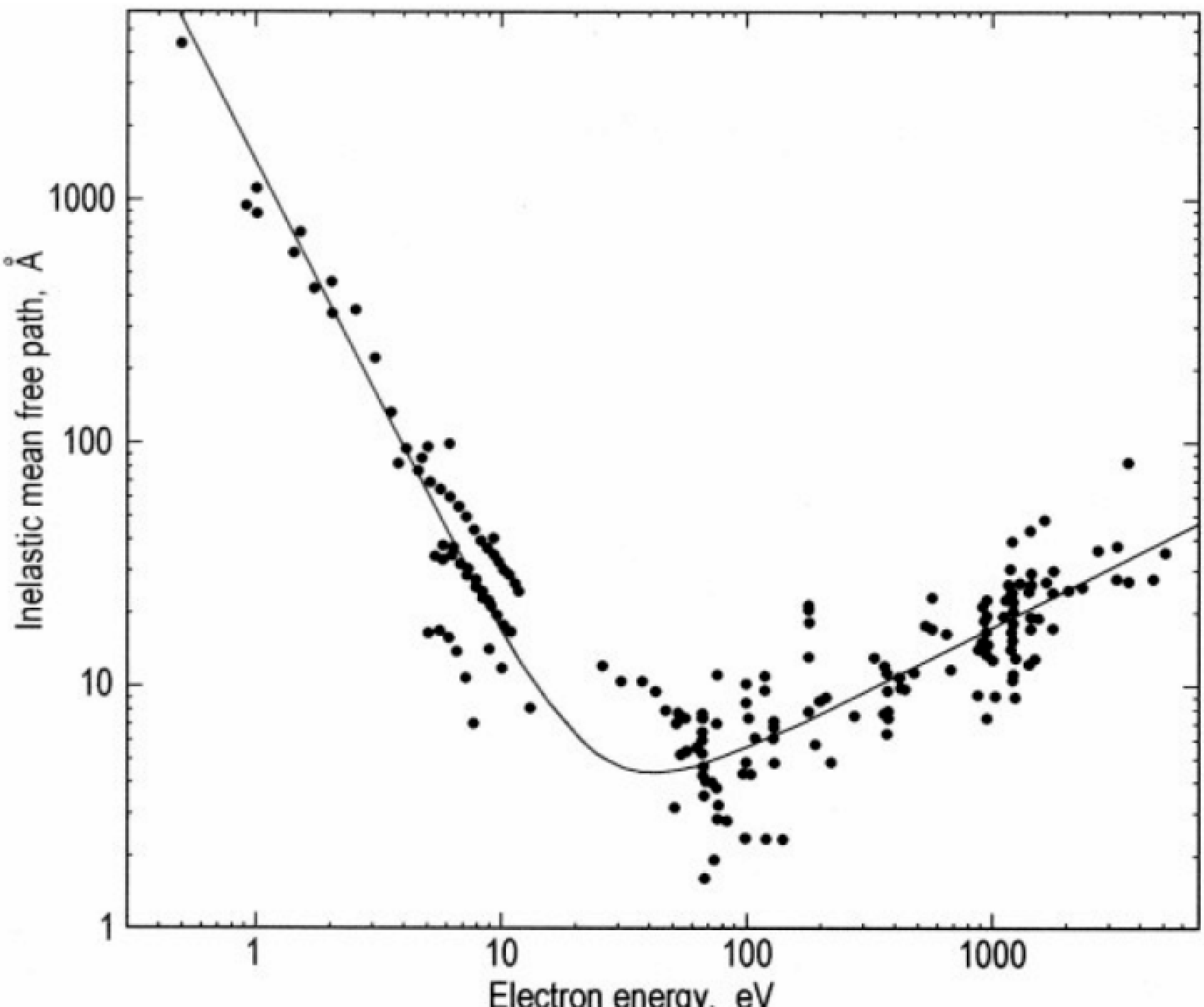

Nobel price in physics 1937 for Davisson (shared with Thomson) *"for their experimental discovery of the diffraction of electrons by crystals"*

Schematics for a Rear View LEED System

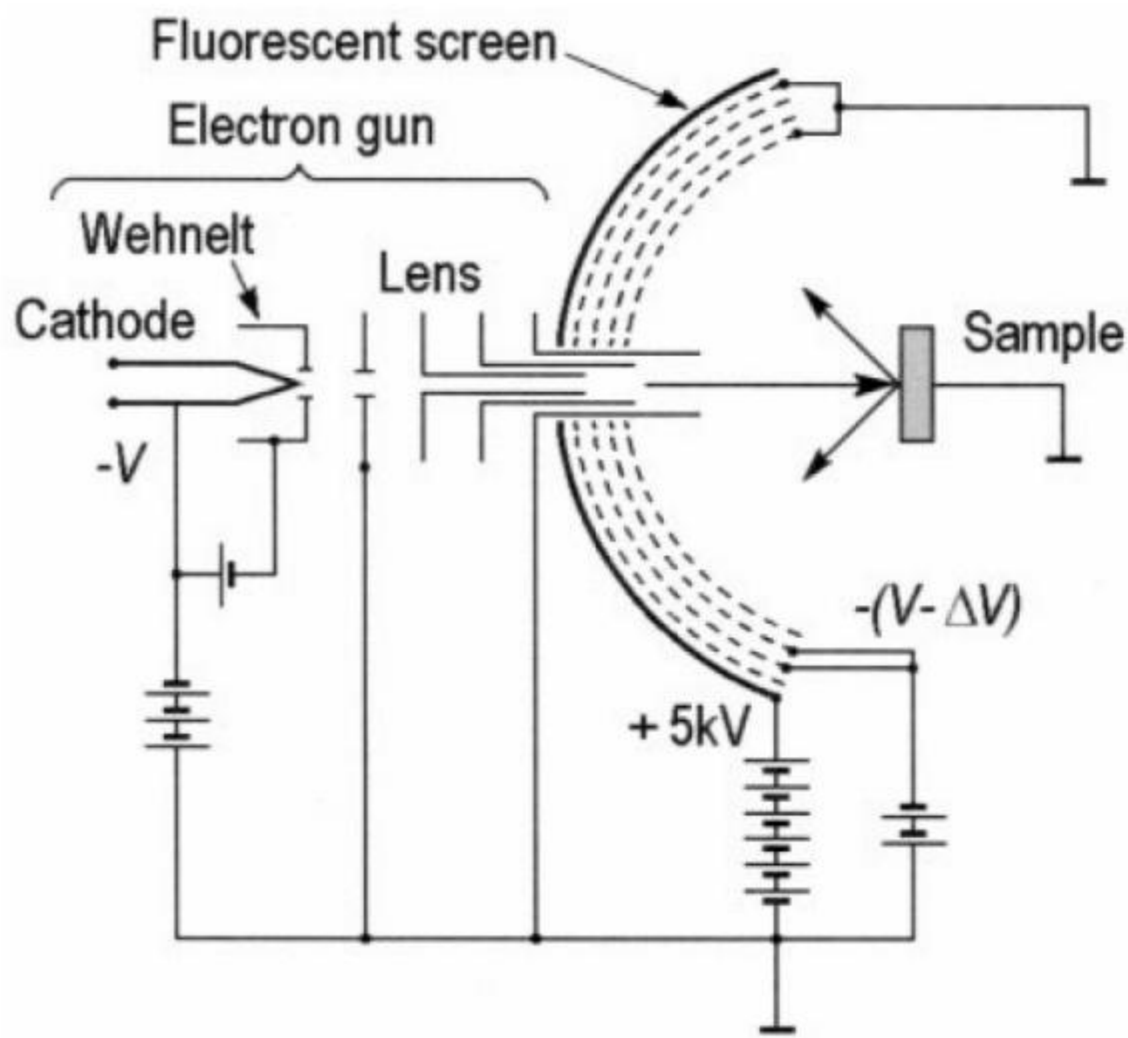

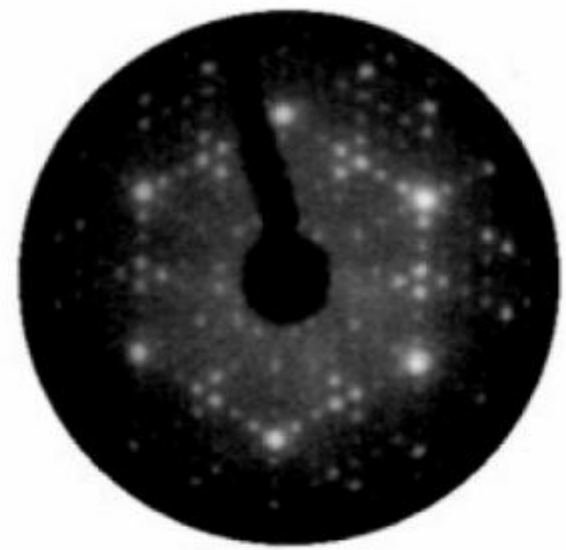

Ewald Construction for a 2D Lattice

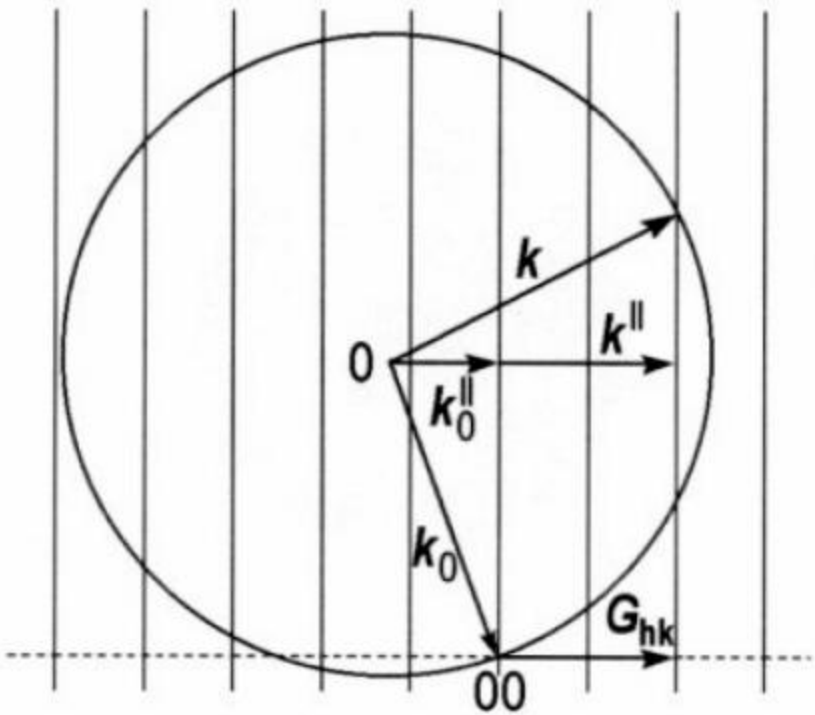

$$k^{\parallel} - k_0^{\parallel} = G_{hk}$$

general situation

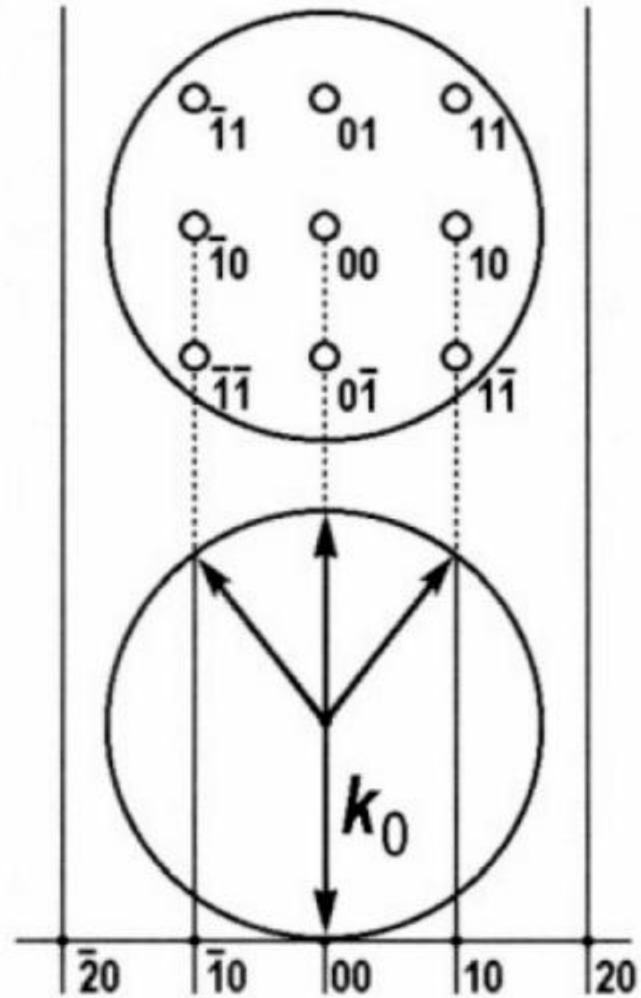

spot indexing and typical LEED situation
with normal electron incidence

2D Real Space and Reciprocal Space Unit Meshes and Primitive Translations

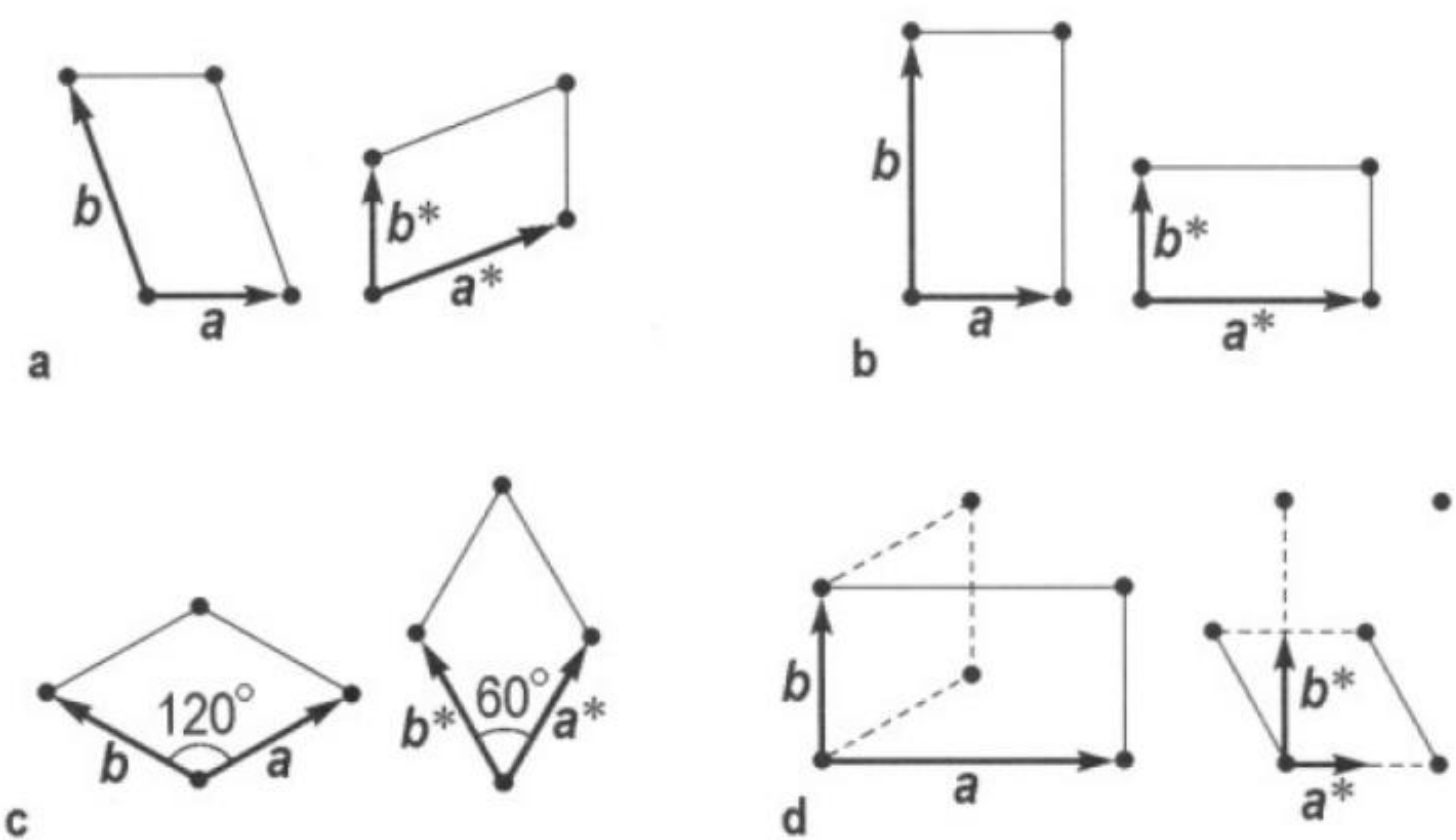

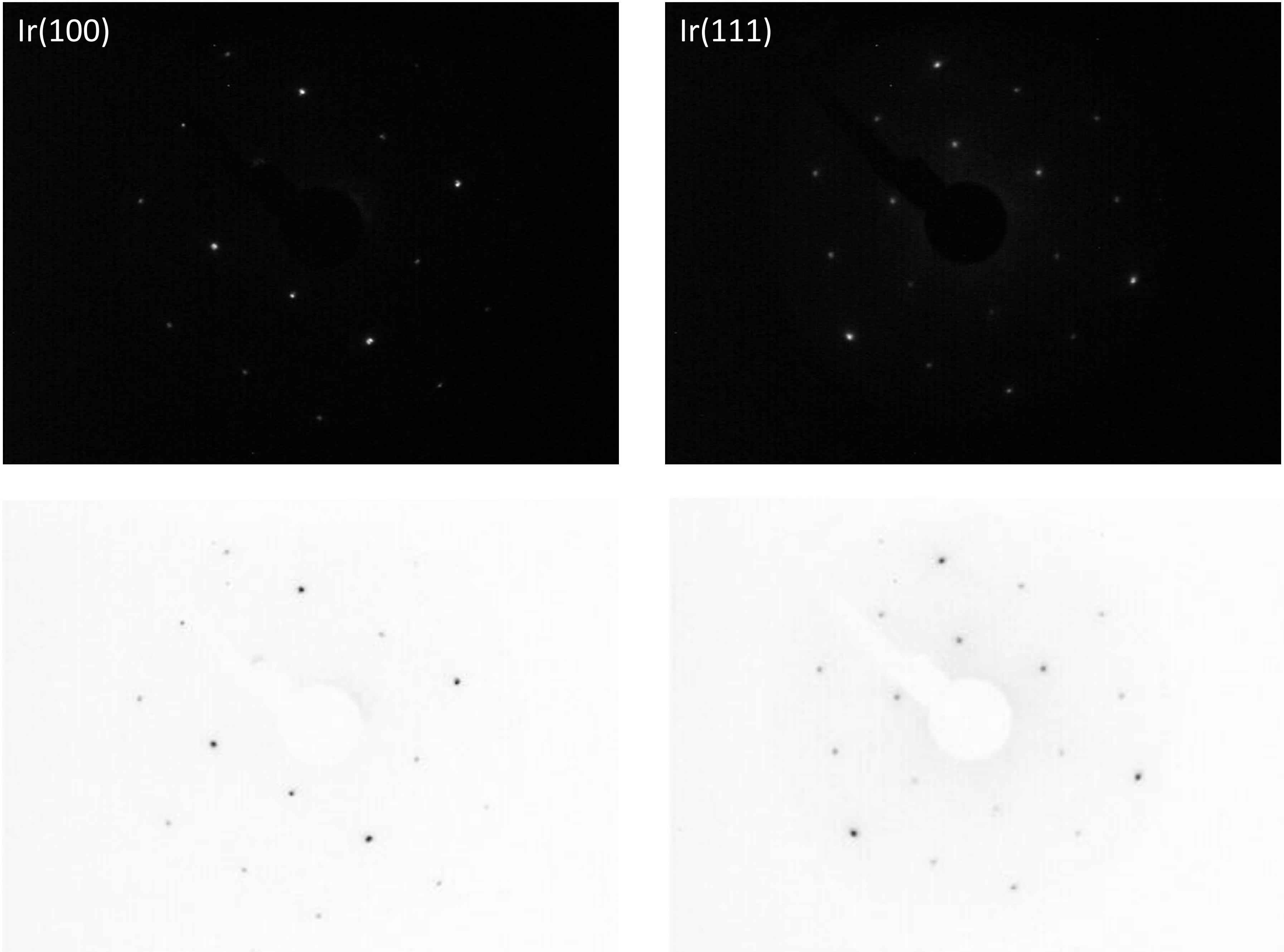

Ir(100)
Ir(111)

Nobel price in physics 1943"*for his contribution to the development of the molecular ray method (and his discovery of the magnetic moment of the proton)*”

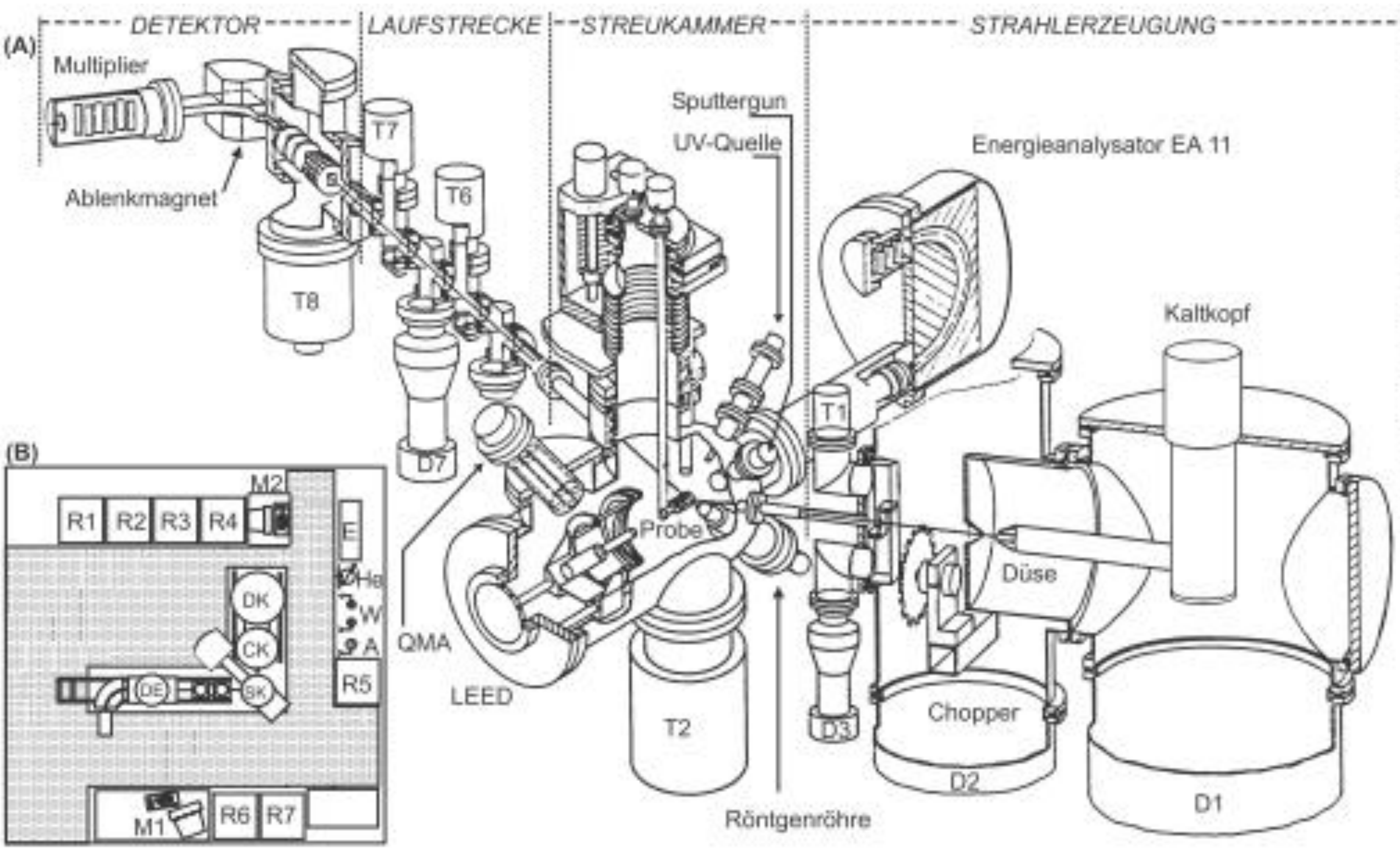

DETEKTOR
LAUFSTRECKE
STREUKAMMER
STRAHLERZEUGUNG
(A)
Multiplier
Ablenkmagnet
T8
T7
T6
D7
Sputtergun
UV-Quelle
Energieanalysator EA 11
Kaltkopf
T1
Probe
Düse
QMA
LEED
T2
Röntgenröhre
D3
Chopper
D2
D1
(B)
M2
R1
R2
R3
R4
E
He
W
A
DK
CK
DE
SK
R5
M1
R6
R7

HAS

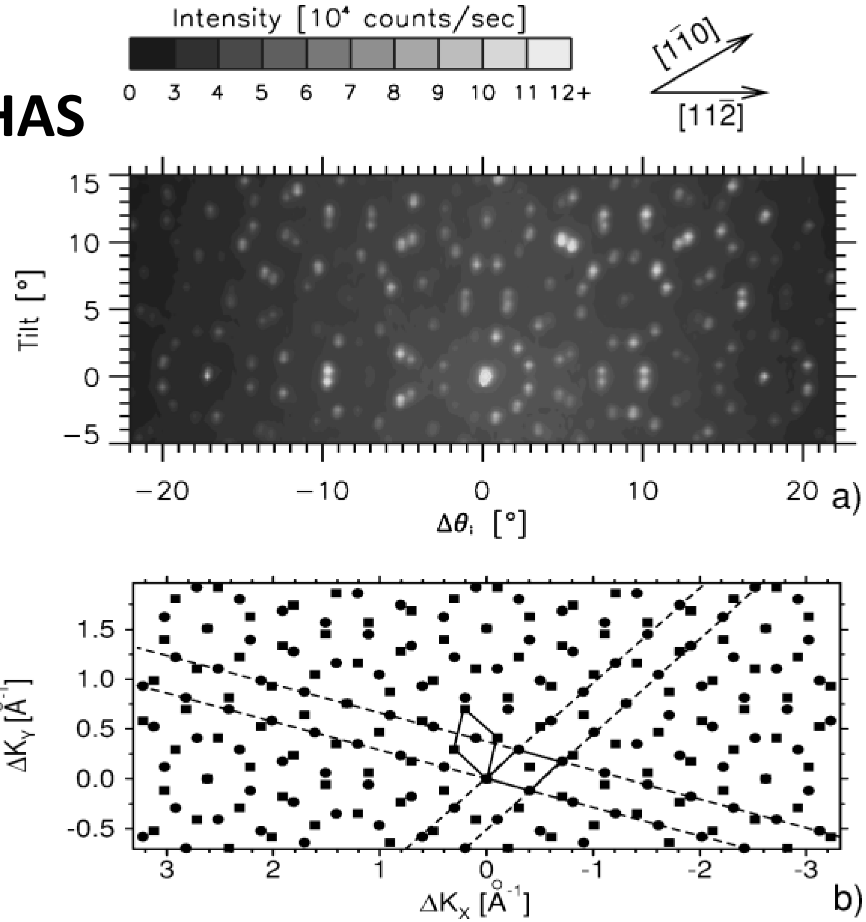

FIG. 2. (a) Two-dimensional helium diffraction pattern for a complete bilayer (Phase II) of D_2O on Pt(111) at an incident helium energy of 22 meV, and a temperature of $T_s = 130$ K. The complete diffraction pattern can be constructed from two domains of a epitaxially rotated water overlayer whose reciprocal unit cells are $(\sqrt{39} \times \sqrt{39})R16.1°$, as shown in (b). The two different domains are shown by the filled circles and squares, respectively. Exactly the same diffraction pattern was observed for H_2O.

A. Glebov, A. P. Graham, A. Menzel, and J. P. Toennies

Max Planck Institut für Strömungsforschung, Bunsenstrasse 10, Göttingen, Germany

J. Chem. Phys. **106** (22), 8 June 1997

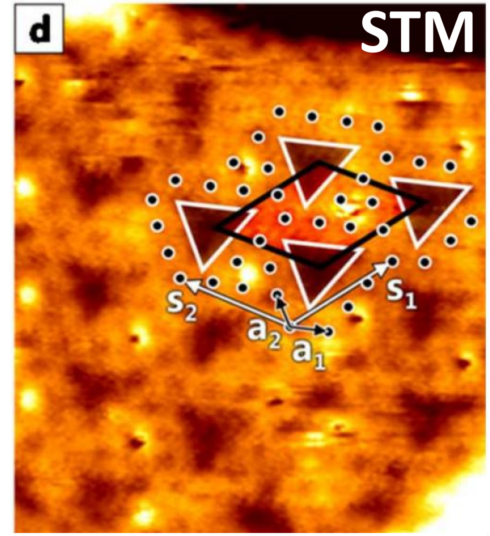

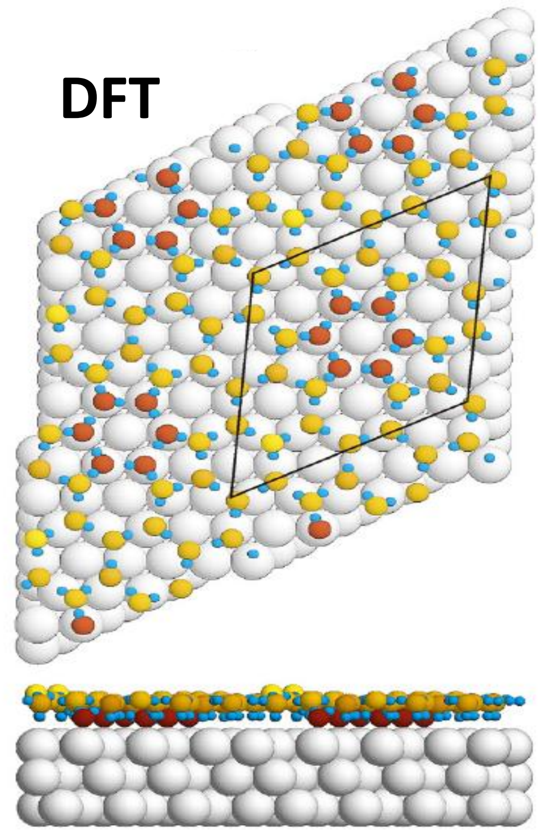

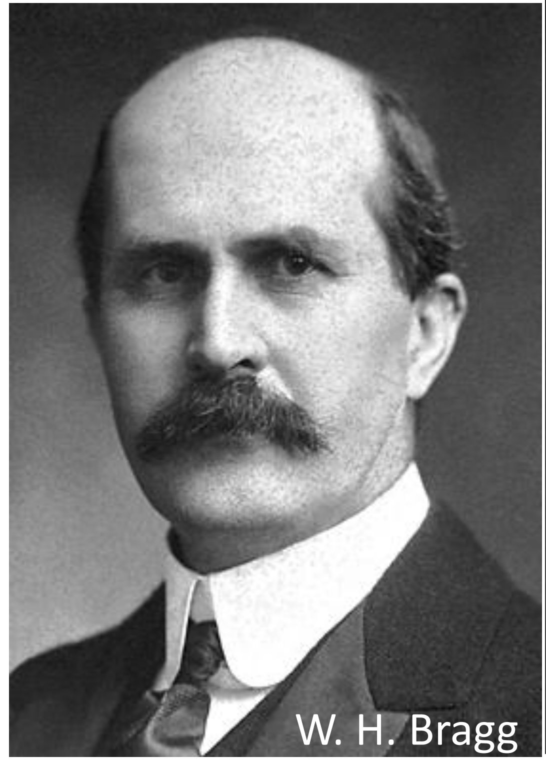

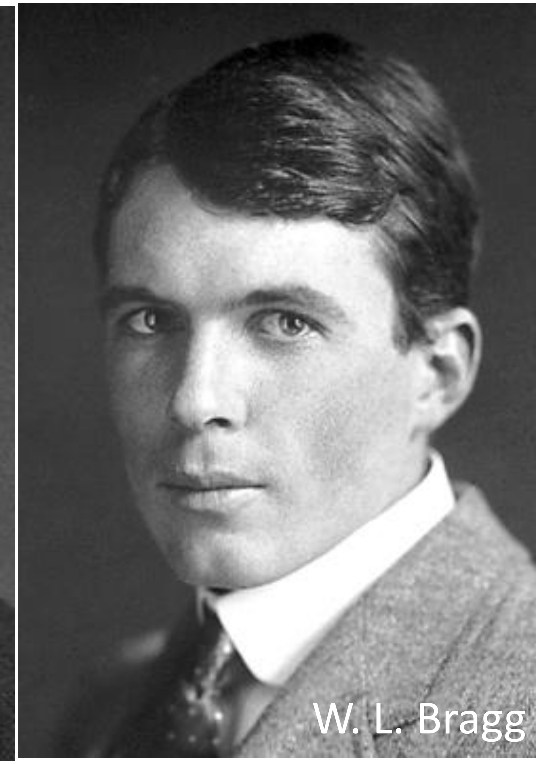

Nobel price in physics 1914 *“for his discovery of the diffraction of X-rays by crystals”*

Nobel price in physics 1915 *"for their services in the analysis of crystal structure by means of X-rays"*

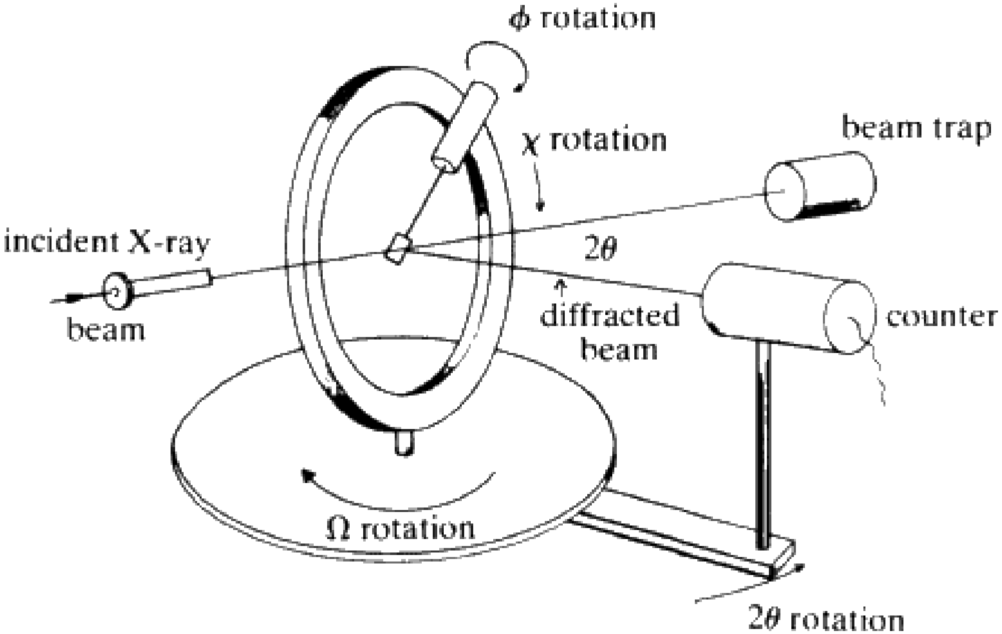

Four circle diffractometer
(Eulerian cradle)

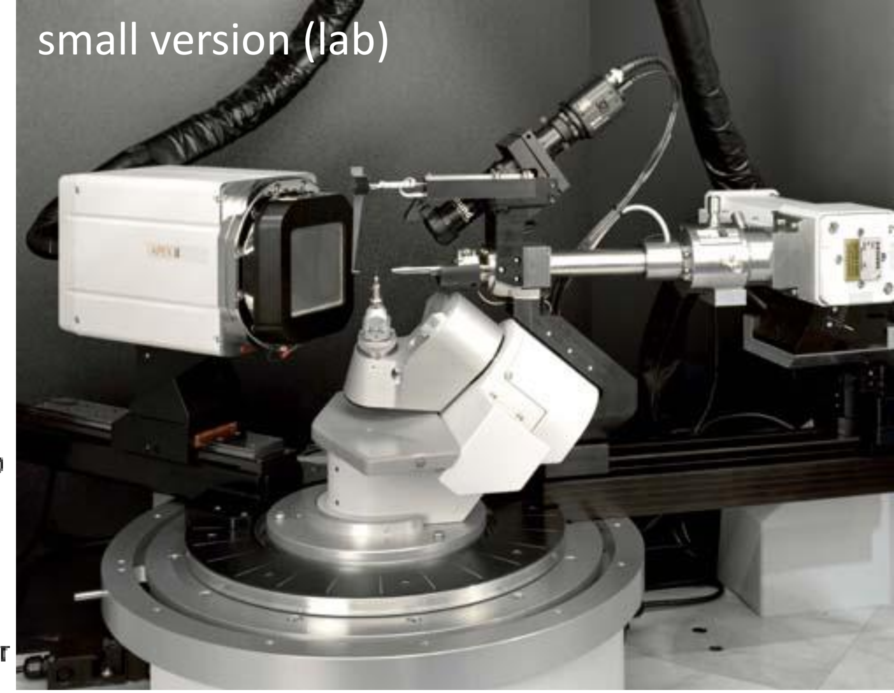

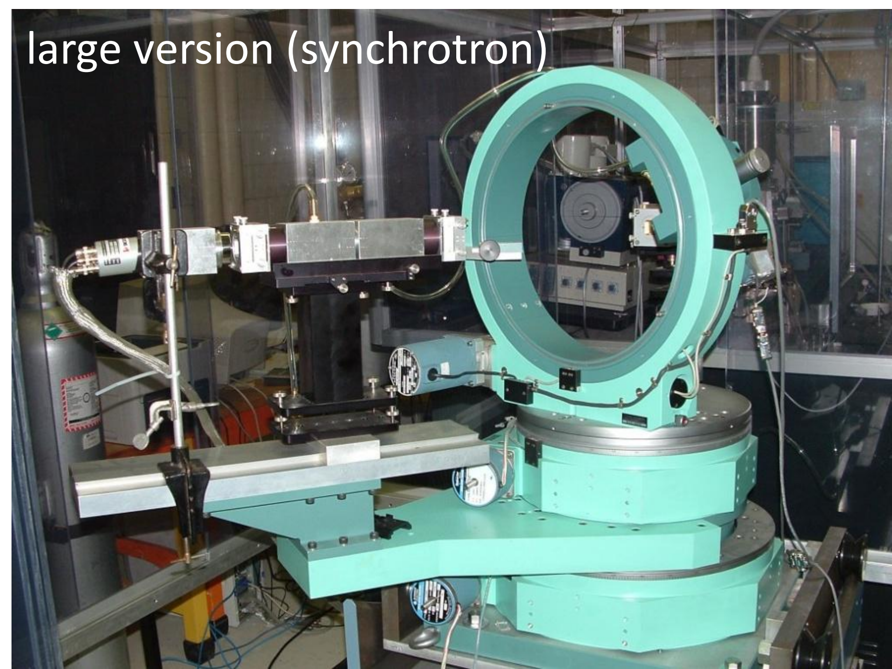

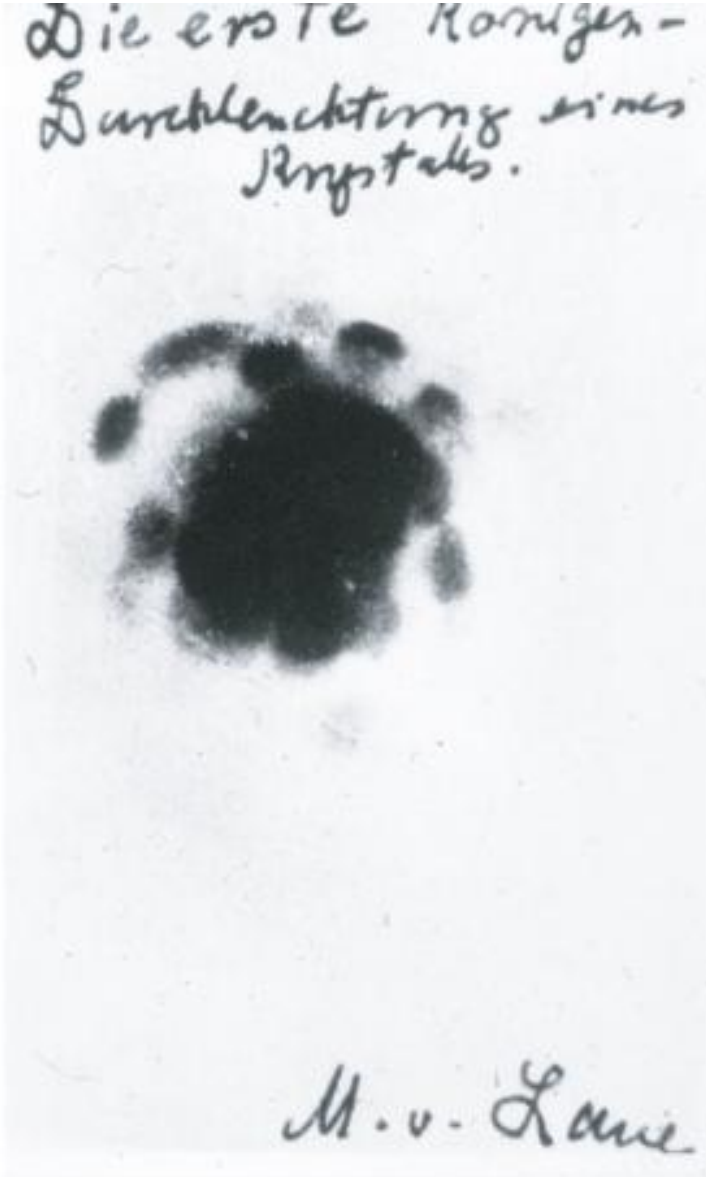

CuSO$_4$

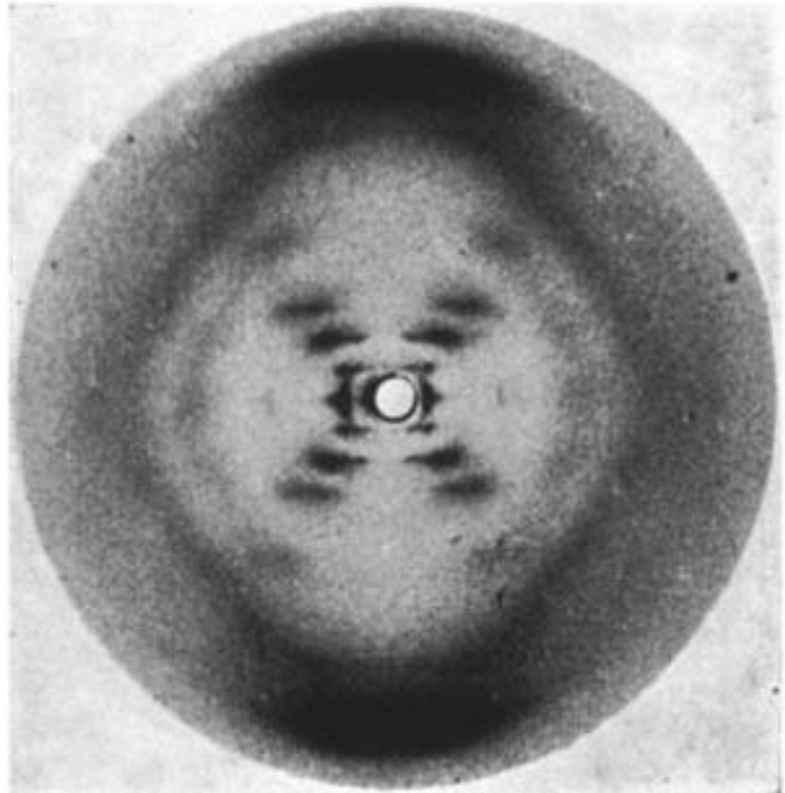

DNA

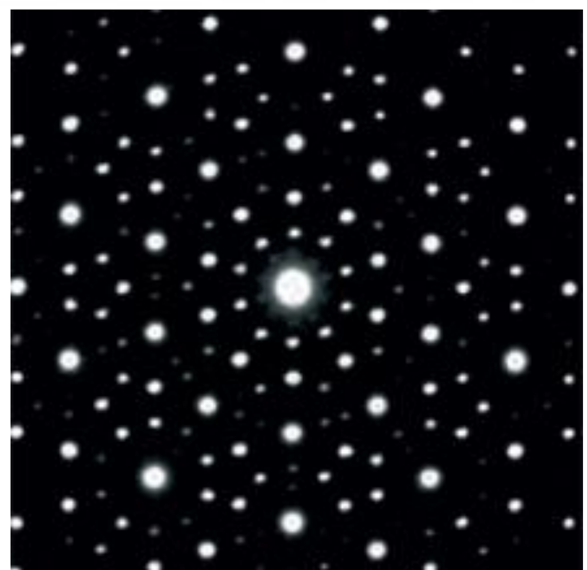

Quasicrystal

Beispiel : Ca_2RuO_4

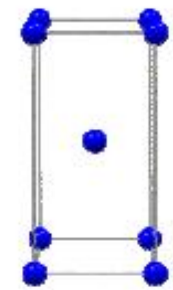

Raumgruppe I4/mmm : Auslöschungsbedingungen

Überstruktur durch Oktaederverkippung

0kl

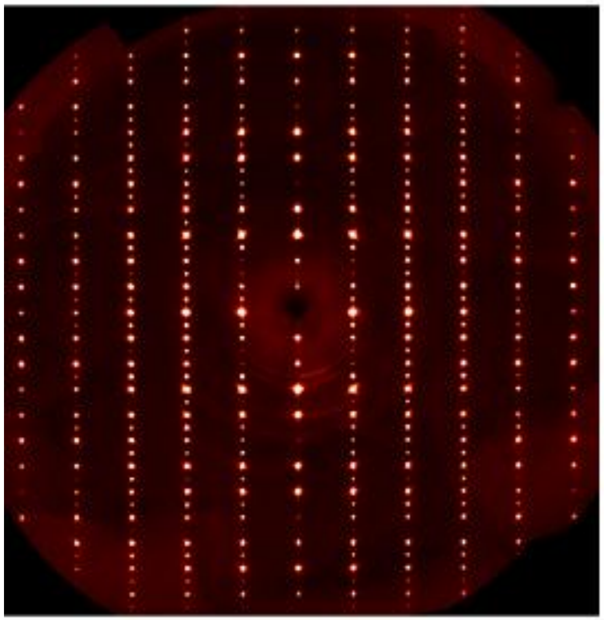

h0l

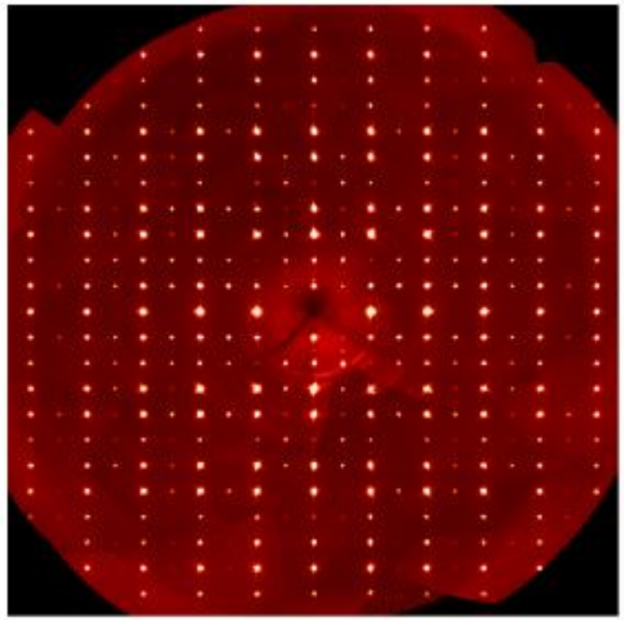

hk0

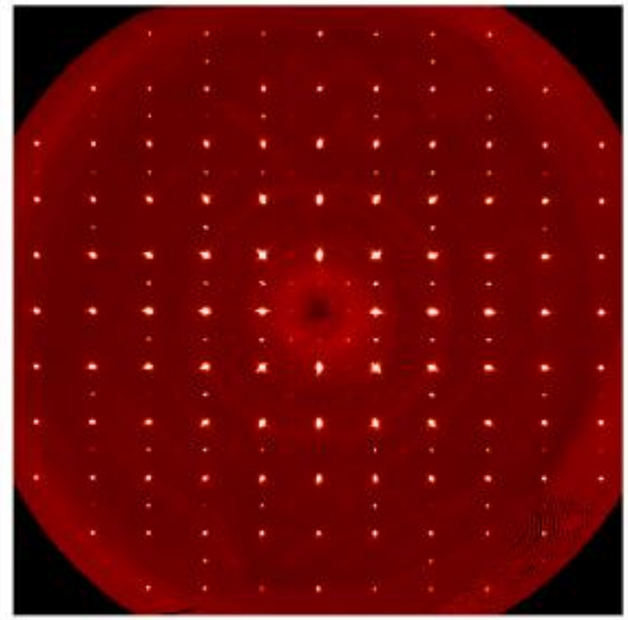

Streukarten entsprechend unterschiedlichen Ebenen im reziproken Raum. Man erkennt starke Fundamental-Reflexe und schwache Überstrukturen aufgrund der strukturellen Verzerrung.

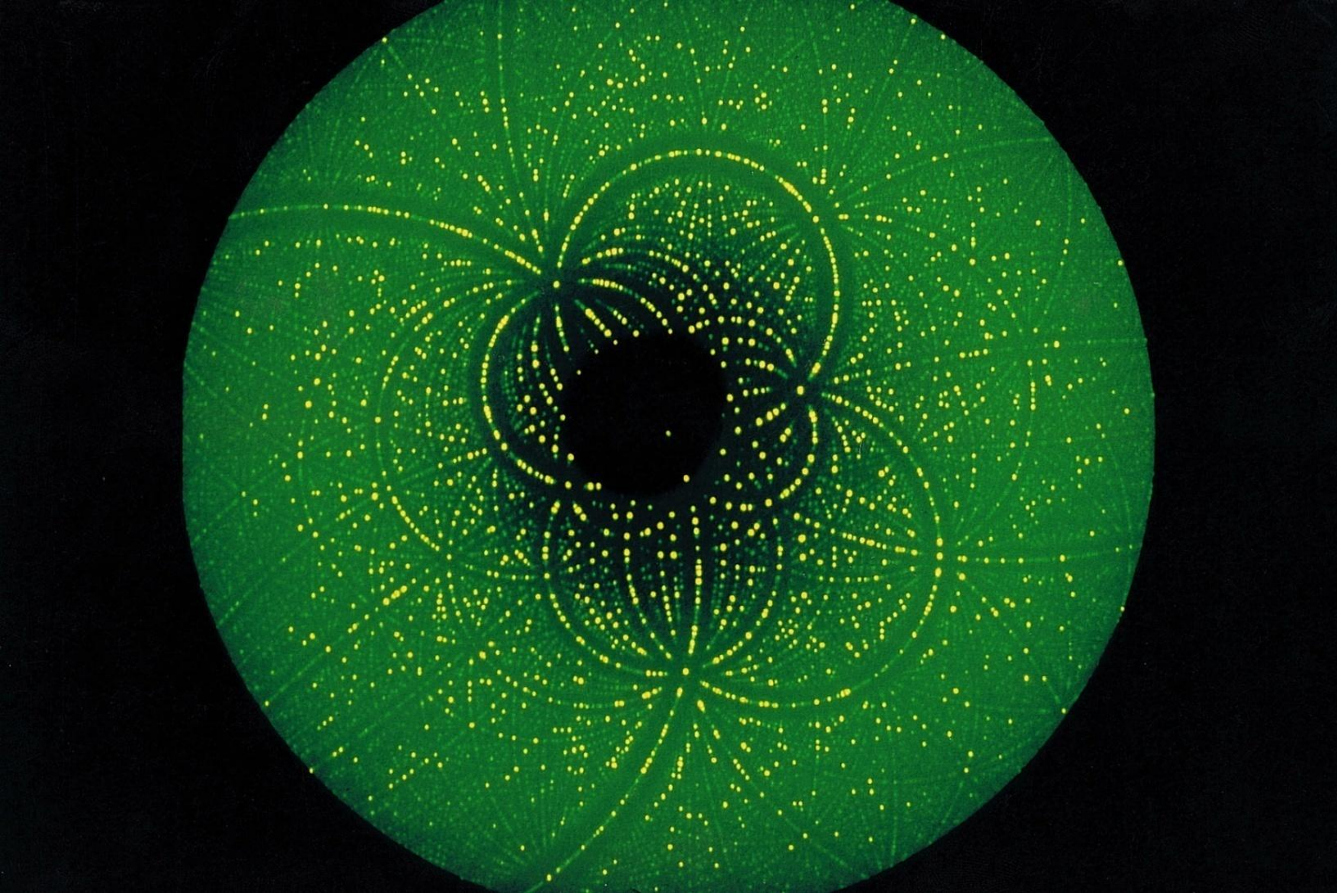

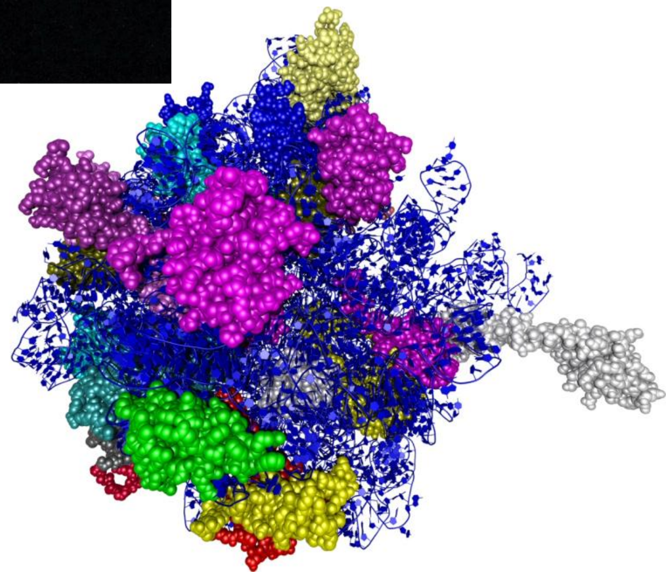

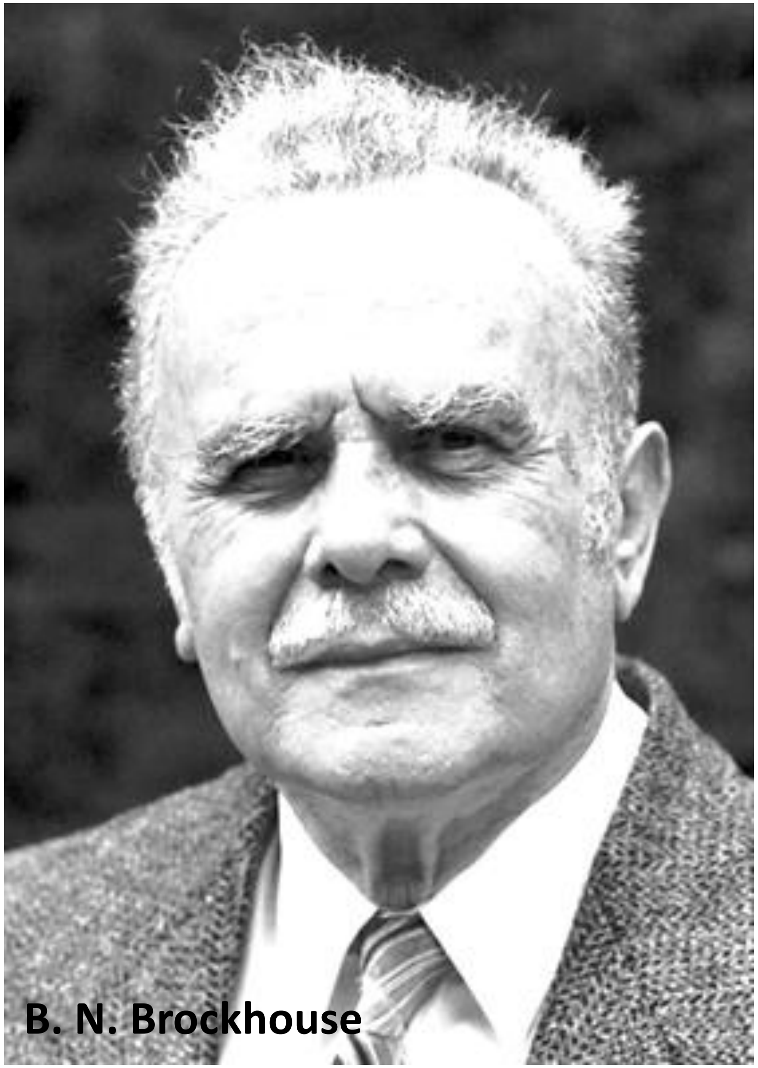

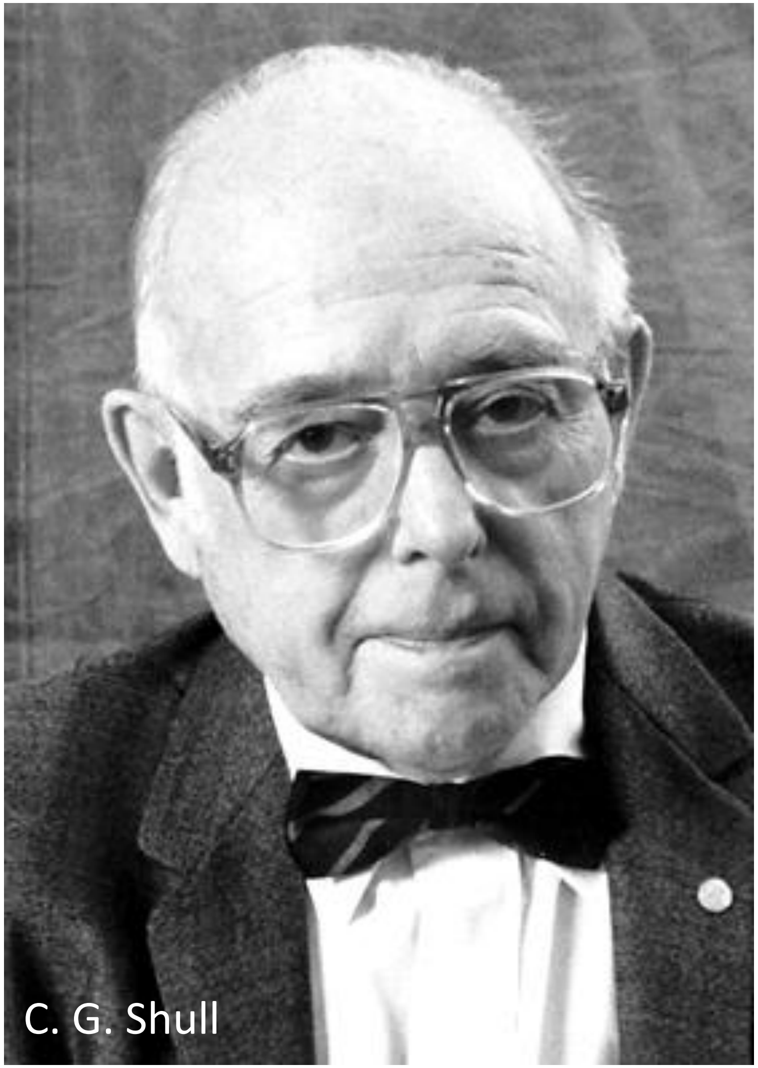

Nobel price in physics 1994 *"for pioneering contributions to the development of neutron scattering techniques for studies of condensed matter"* jointly with one half to Bertram N. Brockhouse *"for the development of neutron spectroscopy"* and with one half to Clifford G. Shull *"for the development of the neutron diffraction technique"* **(work done in the 1950s-1960s)**

Neutrons

Neutrons are **NEUTRAL** particles. They

- are highly penetrating,
- can be used as nondestructive probes, and
- can be used to study samples in severe environments.

Neutrons have a **MAGNETIC** moment. They can be used to

- study microscopic magnetic structure,
- study magnetic fluctuations, and
- develop magnetic materials.

Neutrons have **SPIN**. They can be

- formed into polarized neutron beams,
- used to study nuclear (atomic) orientation, and
- used for coherent and incoherent scattering.

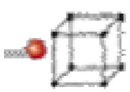

The **ENERGIES** of thermal neutrons are similar to the energies of elementary excitations in solids. Both have similar

- molecular vibrations,
- lattice modes, and
- dynamics of atomic motion.

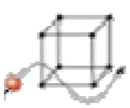

The **WAVELENGTHS** of neutrons are similar to atomic spacings. They can determine

- structural sensitivity,
- structural information from 10^{-13} to 10^{-4} cm, and
- crystal structures and atomic spacings.

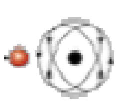

Neutrons "see" **NUCLEI**. They

- are sensitive to light atoms,
- can exploit isotopic substitution, and
- can use contrast variation to differentiate complex molecular structures.

$$M_n = 1.674928.10^{-27}\text{kg}$$
$$= 1.001\ M_{\text{Proton}}$$

$\tau = 885$ s (β decay)

$n \rightarrow p + e^- + \nu_e + 0.78\text{MeV}$

n: $E = h^2/2M_n\lambda^2 = 81.1\text{meV}/\lambda^2$

photon: $E = hf = hc/\lambda = 12398\text{eV}/\lambda$

$k = 2\pi/\lambda \qquad p = h/\lambda$

units:

1 meV=11.6 K=8.066/cm=0.241THz

		λ[Å]	k[1/Å]	v(m/s)	E	best $\Delta E/E$
Photon	light	5000	10^{-3}	3.10^8	eV	10^{-8}
	X-ray	1	1	3.10^8	keV	10^{-6}
electron		1	1	6.10^7	150eV	10^{-5}
neutron		1	1	400	meV	10^{-6}

-Neutronen sind neutral ($Q<10^{-20}e$)
-Wechselwirkung mit den Atomkernen
→lokal
→nicht direkt von Z abhängig
→Bestimmung leichter **und** schwerer Atome !!!

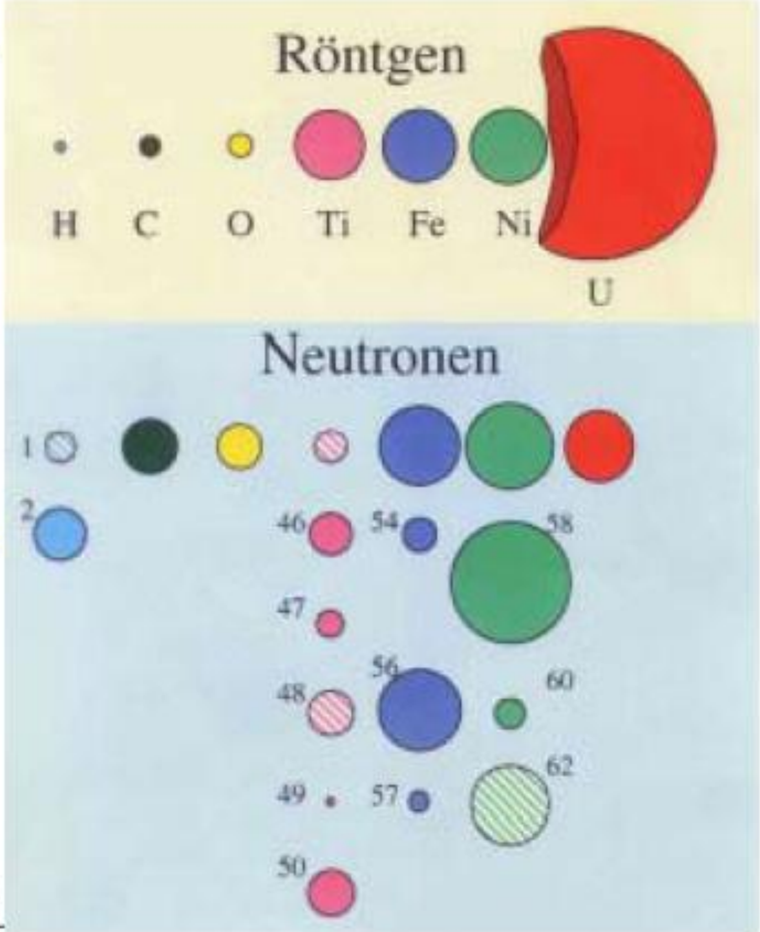

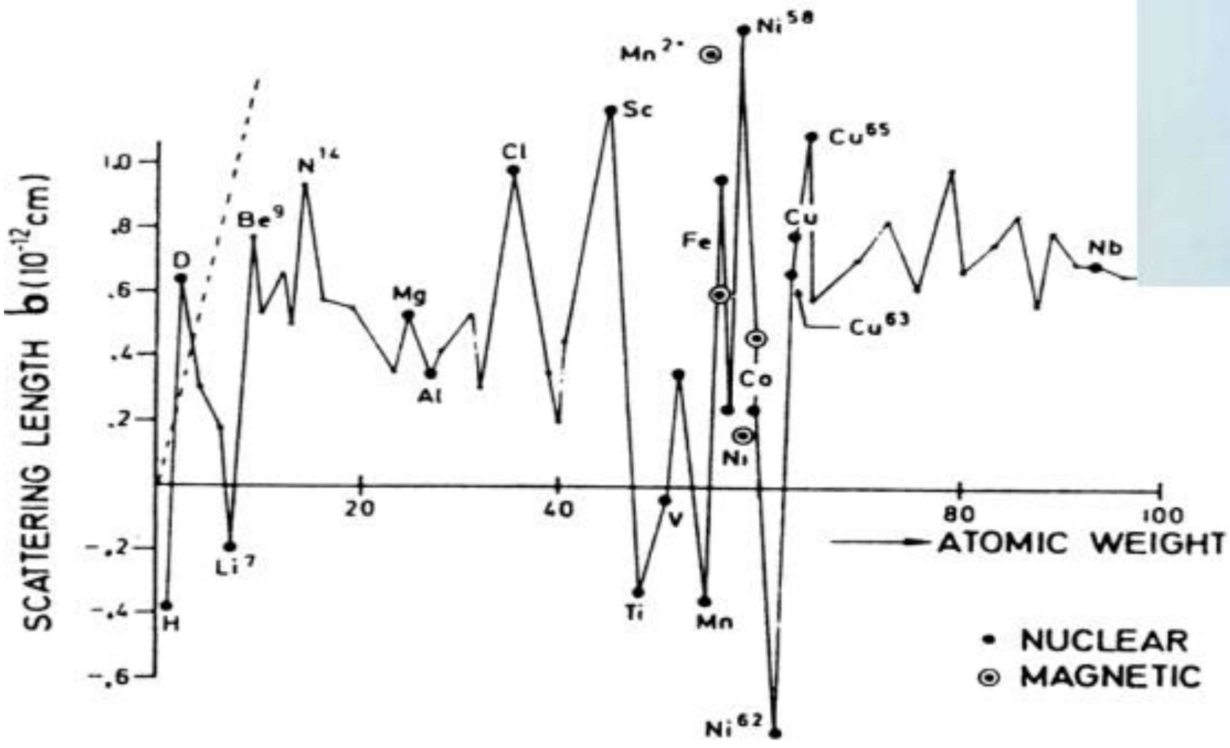

Neutrons – Photons

Neutrons:

Particle beam (neutral)
$E=h^2/2m_N\lambda^2=81.1\text{meV}/\lambda^2$
Low brilliance (particles/cm2/sr/meV)
Interactions with the nuclei and the magnetic moment of unpaired electrons

Scattered by all elements, also the light ones like the hydrogen isotopes

Deep penetration depth (bulk studies of samples)

Less intense beam measuring larger samples

Applications:
Magnetic structures & excitations, critical scattering

Photons:

Light beam
$E=hf=hc/\lambda=12398\text{eV}/\lambda$
High brilliance
Interactions with the electrons surrounding the nuclei

Mainly scattered by heavy elements

Small penetration depth (surface studies of samples)

Very intense beam measuring small or ultra-dilute samples

Applications:
Surface studies, element and shell sensitive resonant magnetic scattering, magnetic dichroism, magnetic Materials with high neutron absorption

Where do the Magnetic Reflections appear?

assuming one atom per unit cell

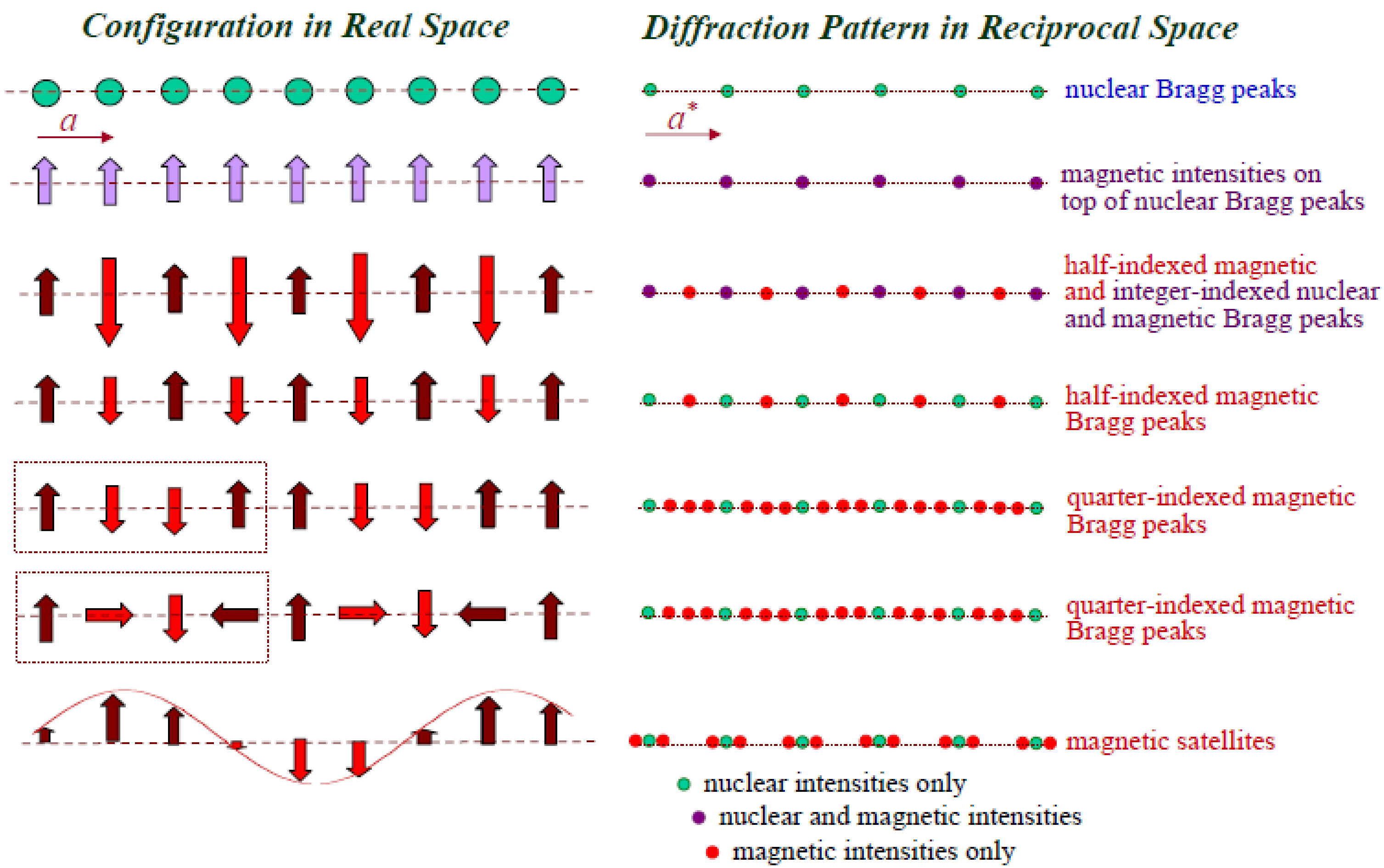

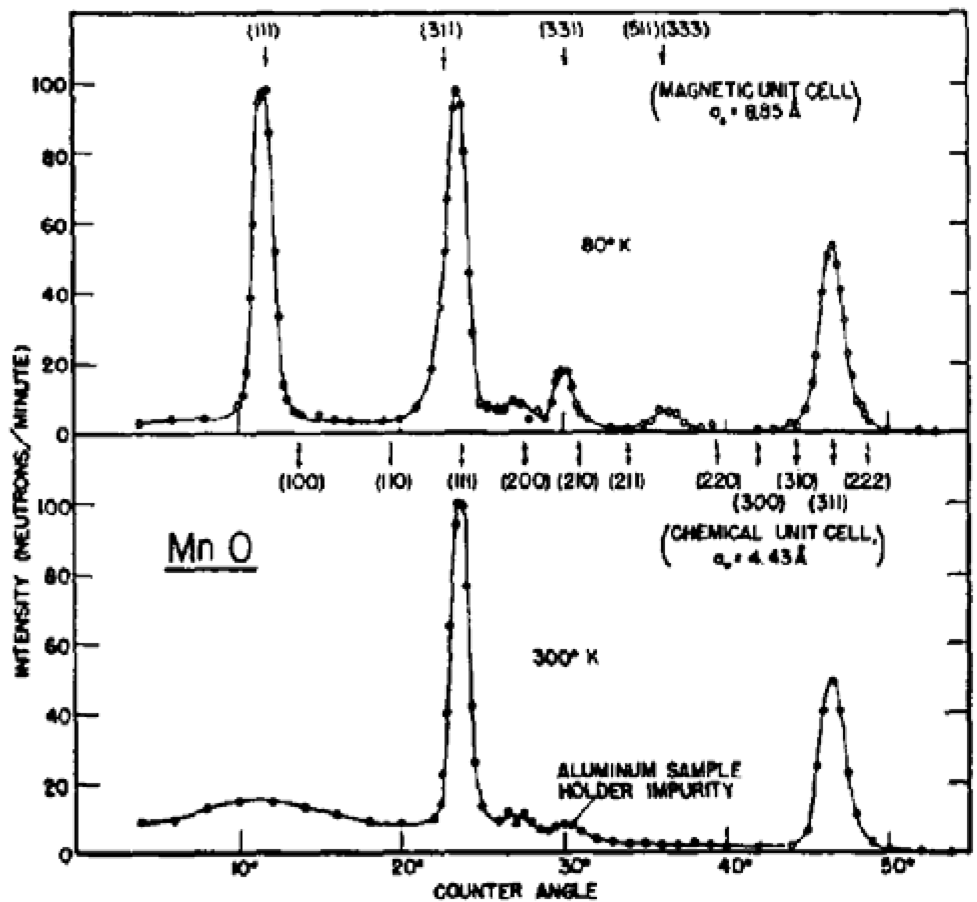

FIG. 1. Neutron diffraction patterns for MnO at room temperature and at 80°K.

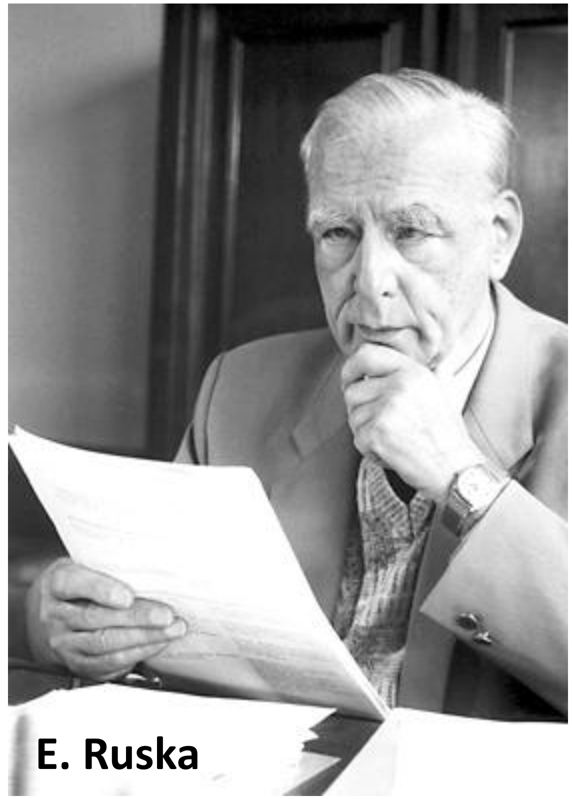

E. Ruska

Nobel price in physics 1988 *" "for his fundamental work in electron optics, and for the design of the first electron microscope"* **(work done in the 1930s-1940s)**

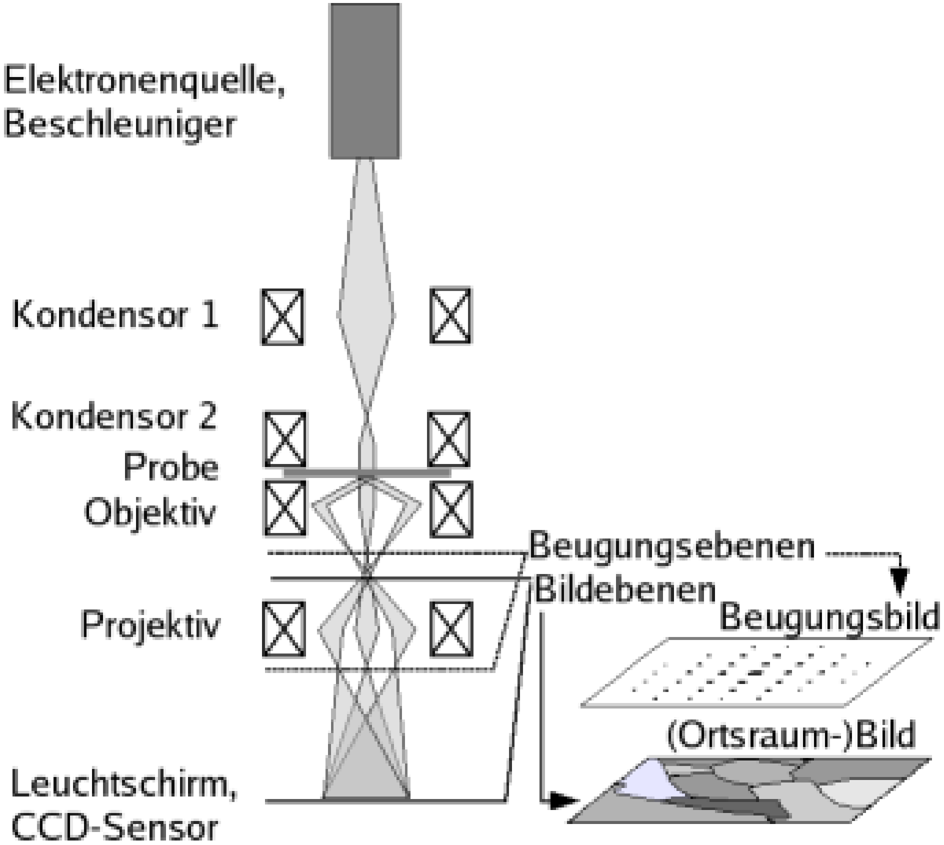

Elektronenquelle,
Beschleuniger
Kondensor 1
Kondensor 2
Probe
Objektiv
Beugungsebenen
Bildebenen
Beugungsbild
Projektiv
(Ortsraum-)Bild
Leuchtschirm,
CCD-Sensor

2004: Tesafilm-Graphen

scotch tape on Si wafer with 300 nm SiO_2 on top

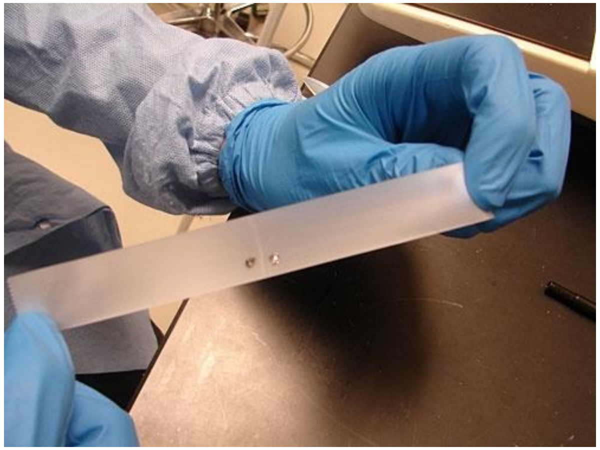

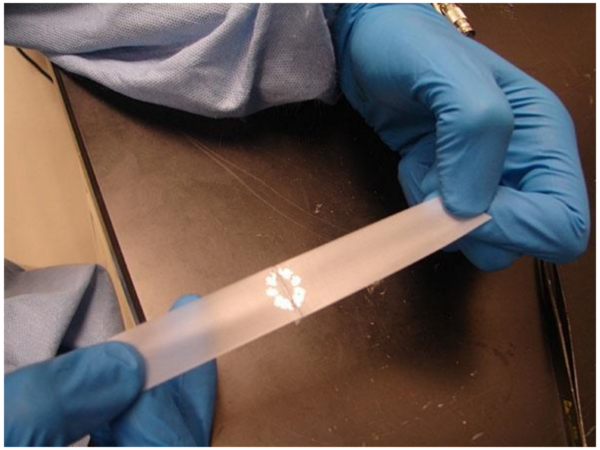

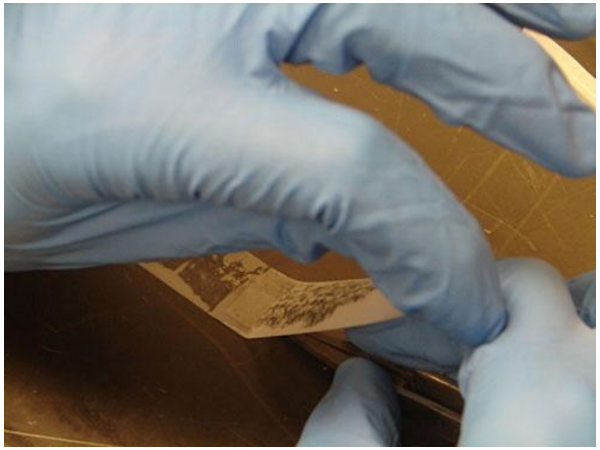

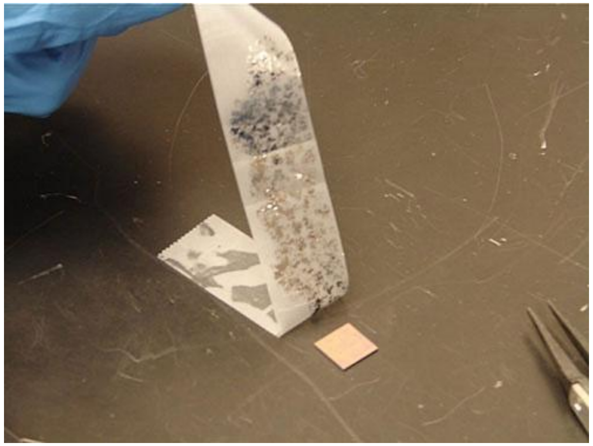

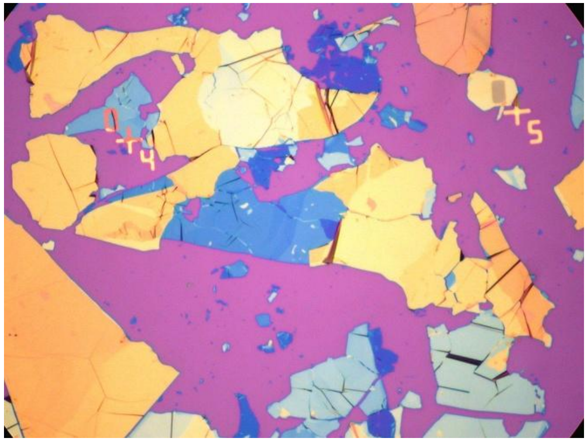

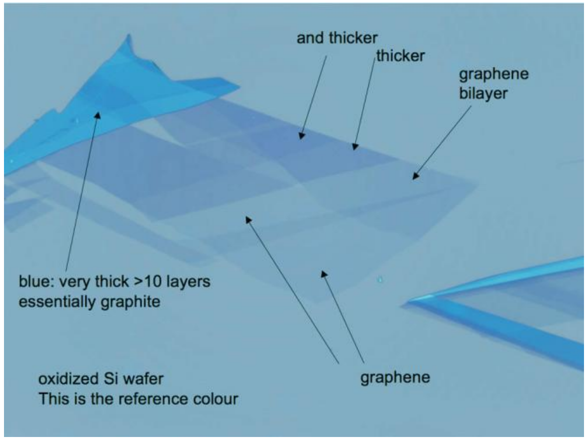

inteference-like constrast in optical microscope allows detection of single-layered graphene

Nobelpreis in Physik 2010

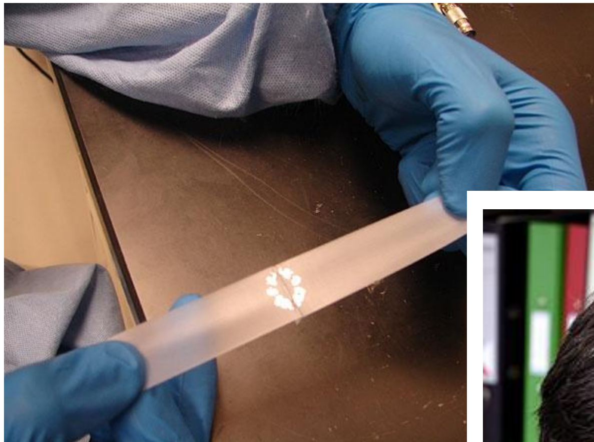

A. Geim

K. Novoselov

"für grundlegende Experimente mit dem zweidimensionalen Material Graphen"

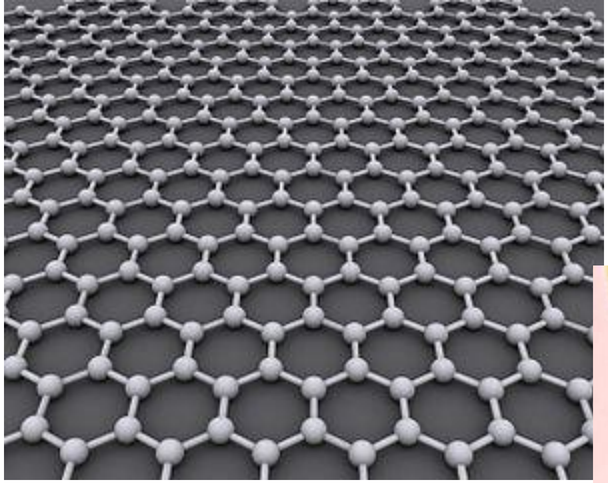
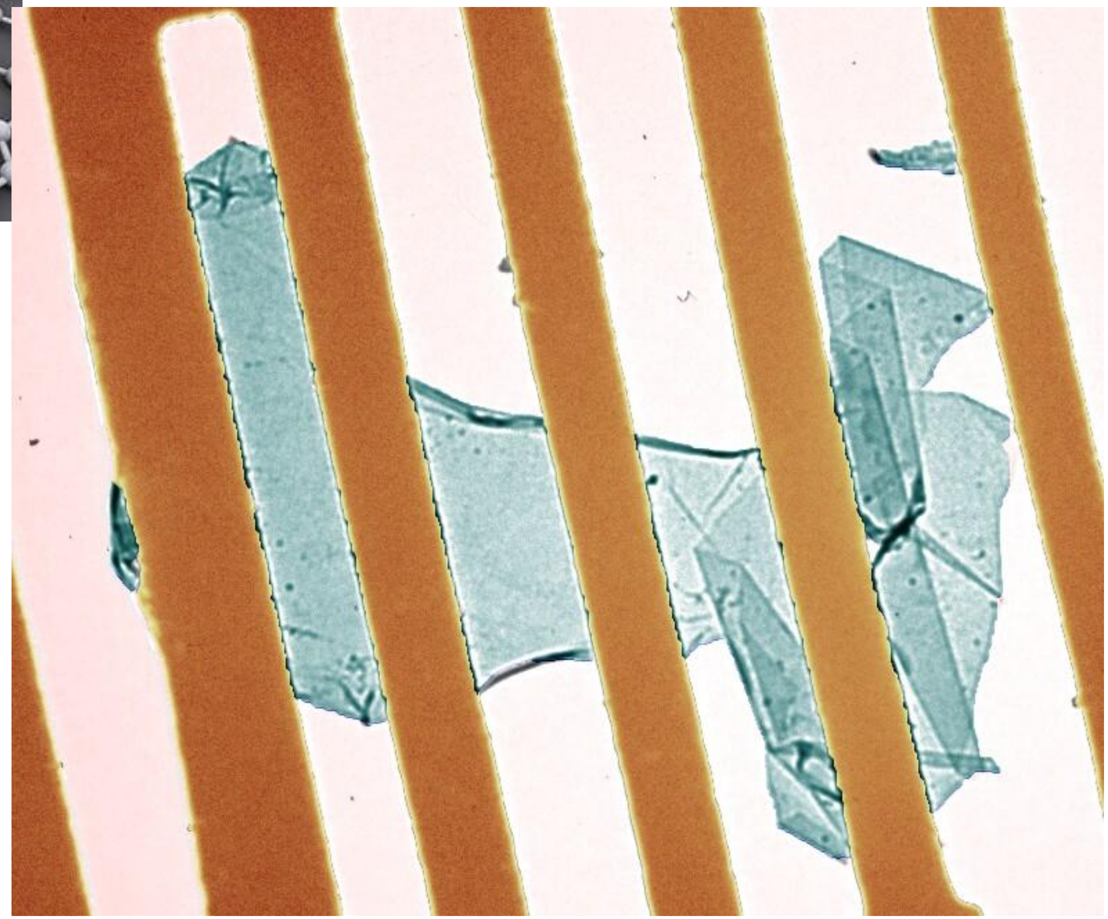

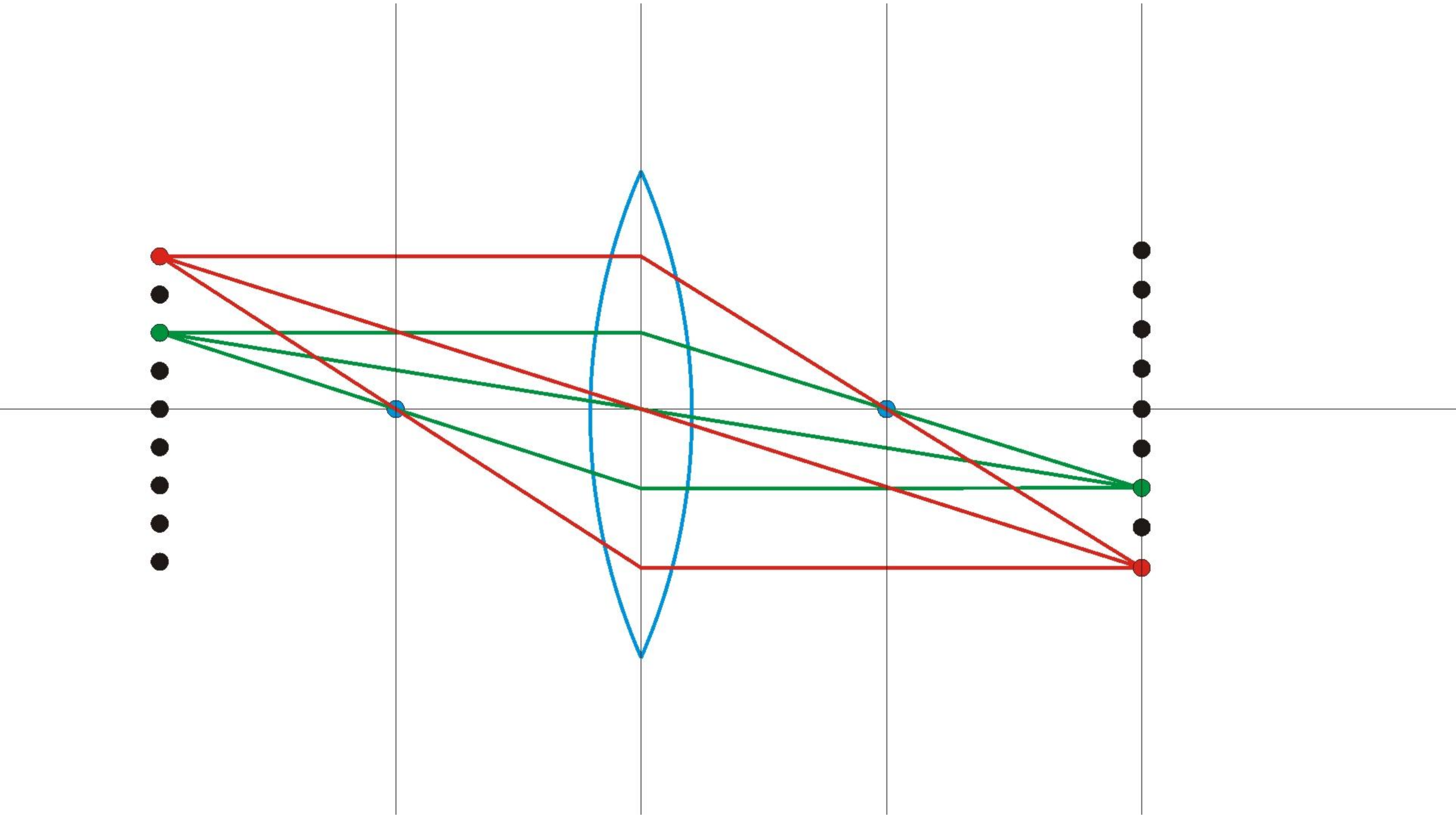

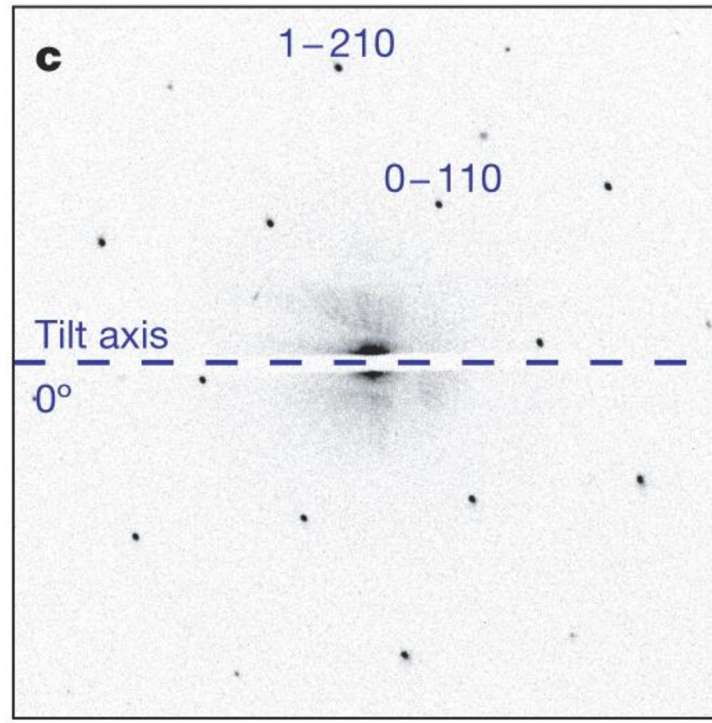
c
1−210
0−110
Tilt axis
0°

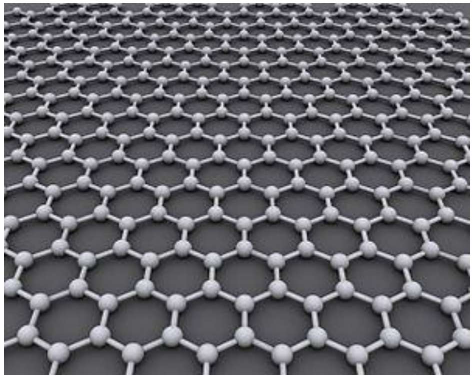

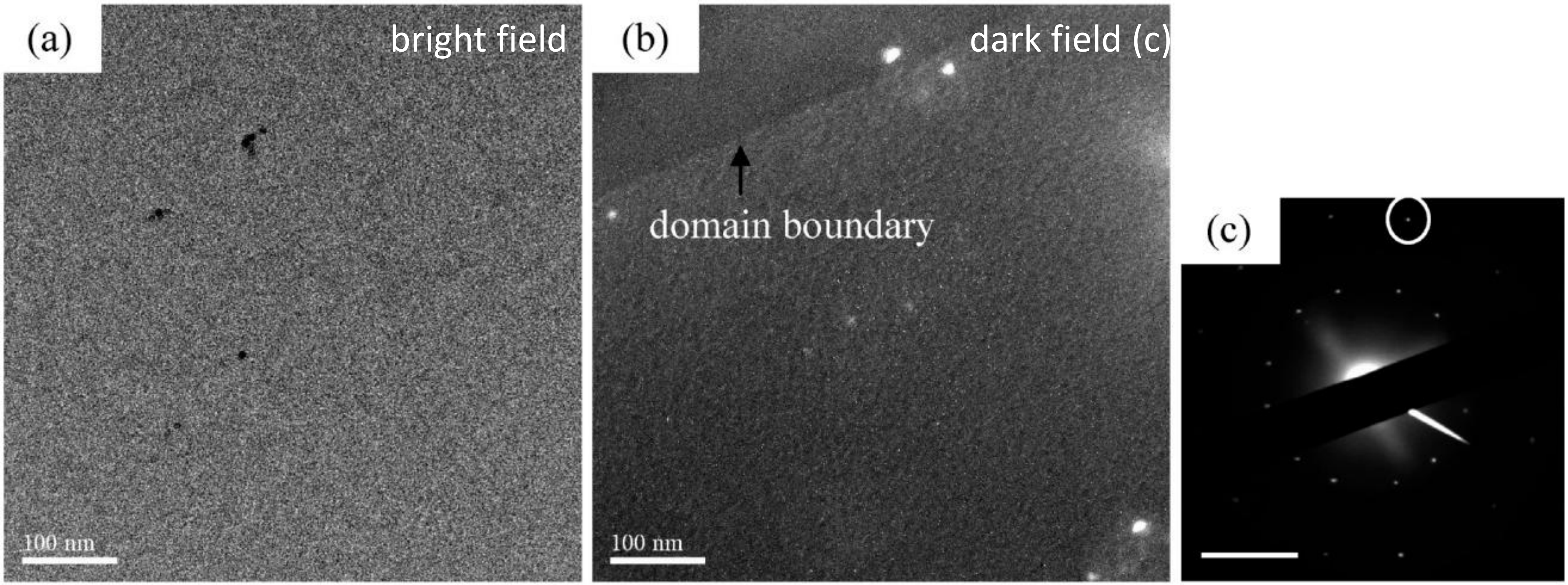
(a)
bright field
100 nm
(b)
dark field (c)
domain boundary
100 nm
(c)

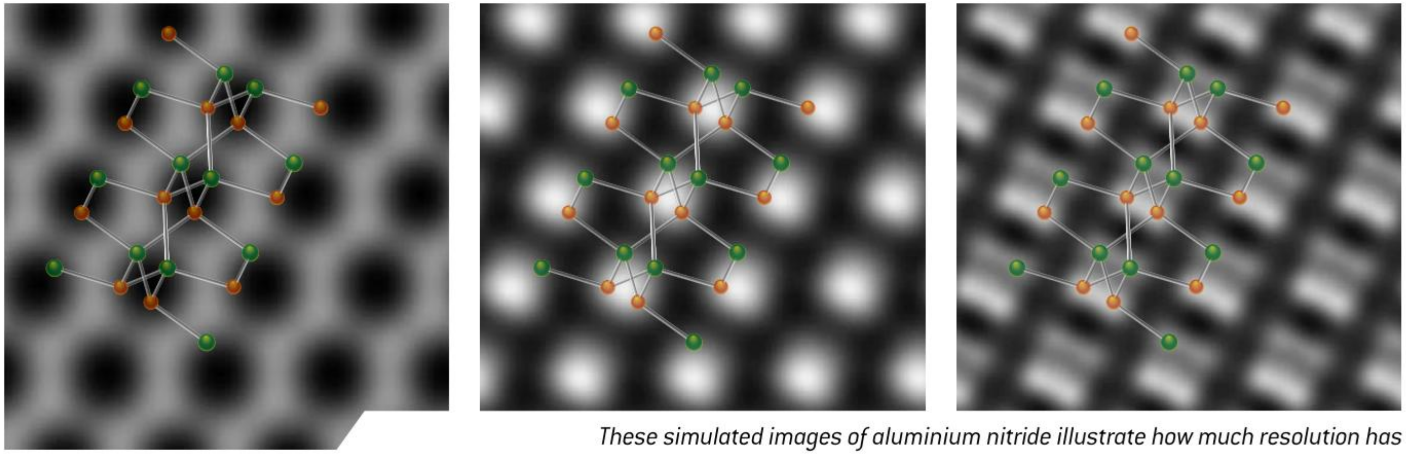

These simulated images of aluminium nitride illustrate how much resolution has improved with each generation of electron microscopes from 1992, 1998 and 2005 up to the present day (from left to right).

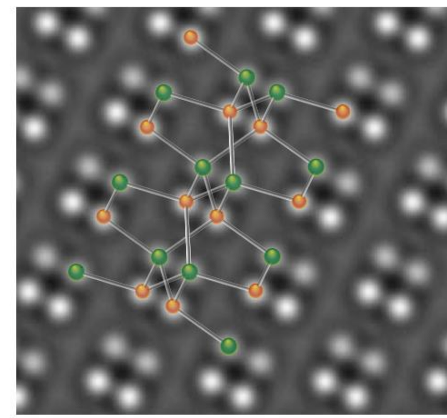

Only PICO makes it possible to actually recognize the atoms in this material. The atoms are shown as green and red spheres as an aid to recognition.

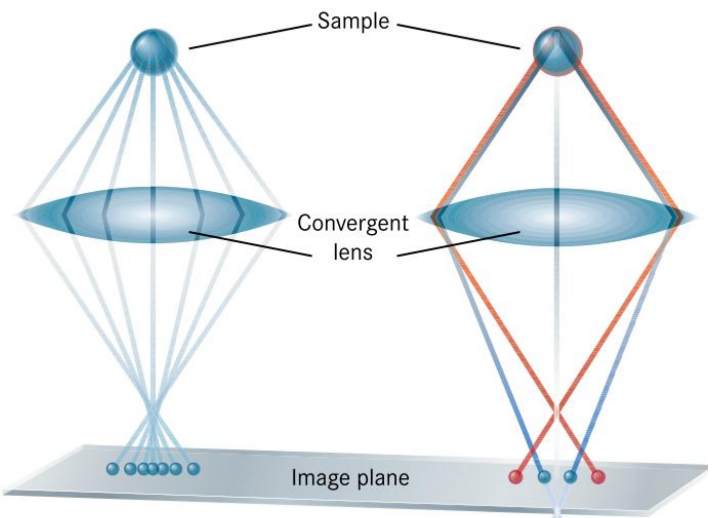

Two lens errors that lead to fuzzy images with reduced resolution: spherical aberration (left) and chromatic aberration (right)

HRTEM of $SrTiO_3$

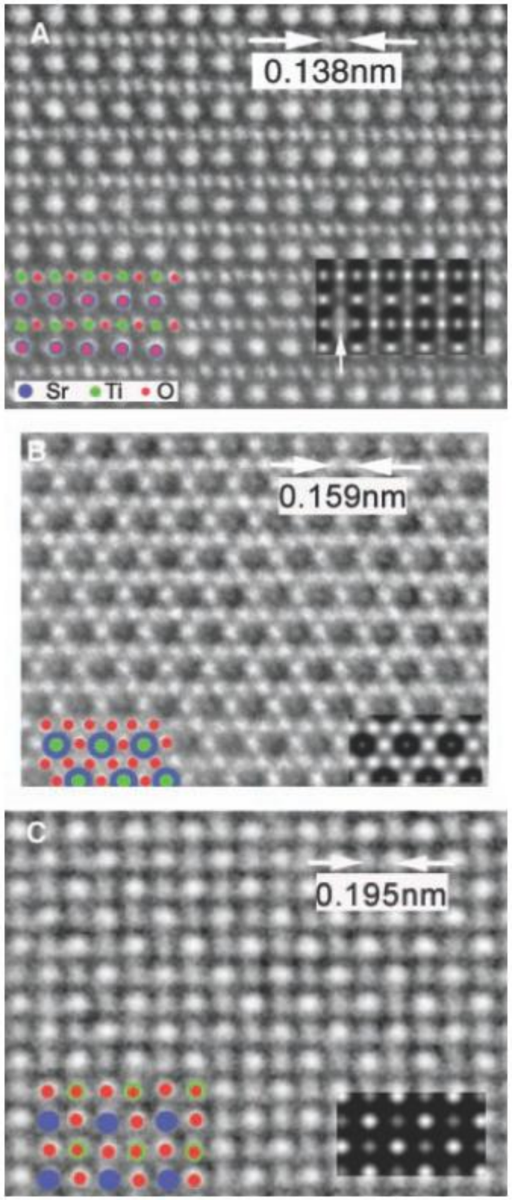

$SrTiO_3$ (strontium titanate) perovskite structure

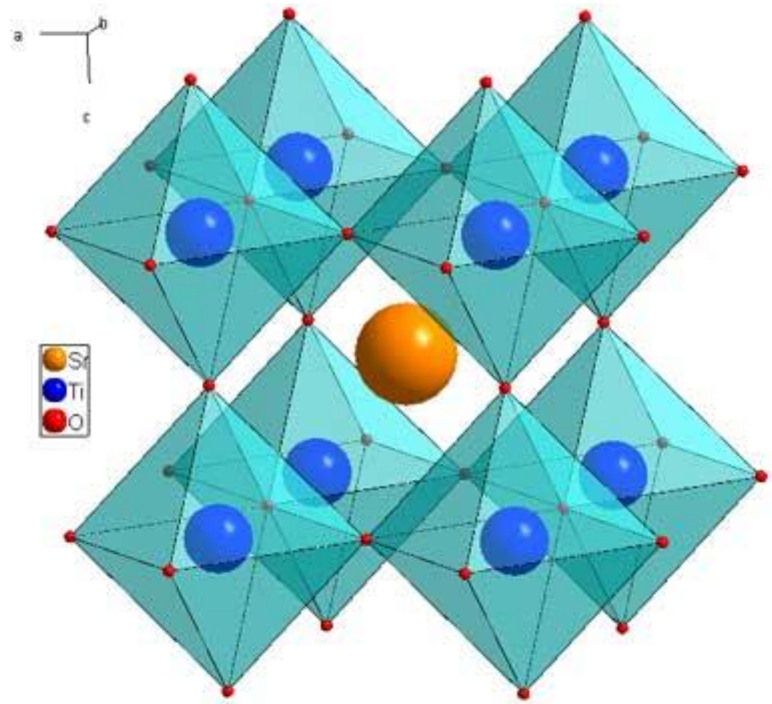

Z. Zhang, W. Sigle, F. Phillipp, M. Rühle, Science 302, 846 (2003)

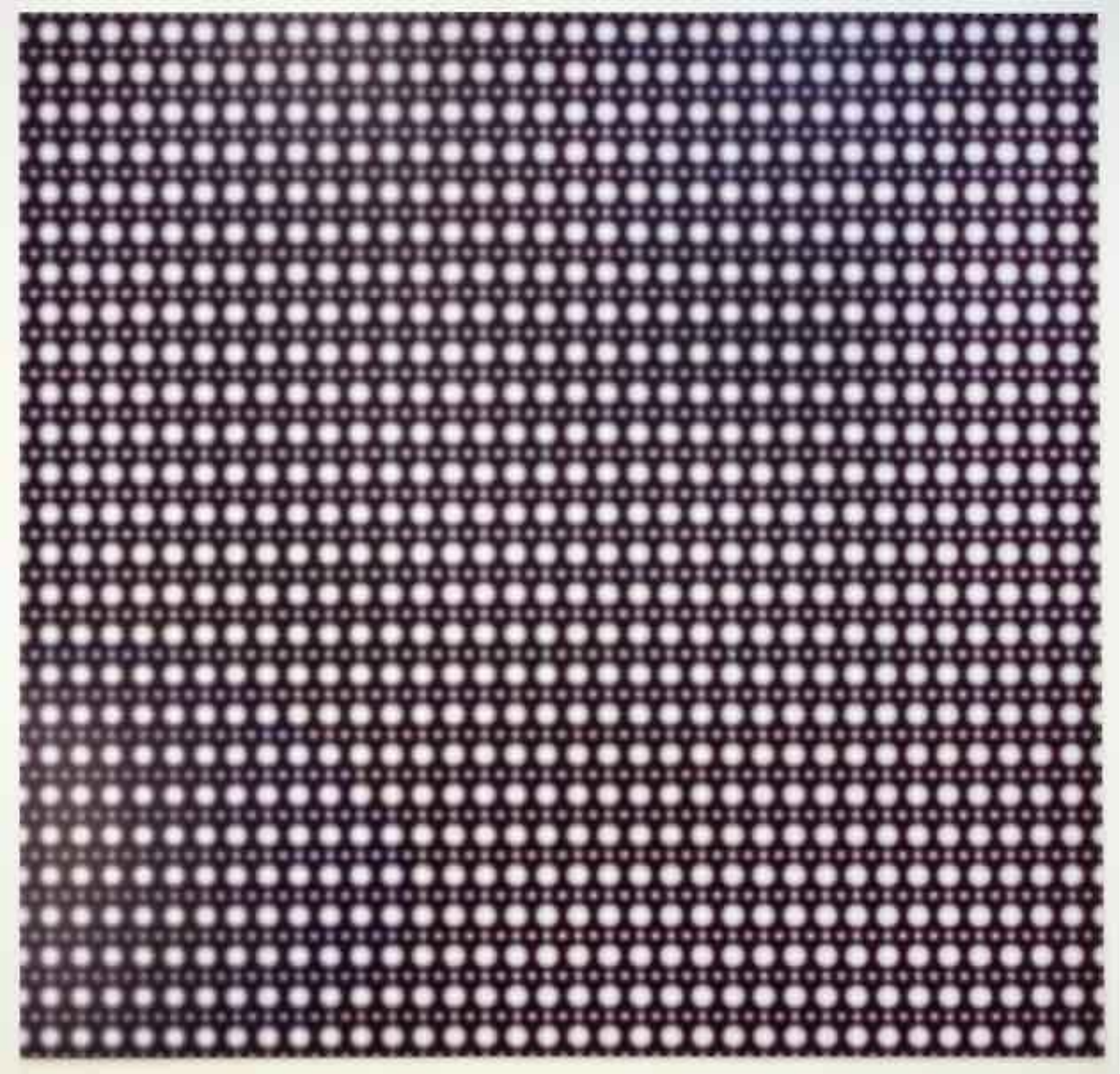

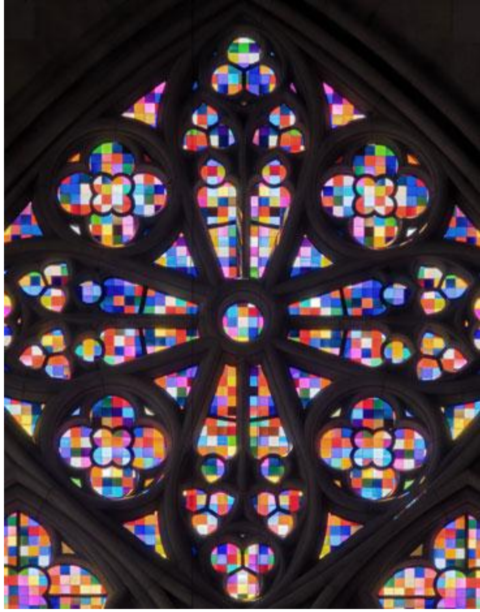

G. Richter, Strontium (2005)

HRTEM of graphene

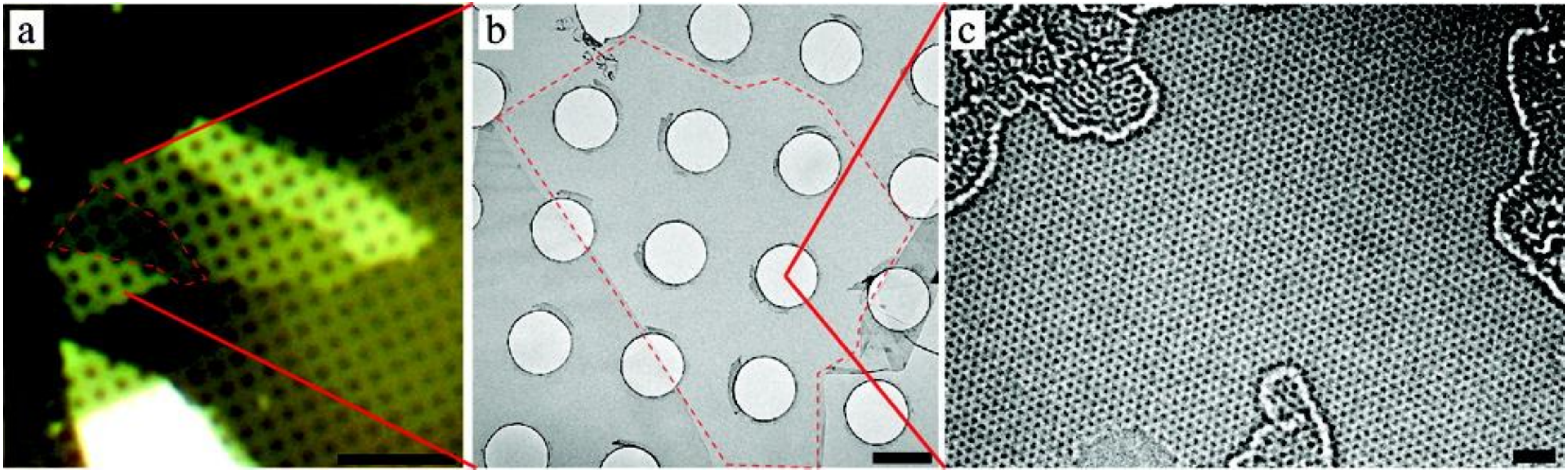

J. C. Meyer, C. Kisielowski, R. Erni, M. D. Rossell,
M. F. Crommie, A. Zettl, Nano Lett. 8, 3582 (2008)

HRTEM of graphene

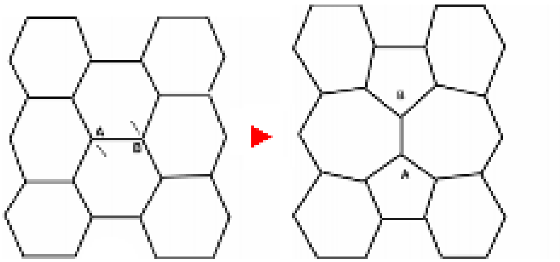

Stone-Wales defect

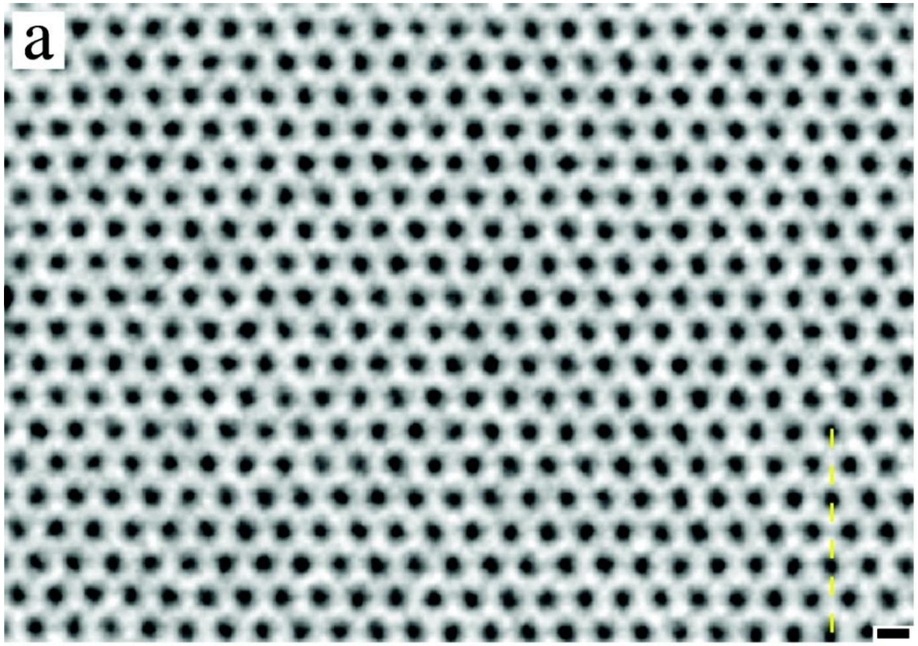

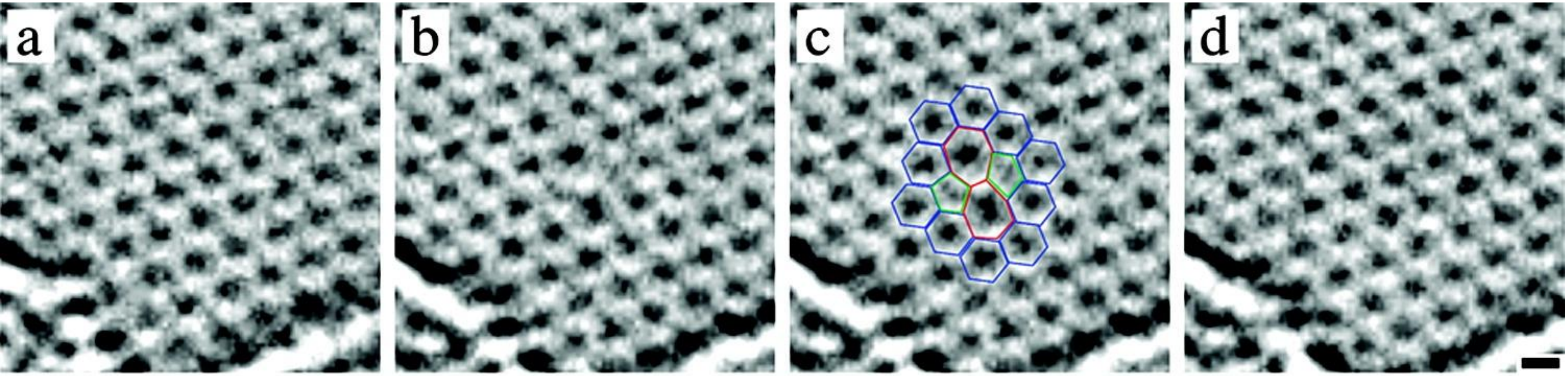

J. C. Meyer, C. Kisielowski, R. Erni, M. D. Rossell,
M. F. Crommie, A. Zettl, Nano Lett. 8, 3582 (2008)

Interaction of e$^-$ with matter

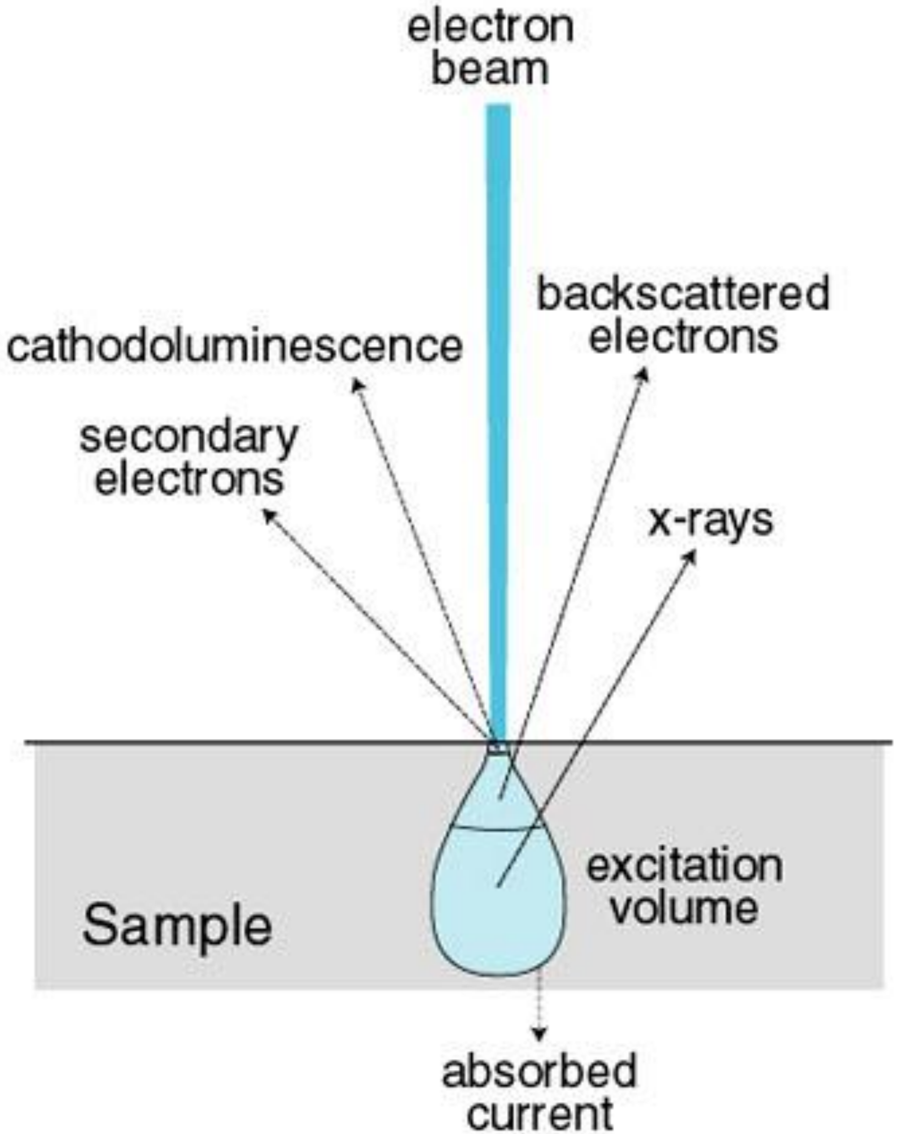

SEM – principle of operation

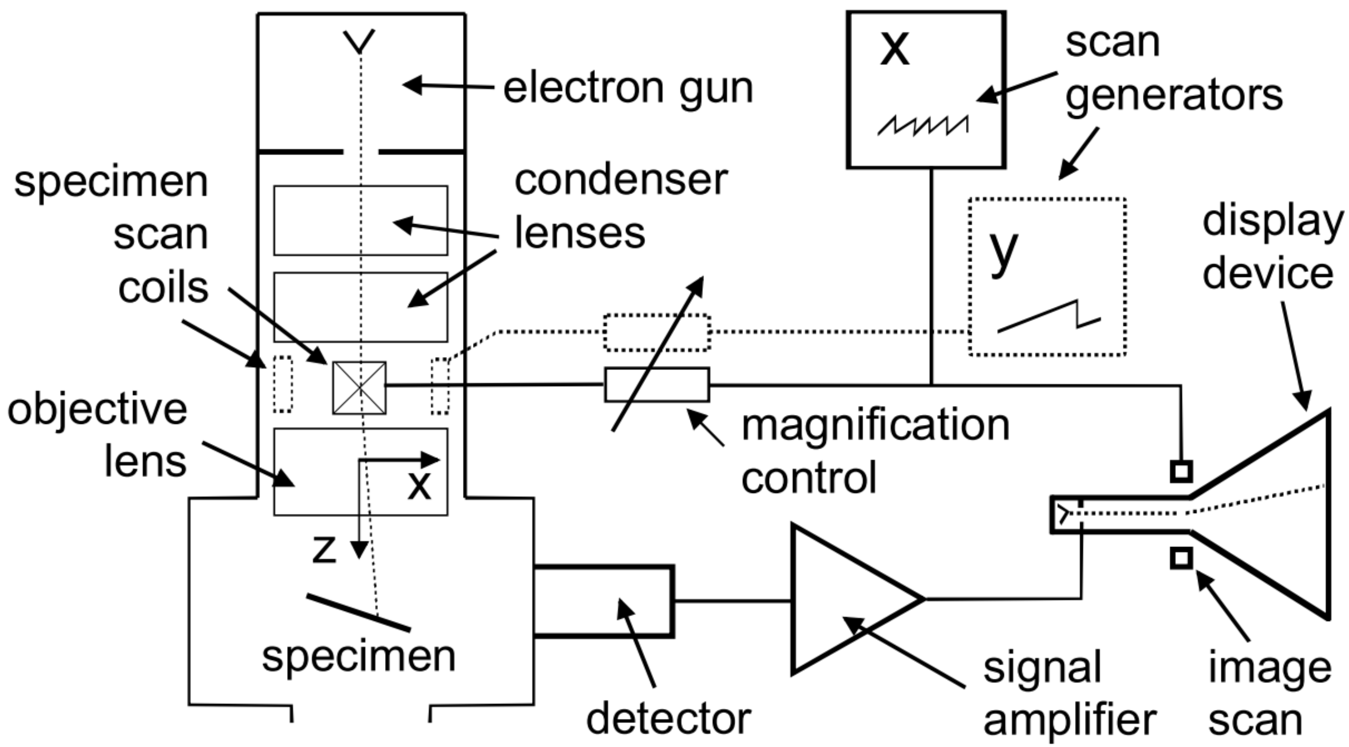

SEM

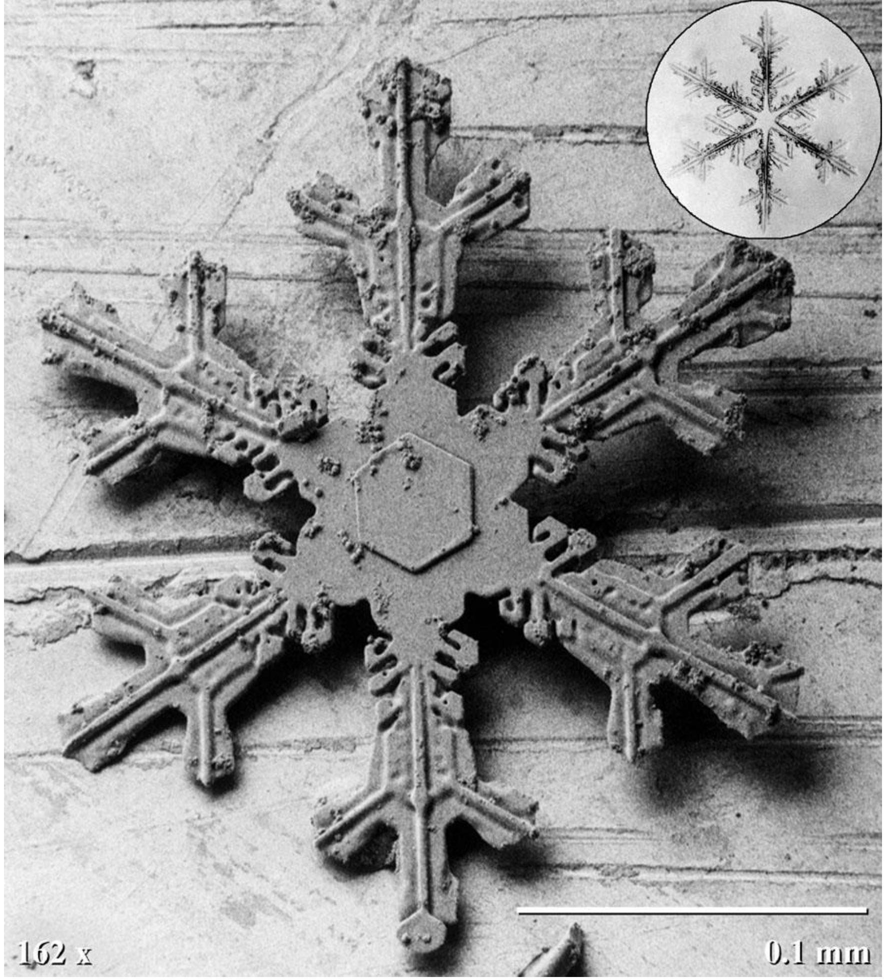

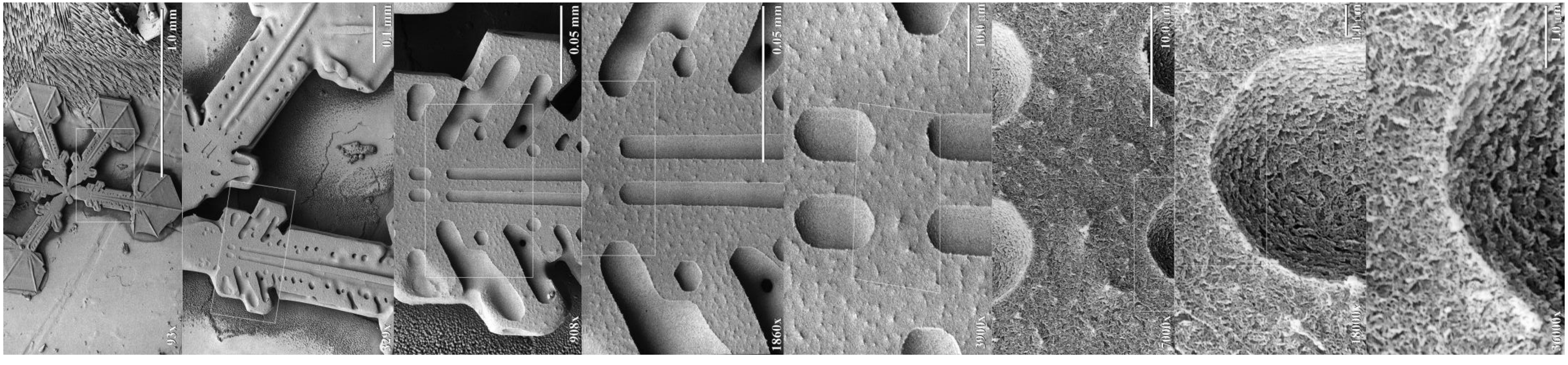

Interaction of electrons with matter

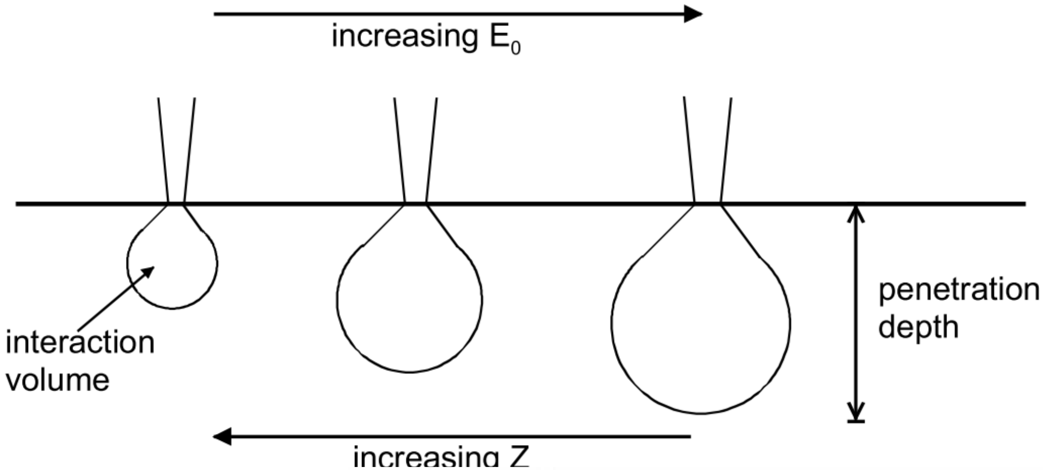

	1 keV	10 keV
C	50 nm	1000 nm
Au	10 nm	200 nm

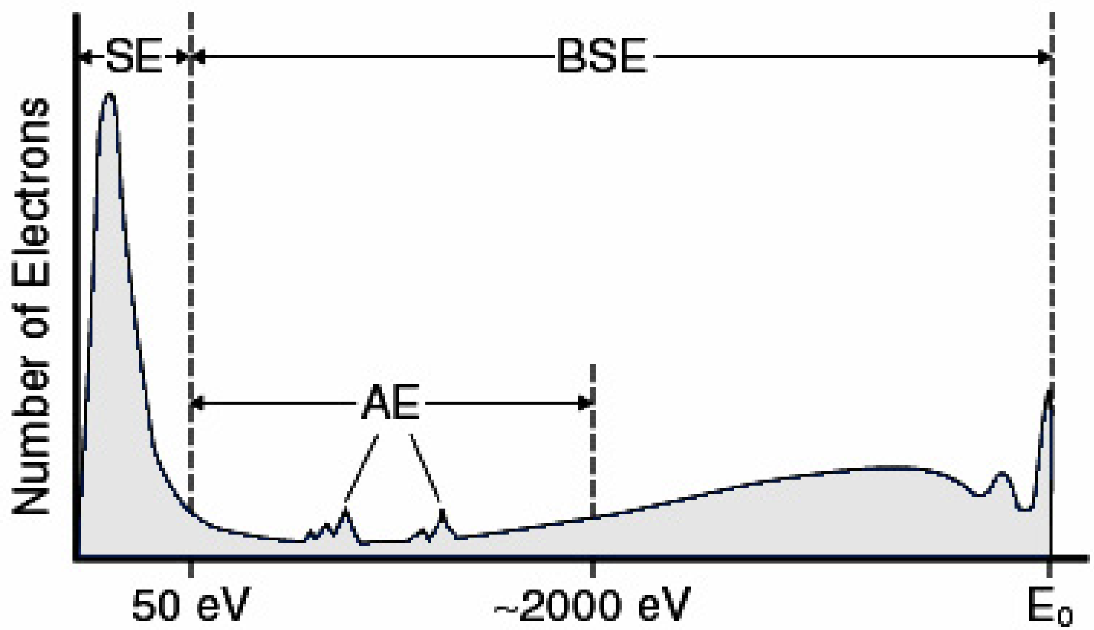

Contrast formateion by secondary e^-

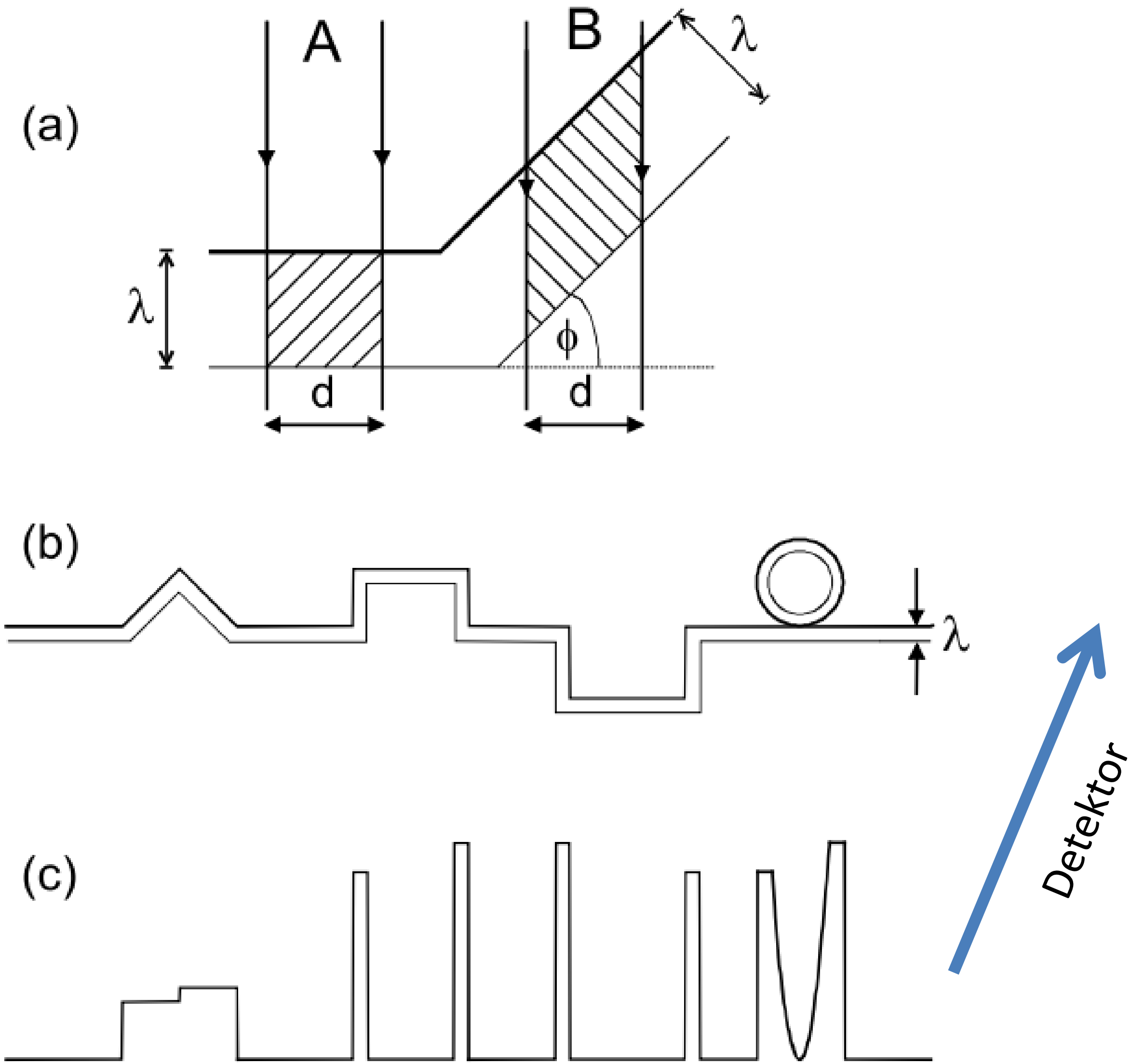

SEM of graphene on Ir(111)

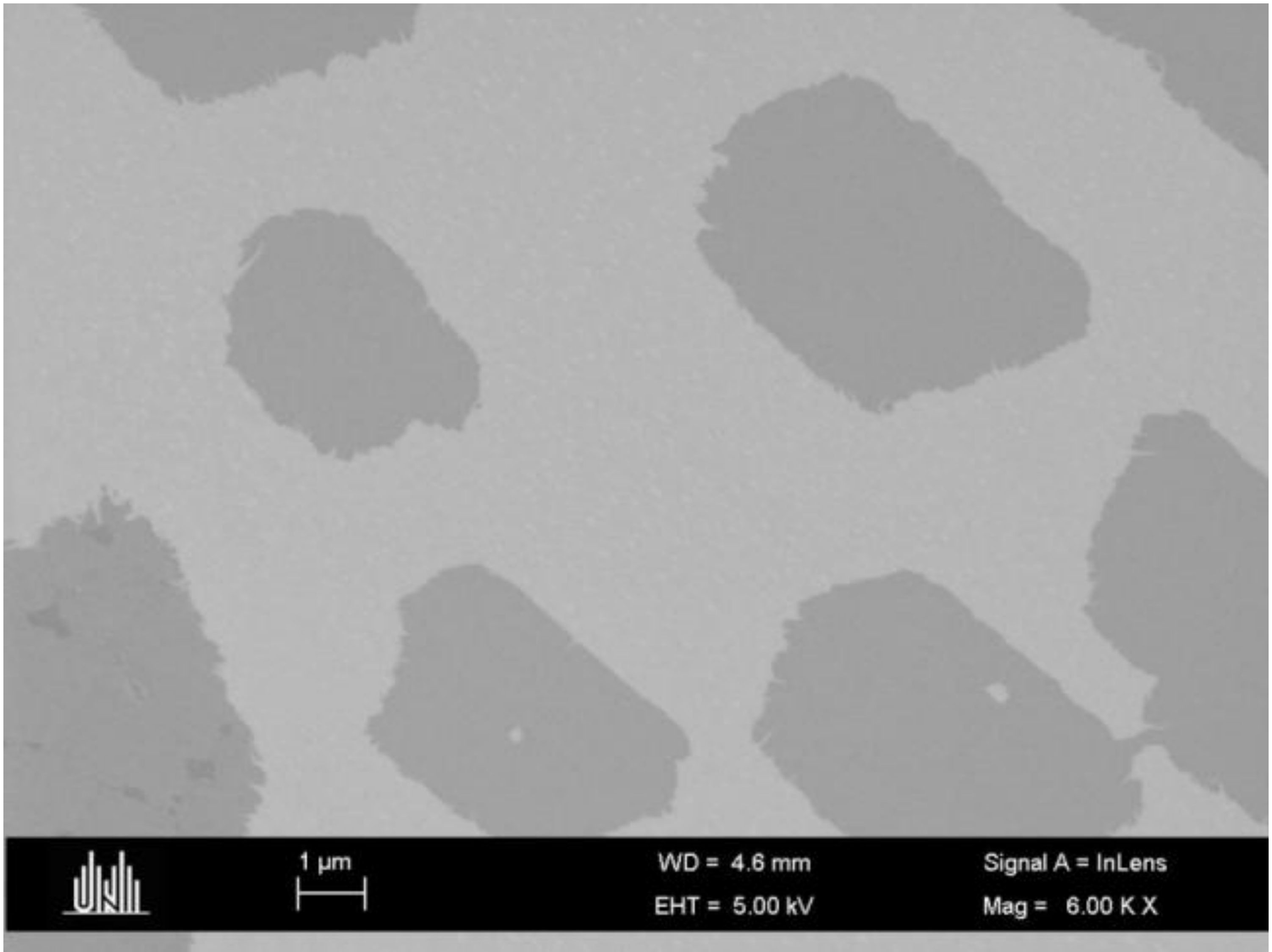

LEEM

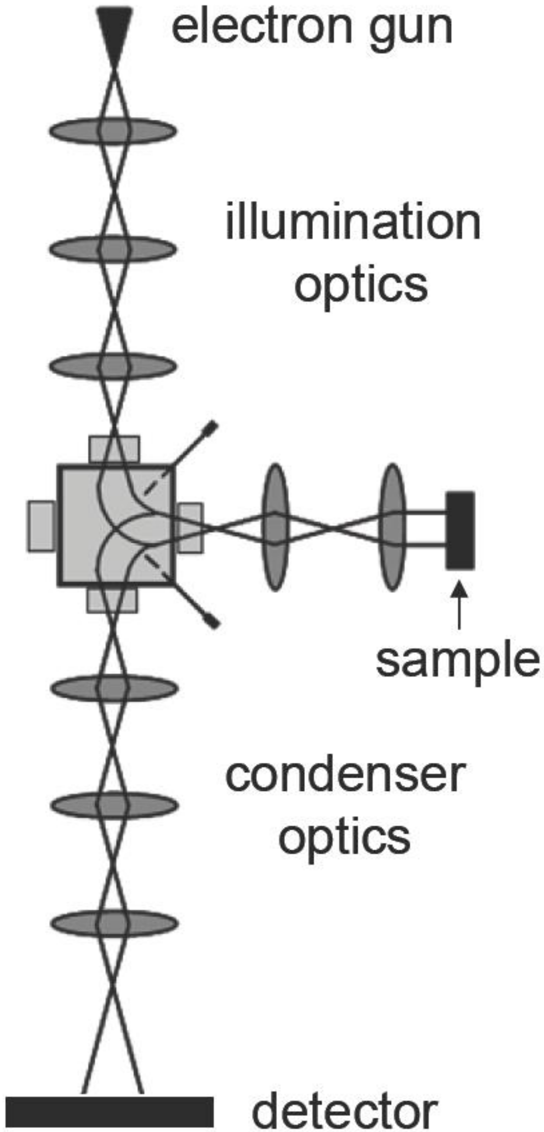

electron gun
illumination
optics
sample
condenser
optics
detector

Dark Field Imaging: Si(100) – 2x1

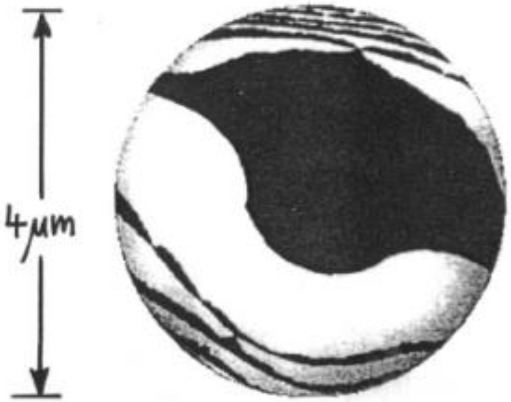

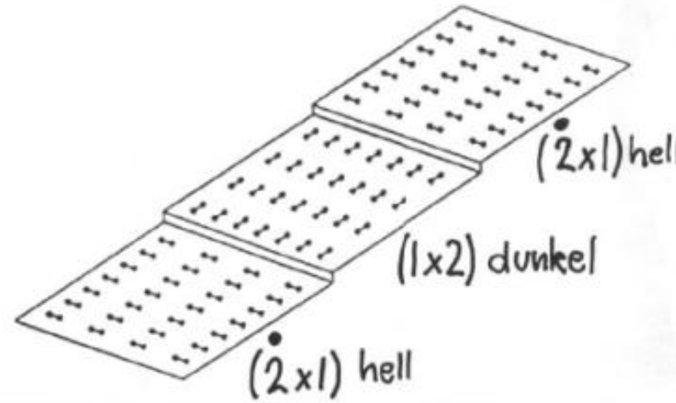

Bright Field Imaging: Pattern Formation by Pb on Cu/Pb on Cu(111)

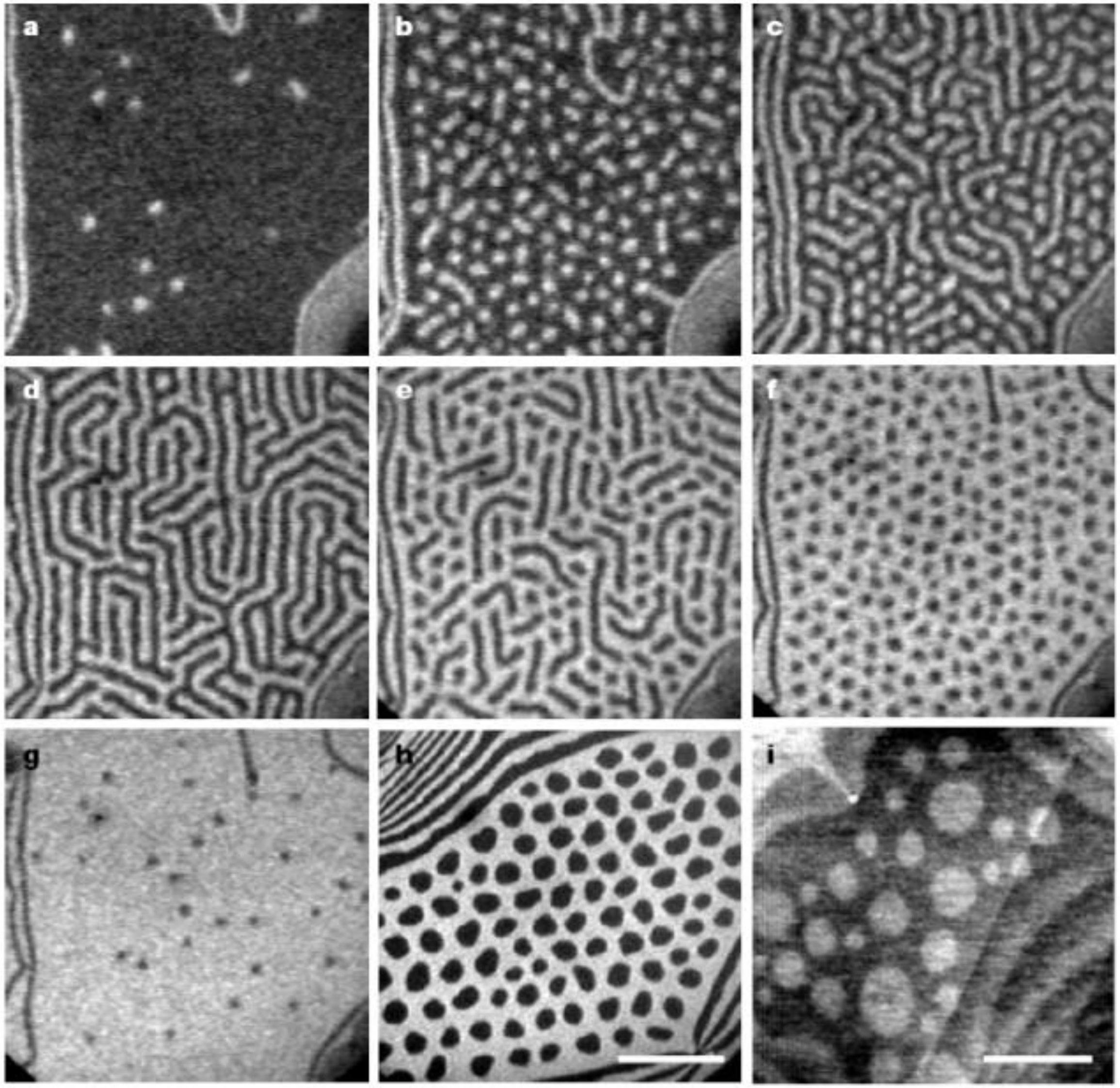

Figure 1 Self-assembly of Pb on Cu(111). Low-energy electron micrographs of the Cu(111) surface at 673 K with different area fractions of the lead-overlayer phase (bright) in the surface alloy phase (dark). **a–g,** Area fractions 0.03, 0.28, 0.35, 0.50, 0.65, 0.73 and 0.95, respectively. The domain pattern evolves from circular islands (droplets) to stripes, to vacancy islands (inverted droplets) with increasing lead coverage. **h,** Ordered droplet configuration at 623 K. Scale bar, 0.5 μm. **i,** Atomic-force micrograph of a droplet pattern after cooling down to room temperature and 2 hours of exposure to air. Scale bar, 0.3 μm.

R. Plass, J.A. Last, N.C. Bartelt, G.L. Kellogg, Nature 412 (2001) 875L

Fig. 21b

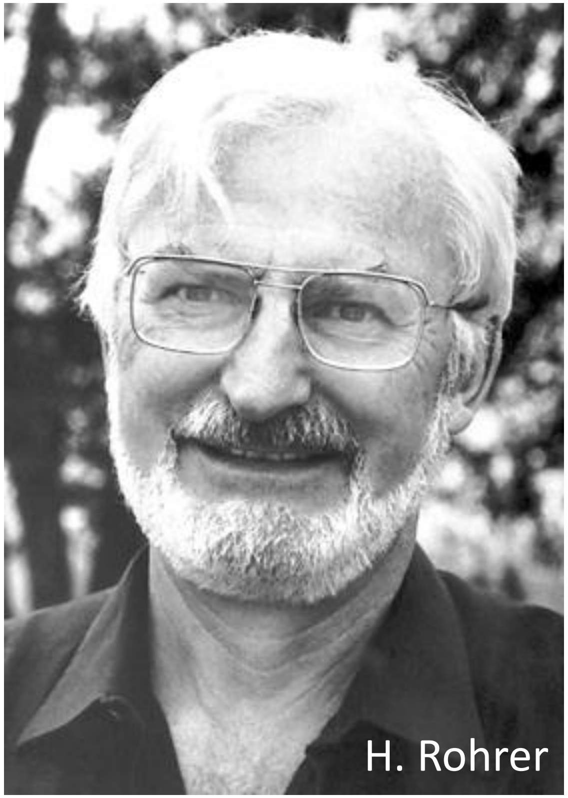

Nobel price in physics 1986 for Binnig and Rohrer (shared with Ruska) *“for their design of the scanning tunneling microscope"*.

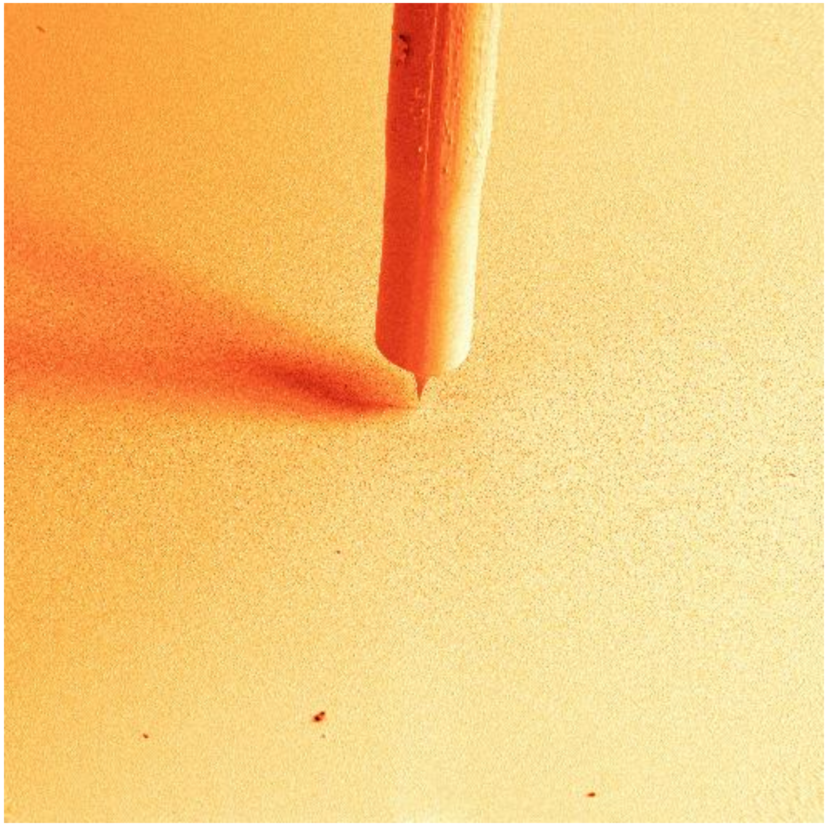

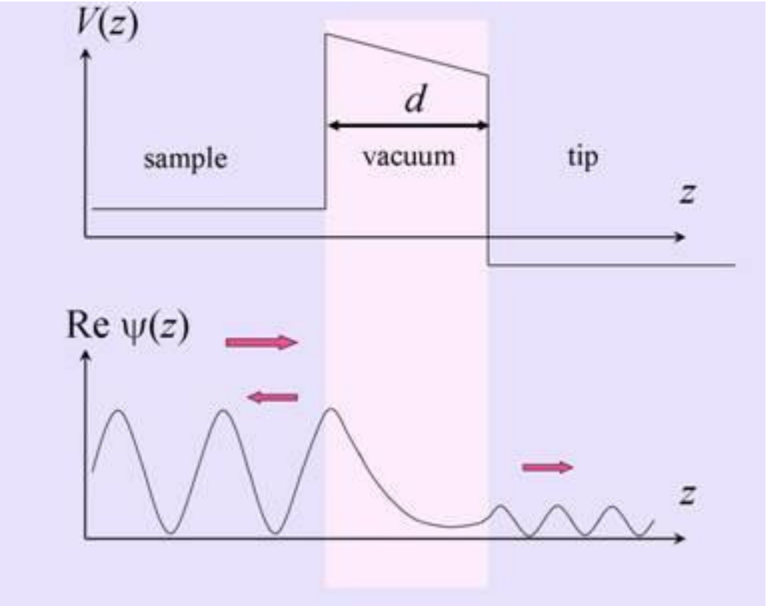

$$I \propto e^{-2\kappa d}$$

Schema zur Besetzung von Bändern

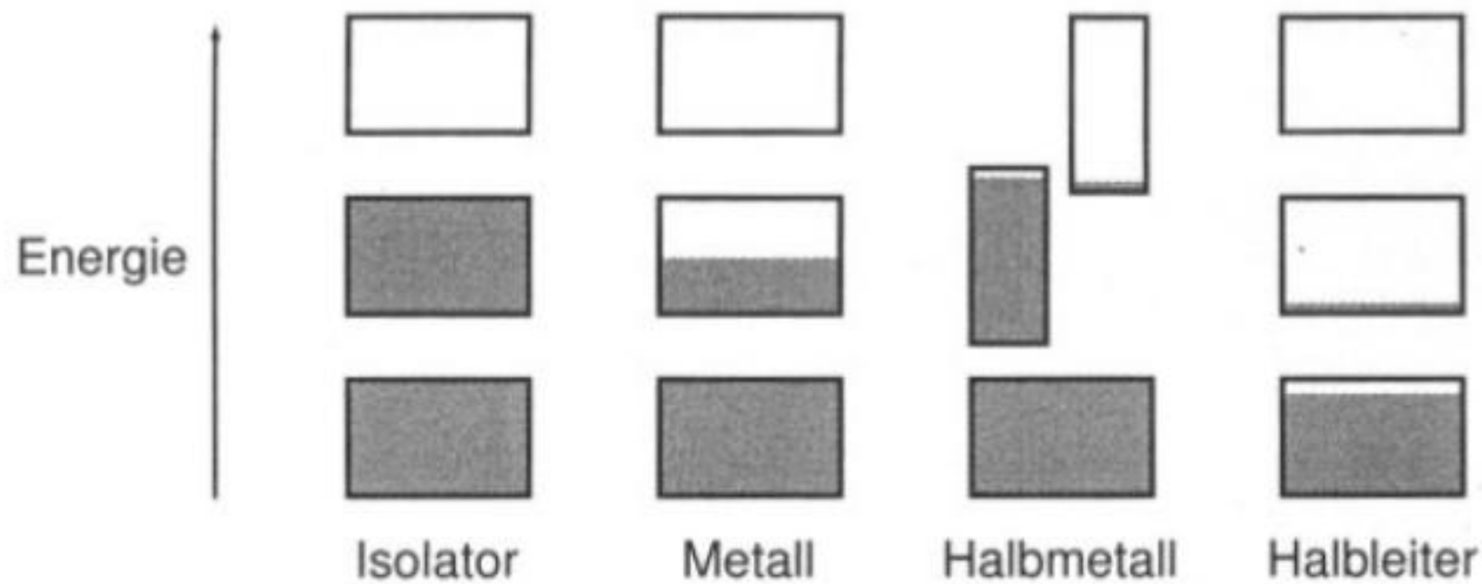

Bild 7.1: Schematische Darstellung der Besetzung erlaubter Energiebänder durch Elektronen für Isolator, Metall, Halbmetall und Halbleiter. Die Vertikalausdehnung der Rechtecke kennzeichnet die erlaubten Energiebereiche, die schattierten Flächen die mit Elektronen besetzten Bereiche.

Band structure of Aluminium

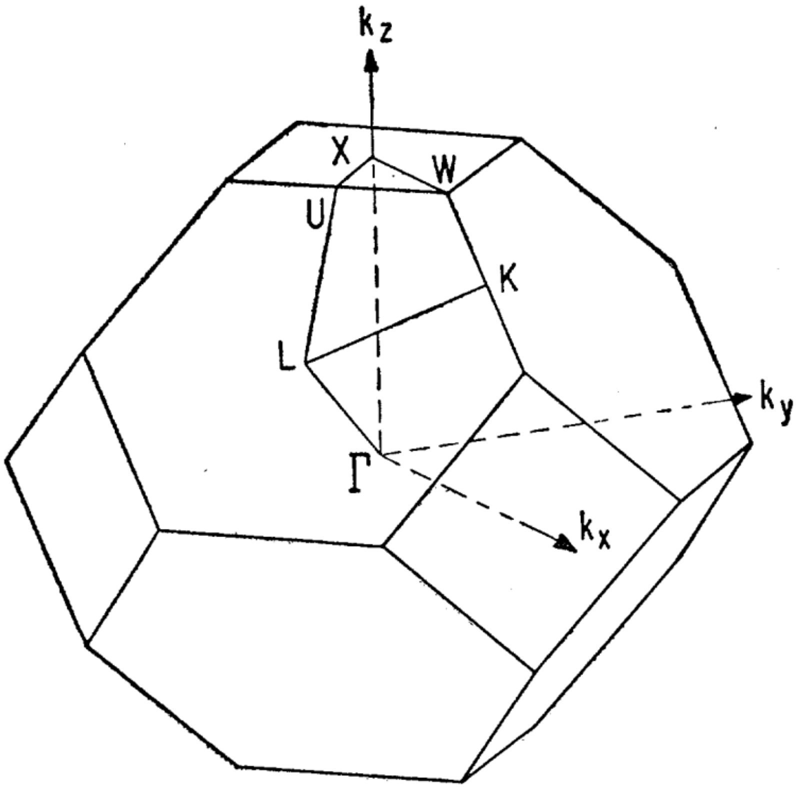

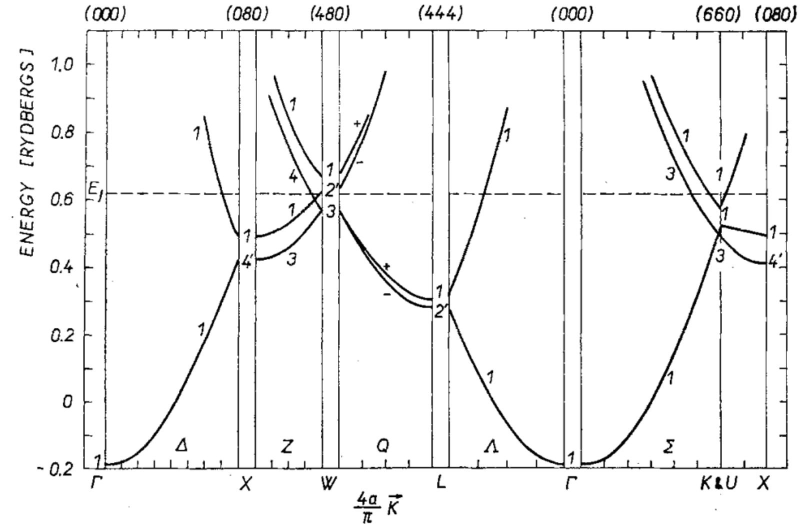

Fig. 2. Energy bands in directions of high symmetry.

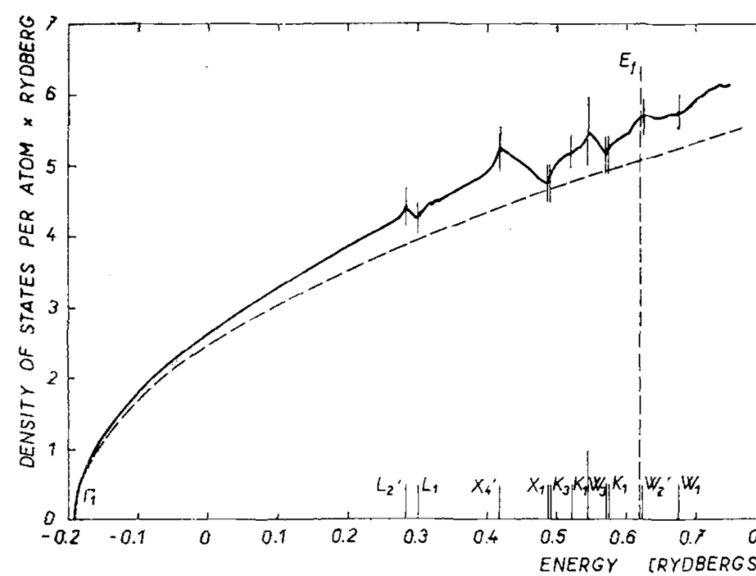

Fig. 3. The density of states. ——— present, - - - - - - - free electron approximation.

Band structure of copper

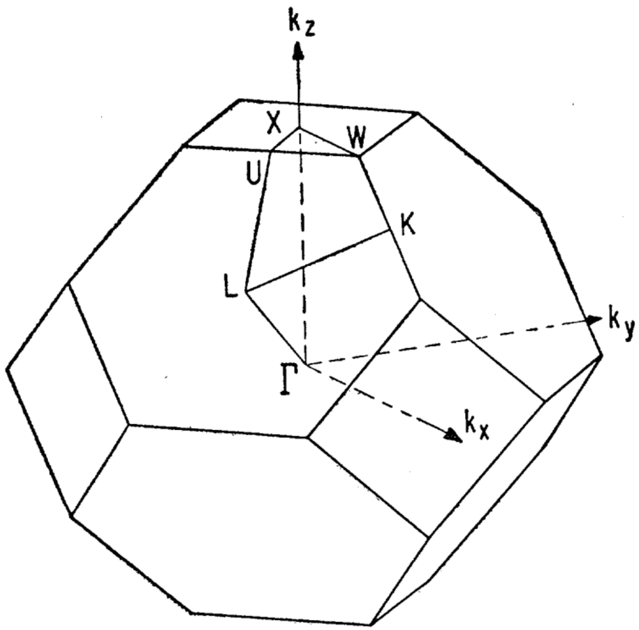

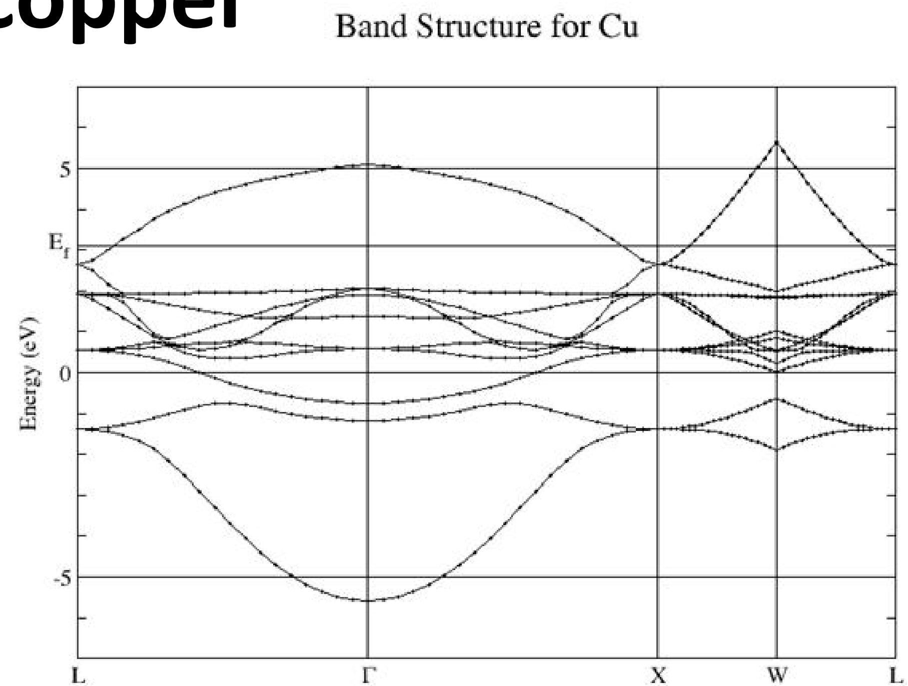

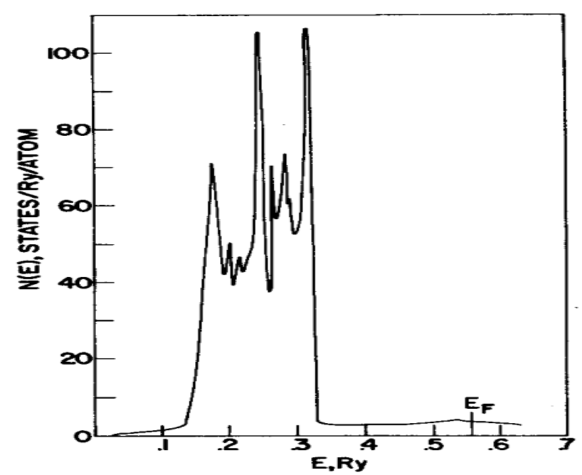

Tersoff-Haman Theory for Au(110)- 2x1 and 3x1

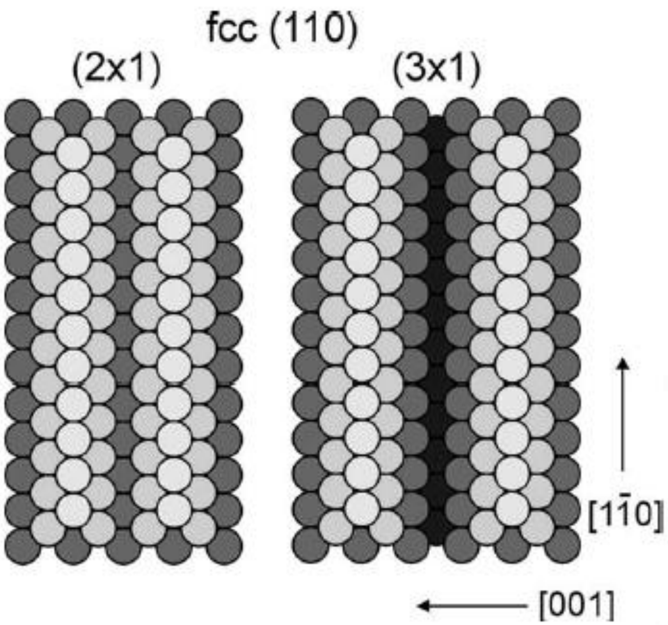

experiment: corrugation 0.45 Å (2x1) and 1.4 Å (3x1) with identical tip.

theory: R = 9Å, d= 6 Å, such that corrugation 0.45 Å for 2x1. This Implies a corrugation of 1.4 Å for the 3x1

tip model

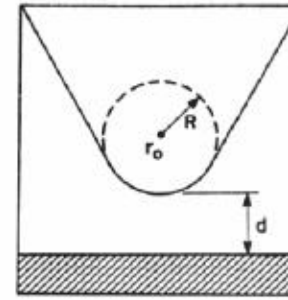

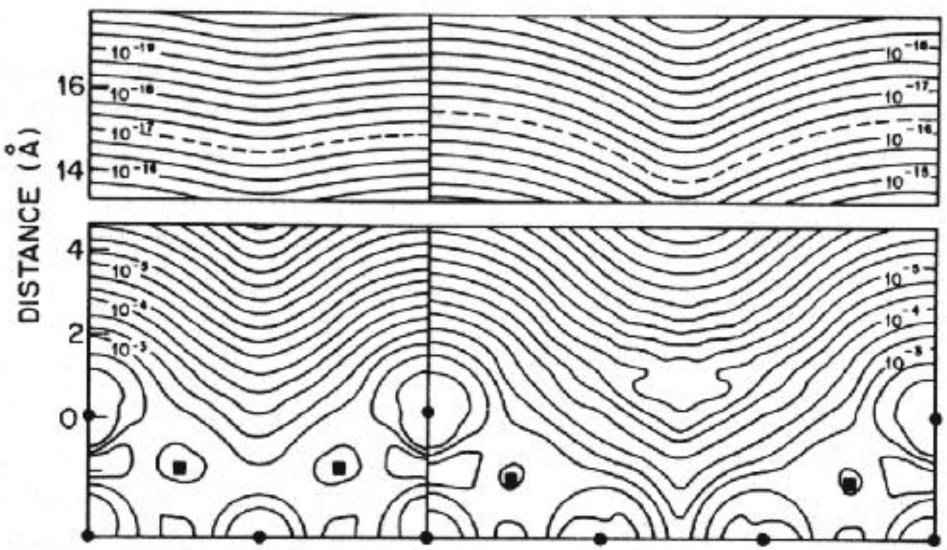

FIG. 3. Calculated $\rho(\mathbf{r}, E_F)$ for Au(110) 2×1 (left) and 3×1 (right) surfaces. This figure shows (1$\bar{1}$0) plane through outermost atoms. Positions of nuclei are indicated by circles (in plane) and squares (out of plane). Contours of constant ρ are labeled in units of a.u.$^{-3}$eV^{-1}. Note break in vertical distance scale. Assuming a 9 Å tip radius in the *s*-wave tip model, the center of curvature of the tip is calculated to follow the dashed line. (From Ref. 15.)

Fig. 25

Atomic Resolution on Dense-Packed Surfaces

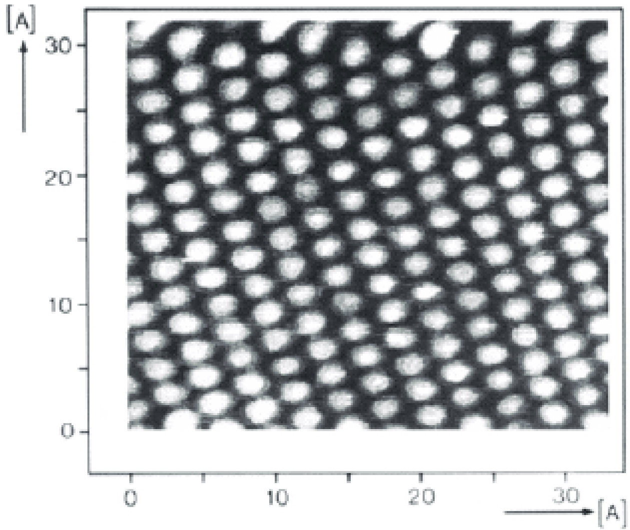

FIG. 1. Grey scale representation of an STM image of the clean Al(111) surface (34×34 Å^2, corrugation amplitude 0.3 Å, $V_t = -50$ mV, $I_t = 6$ nA).

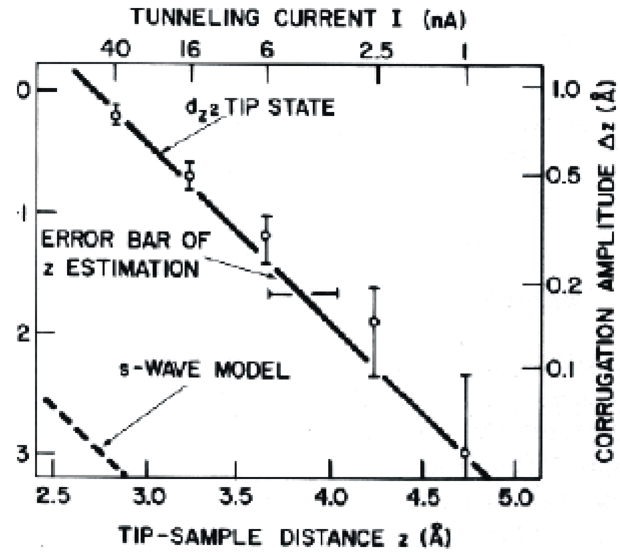

Fig. 7.10. Interpretation of the STM corrugation observed on Al(111). The predicted corrugation amplitude with a d_{z^2} tip state, solid curve, agrees well with the experimental data from Wintterlin et al. (1989), circles with error bars. The parameters of the theoretical curve are taken from a first-principle calculation of Al(111) surface, Wang et al. (1981). The tip-sample distance is defined as the distance from the plane of the top-layer nuclei of the sample to the center of the apex atom of the tip [7.24]

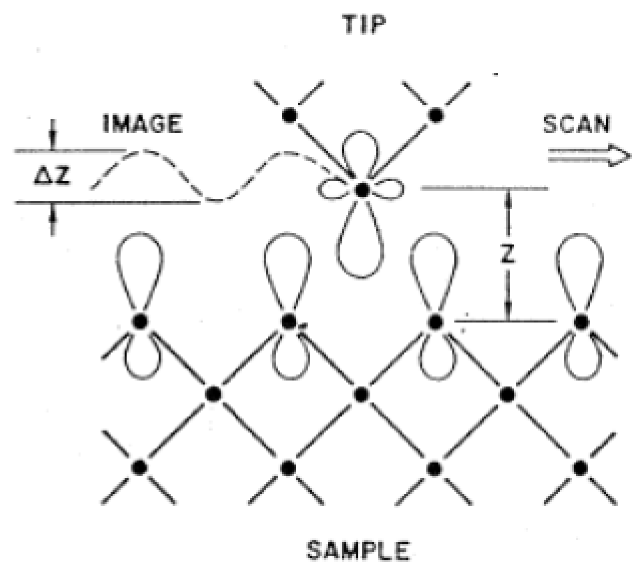

Fig. 26

Piezo-Effekt

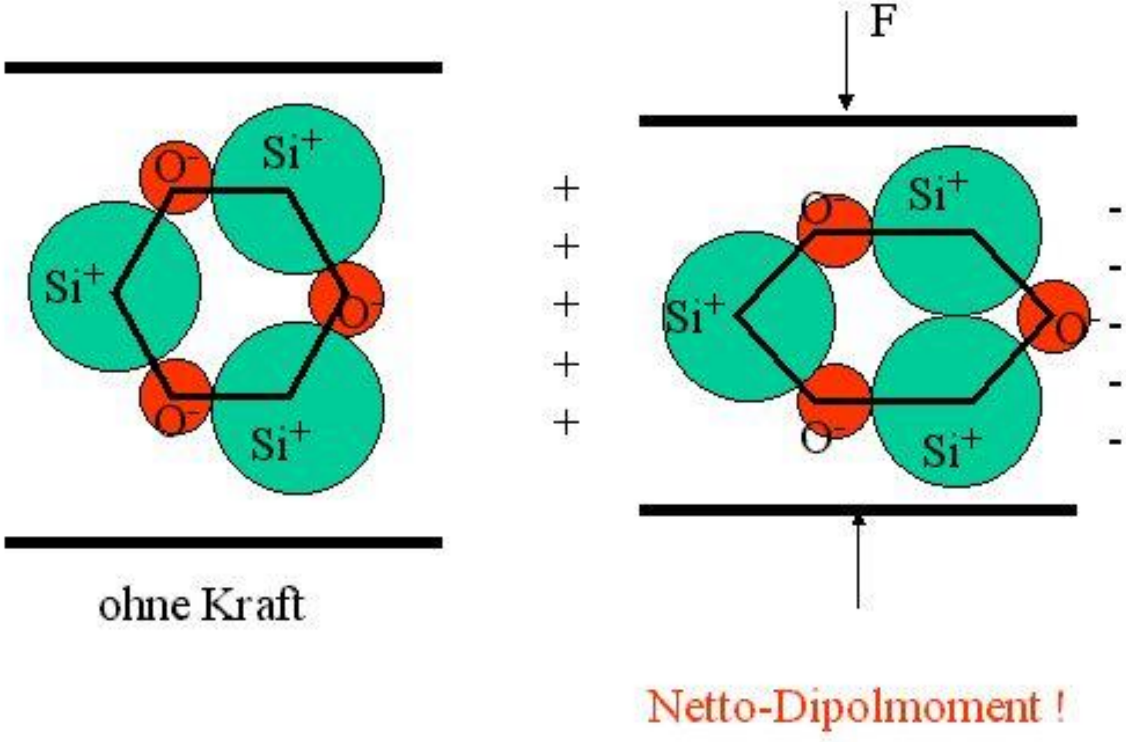

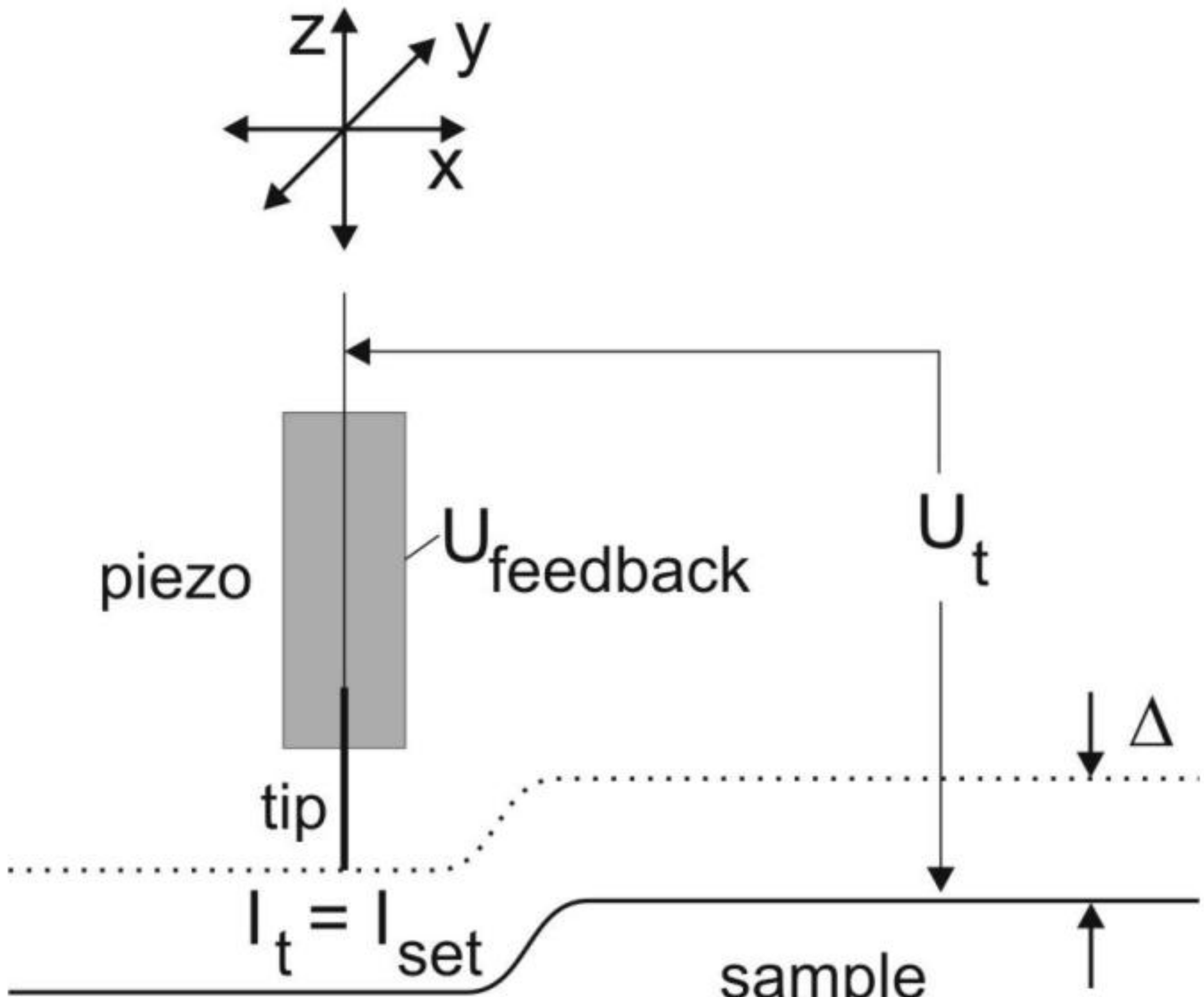
z
y
x
piezo
$U_{feedback}$
U_t
Δ
tip
$I_t = I_{set}$
sample

Beetle STM

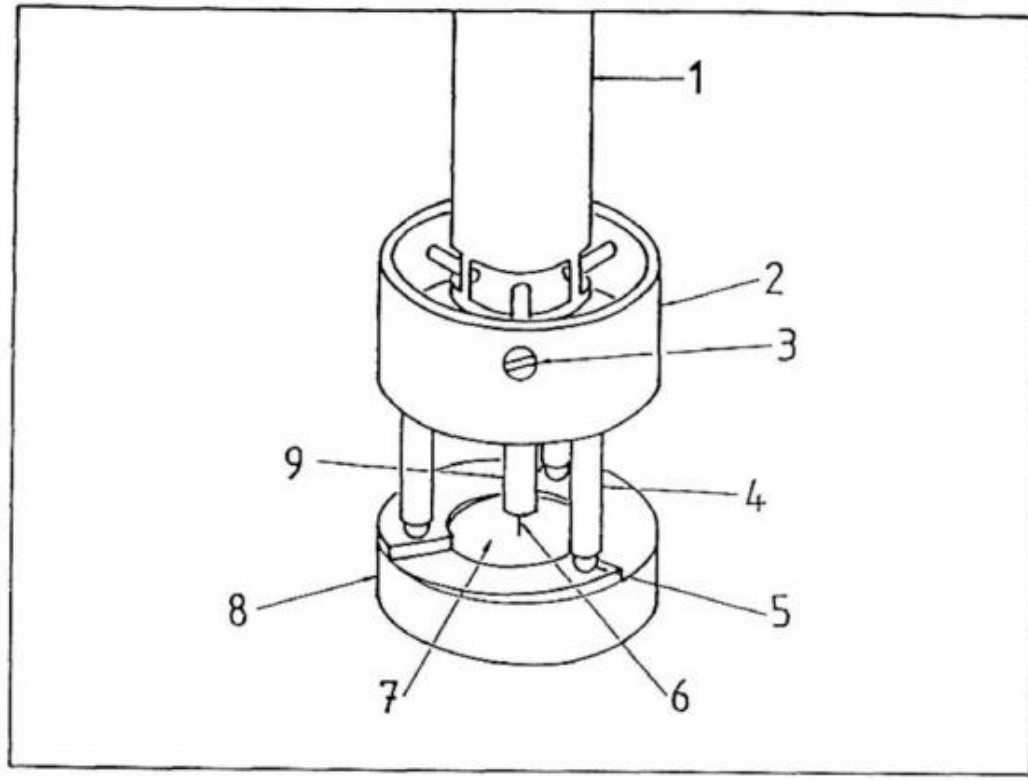

Rastertunnelmikroskop: Perspektivische Ansicht des entwickelten Rastertunnelmikroskops. 1 Halterohr, 2 Mikroskopkörper, 3 Halteschraube, 4 Rasterbein, 5 Stahlkugel, 6 Spitze, 7 Probe, 8 Rampenprobenhalter, 9 Z-Piezo.

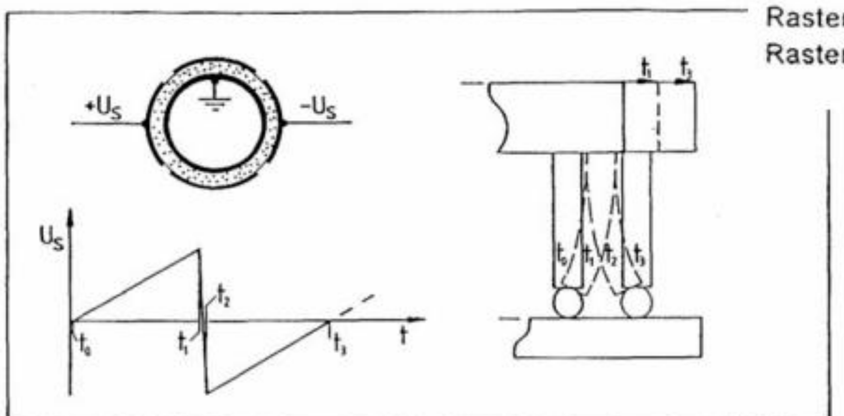

Mikroskopbewegung: Durch Anlegen eines Sägezahnimpulses U_s an zwei gegenüberliegende Elektrodenflächen bewegt sich das Mikroskop wie rechts gezeigt einen "Schritt".

Si(111) – 7x7 Rekonstruktion

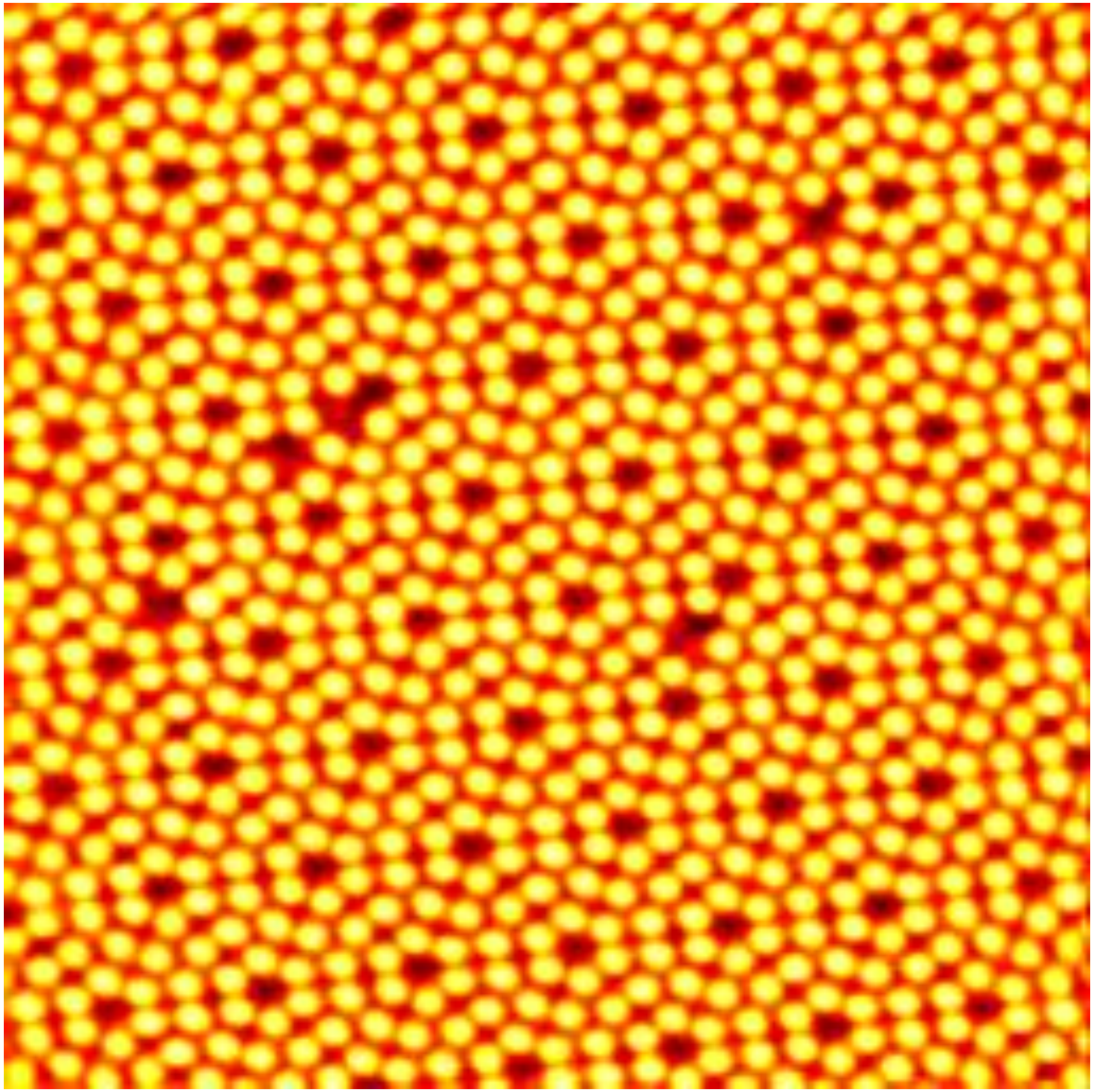

Rekonstruktion von Halbleiteroberflächen: Si(111) – (7x7)

Si(111)-(7×7):

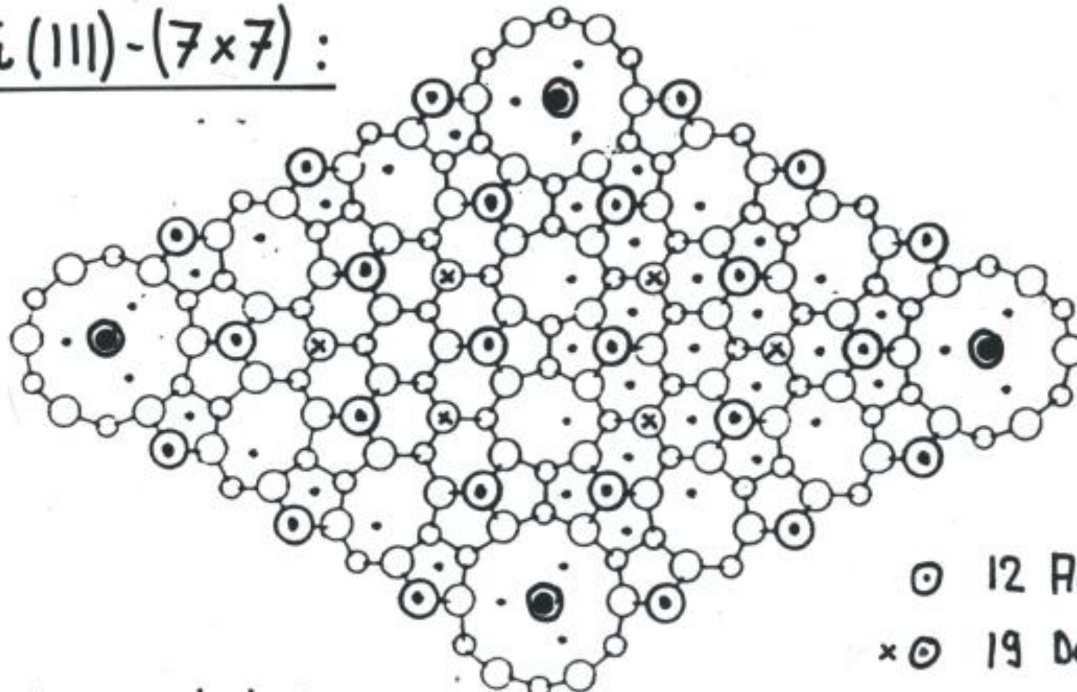

K. Takayanagi et al.
J. Vac. Sci. Tech. A3 (1985) 1502

⊙ 12 Adatome

×⊙ 19 Dangling Bonds (DB)

◉ 1 Corner Hole

Chemischer Kontrast für PtRh-Legierung ((111)-Oberfläche))

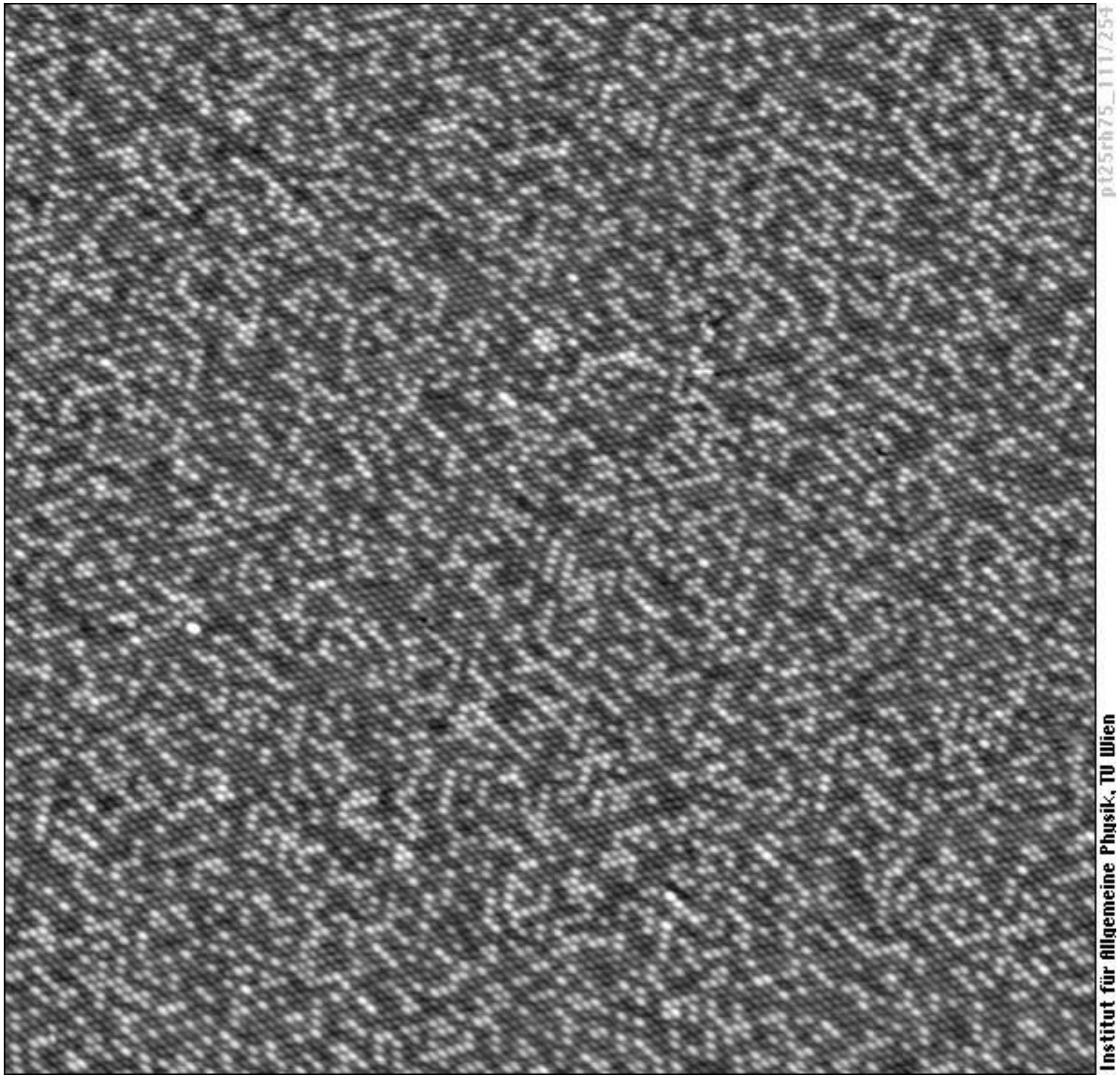

Spitzenherstellung

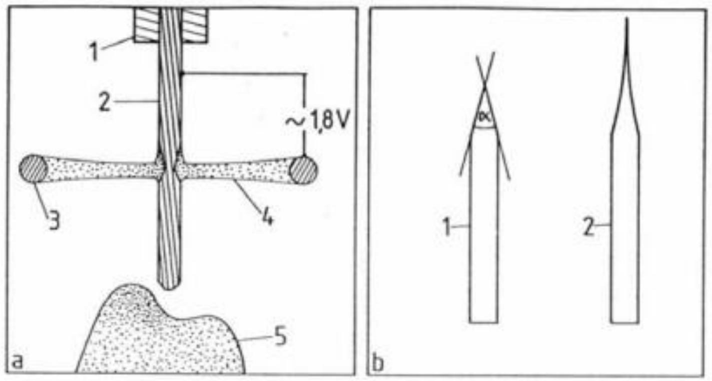

Ätzverfahren und Spitzenform: Abbildung a zeigt den schematischen Aufbau der Ätzanordnung. 1 Drahthalterung, 2 Wolframdraht, 3 Platindrahtschlaufe, 4 Elektrolyt, 5 Schaum. Abbildung b zeigt links eine günstige und rechts eine weniger günstige Spitzenform.

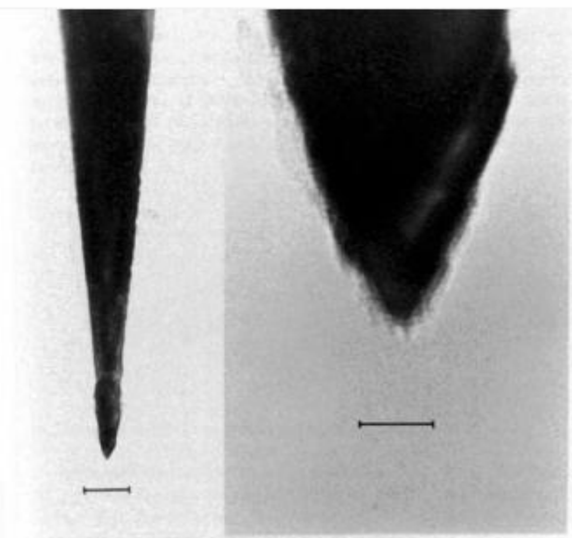

Abbildung 15: TEM-Aufnahmen einer typischen STM-Spitze. Die Markierungen entsprechen links 100 nm und rechts 10 nm.

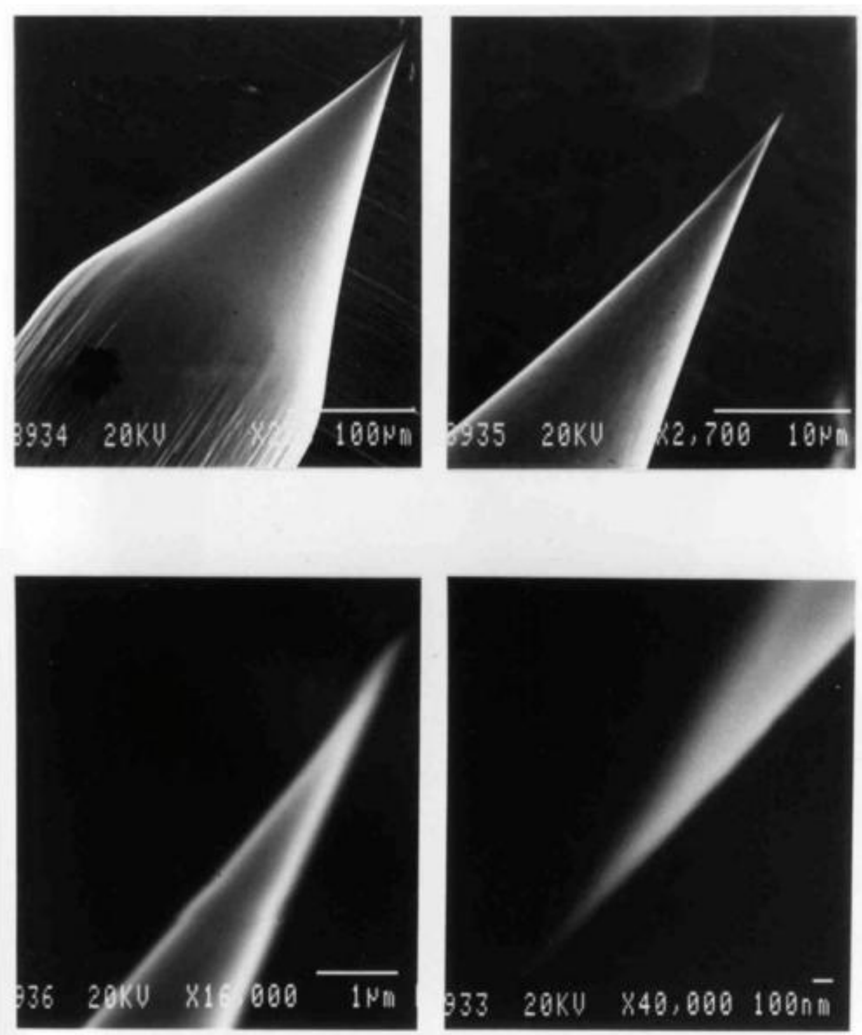

Abbildung 14: SEM-Aufnahmen einer typischen STM-Spitze mit zunehmender Vergrößerung. Strukturen unterhalb von 100 nm sind offensichtlich nicht mehr aufzulösen. (Rechts unten ist die Spitze um 180° gedreht.)

Faltung von Spitzenform und Topographie: In Situ Spitzenformung

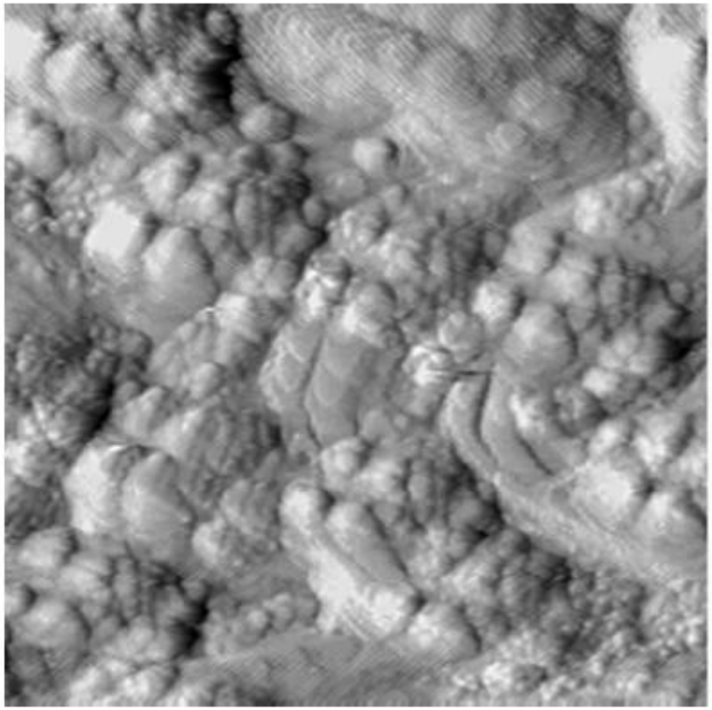

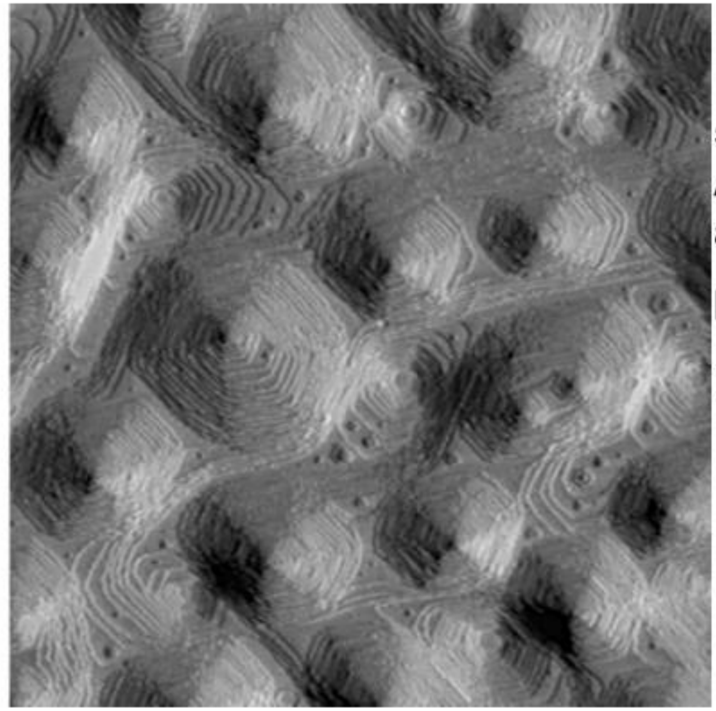

50 ML durch 600 eV Ar Ionenbeschuss abgetragen

bei 625 K

Rasterweite 1650Å

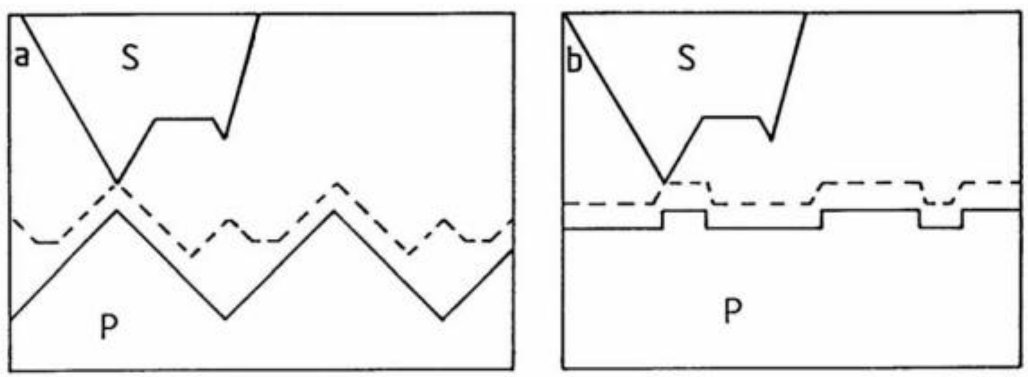

Abb. 20. Abbildungseigenschaften und Probenrauhigkeit: Gestrichelt eingetragen ist der Weg des äußersten Endes der Spitze, der maßgebend für die gemessene Morphologie ist. (a) rauhe Probe, (b) relativ glatte Probe

Faltung von Spitzenform und Topographie: Tip Switch

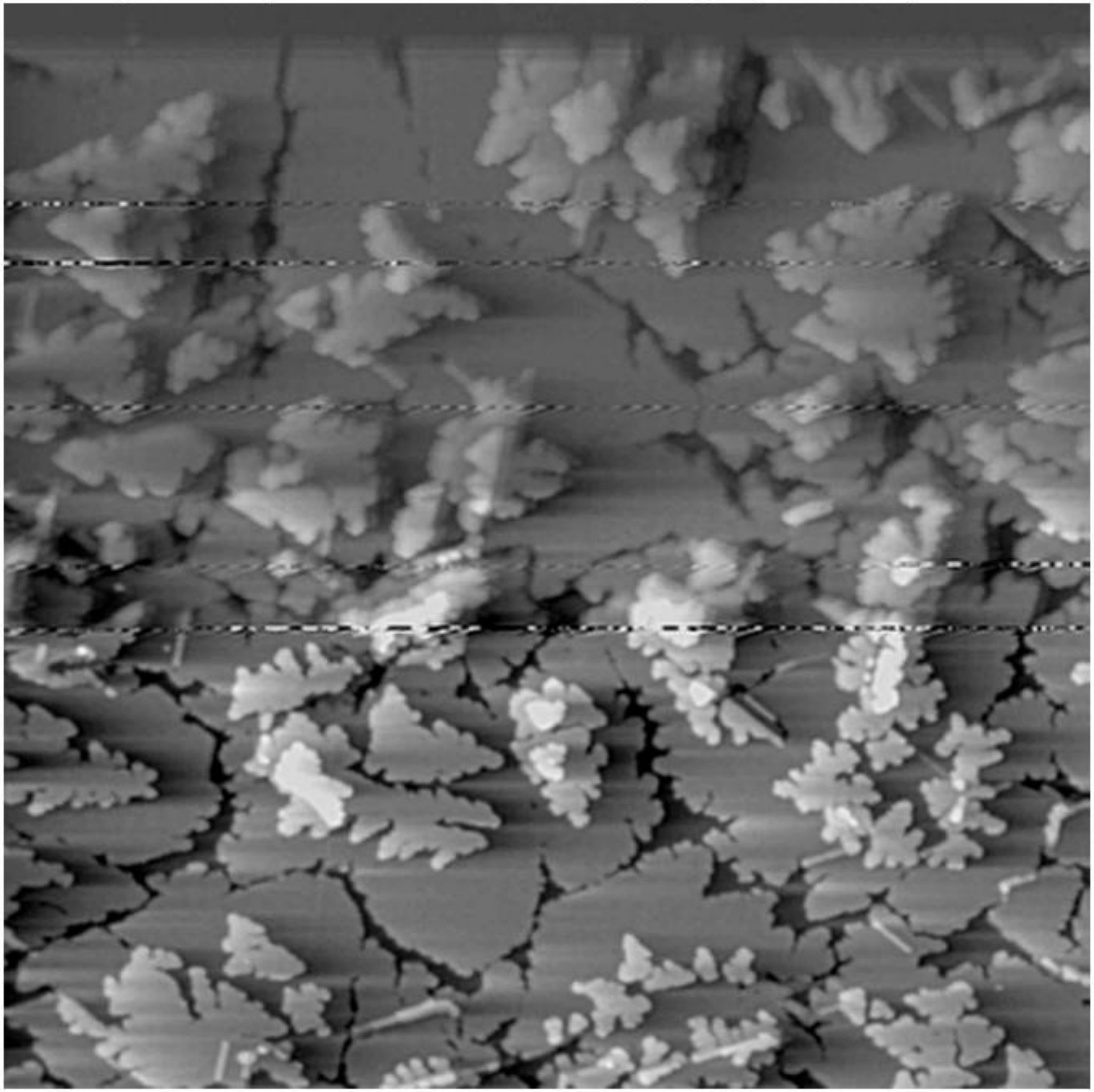

STM Theorie

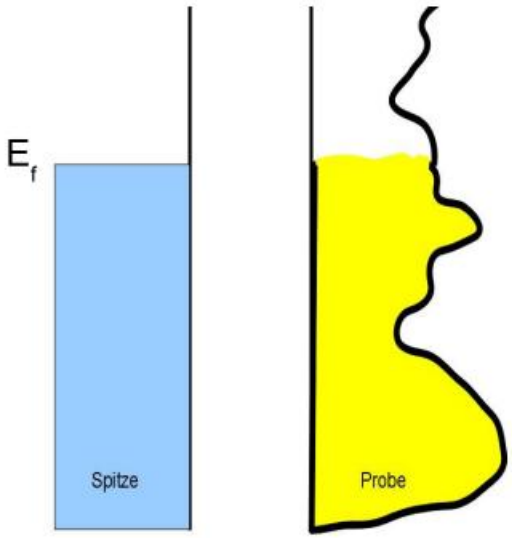

T=0, U=0

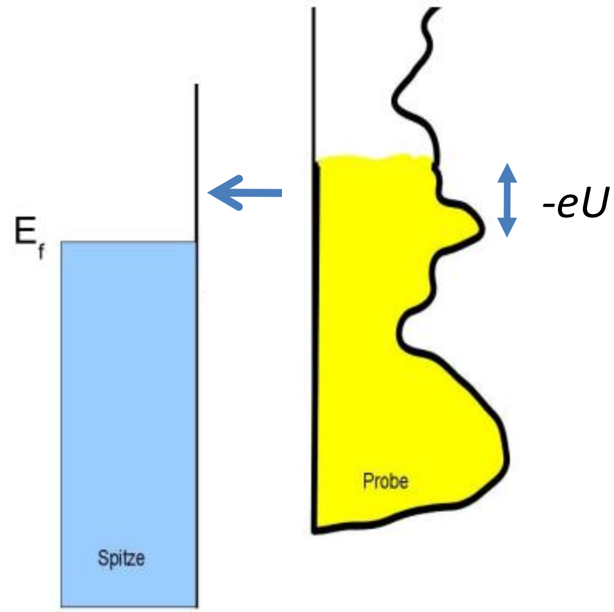

T=0, U_1>0

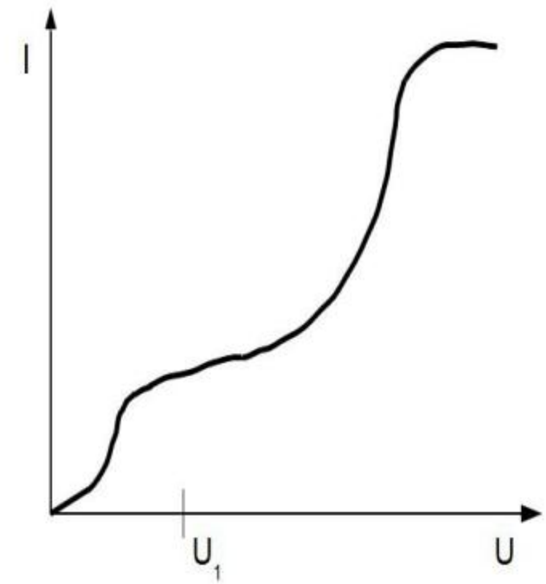

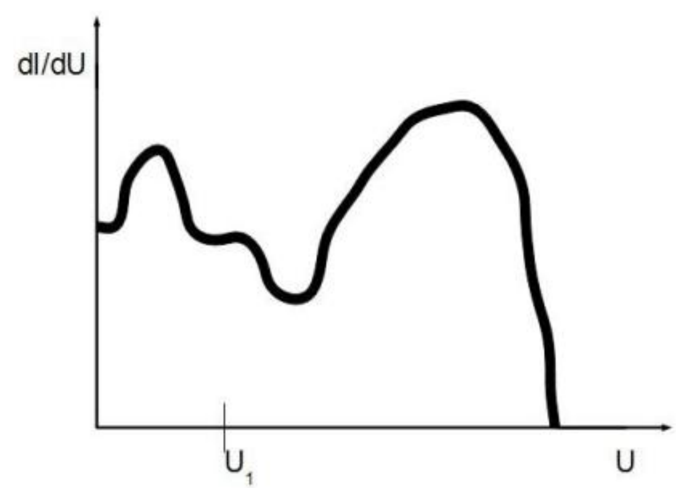

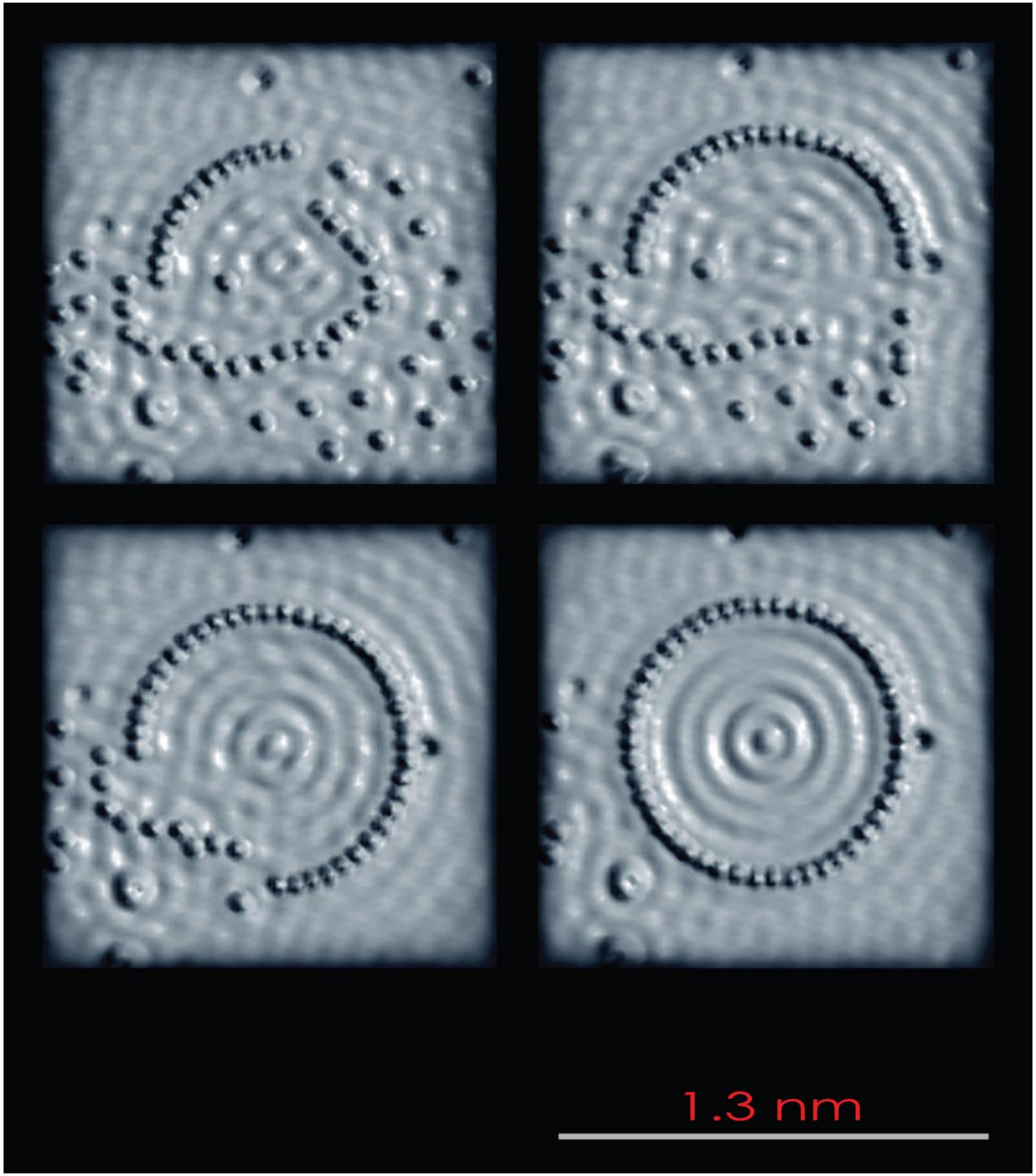
1.3 nm

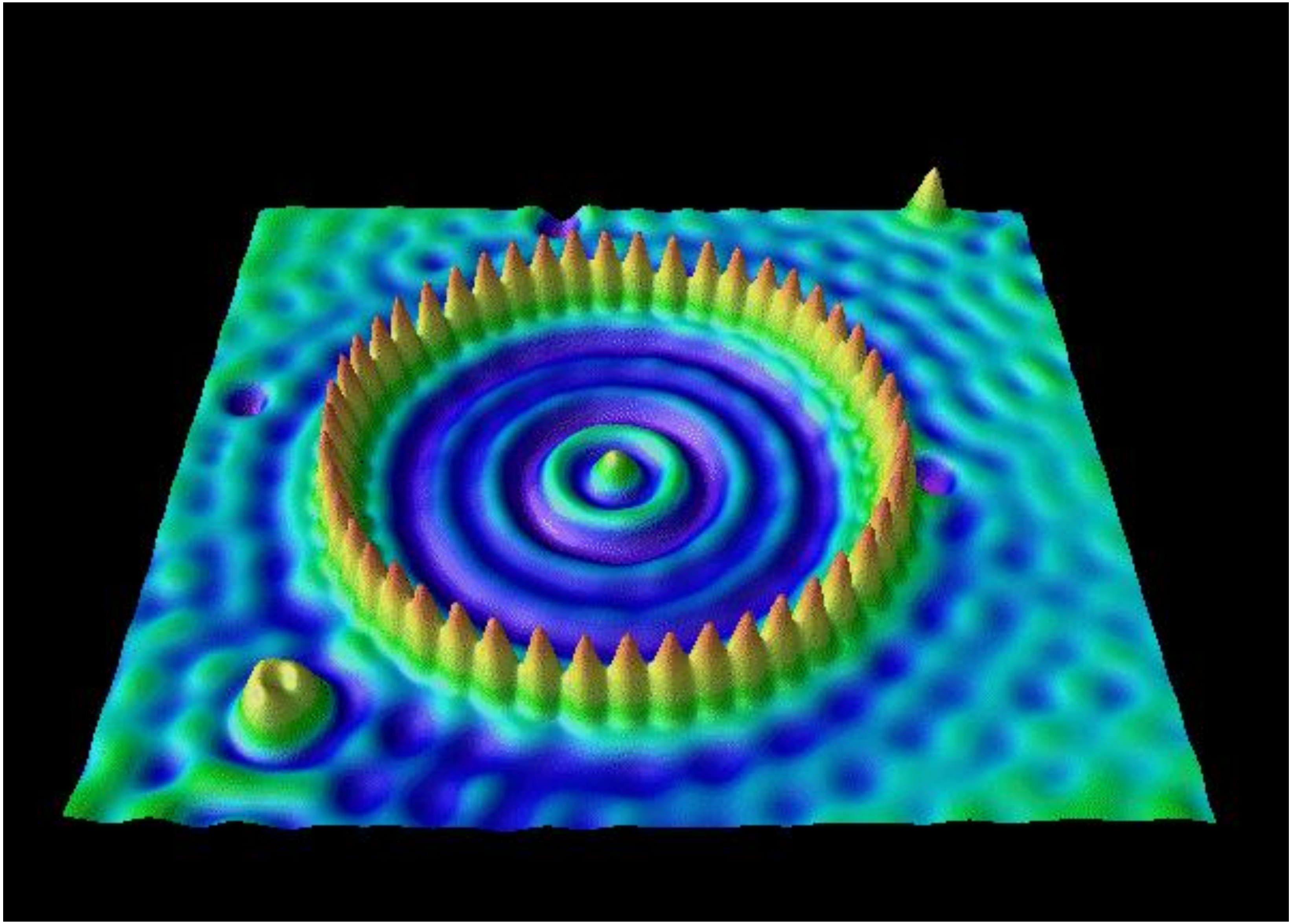

„Quantum Corral", Fe/Cu(111) (Crommie, Lutz, Eigler 1993), image width 1.3 nm

Quantenkäfig

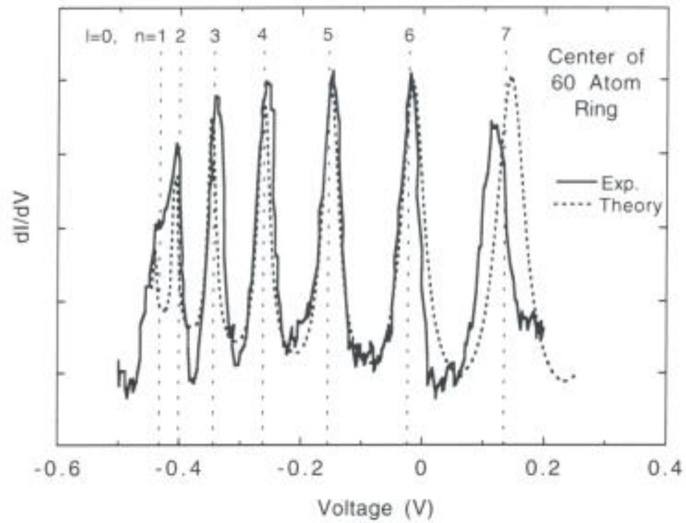

Fig. 9. Solid curve: dI/dV spectrum taken with the STM tip held stationary over the center of the 60 atom Fe ring. The experimental curve has had a smooth background removed. Broken curve: results of multiple-scattering calculation performed in the "black dot" limit (the offset and normalization of the theoretical curve are treated here as free parameters). Vertical lines: theoretical eigenenergies for $l = 0$ states of a round, 2D hard-wall box having the same dimensions as the 60 atom Fe ring.

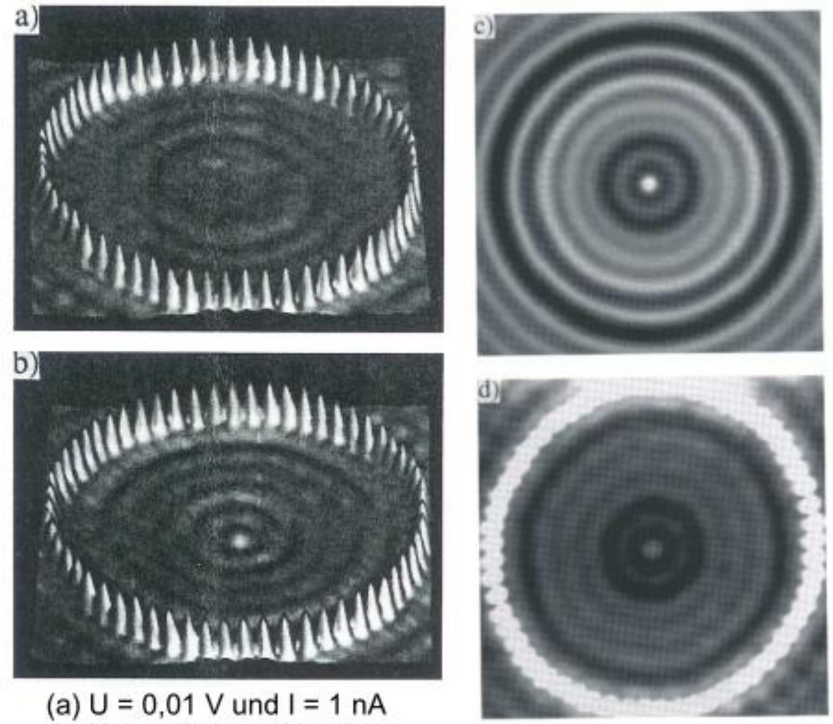

(a) U = 0,01 V und I = 1 nA
(b) U = -0,01 V und I = 1 nA

Aus: Crommie et al., Physica D 83 (1995) 98

Applet for confinement in circular well:

http://www.st-
andrews.ac.uk/~qmanim/animations_2/2D_Circular_Well_V2.
swf

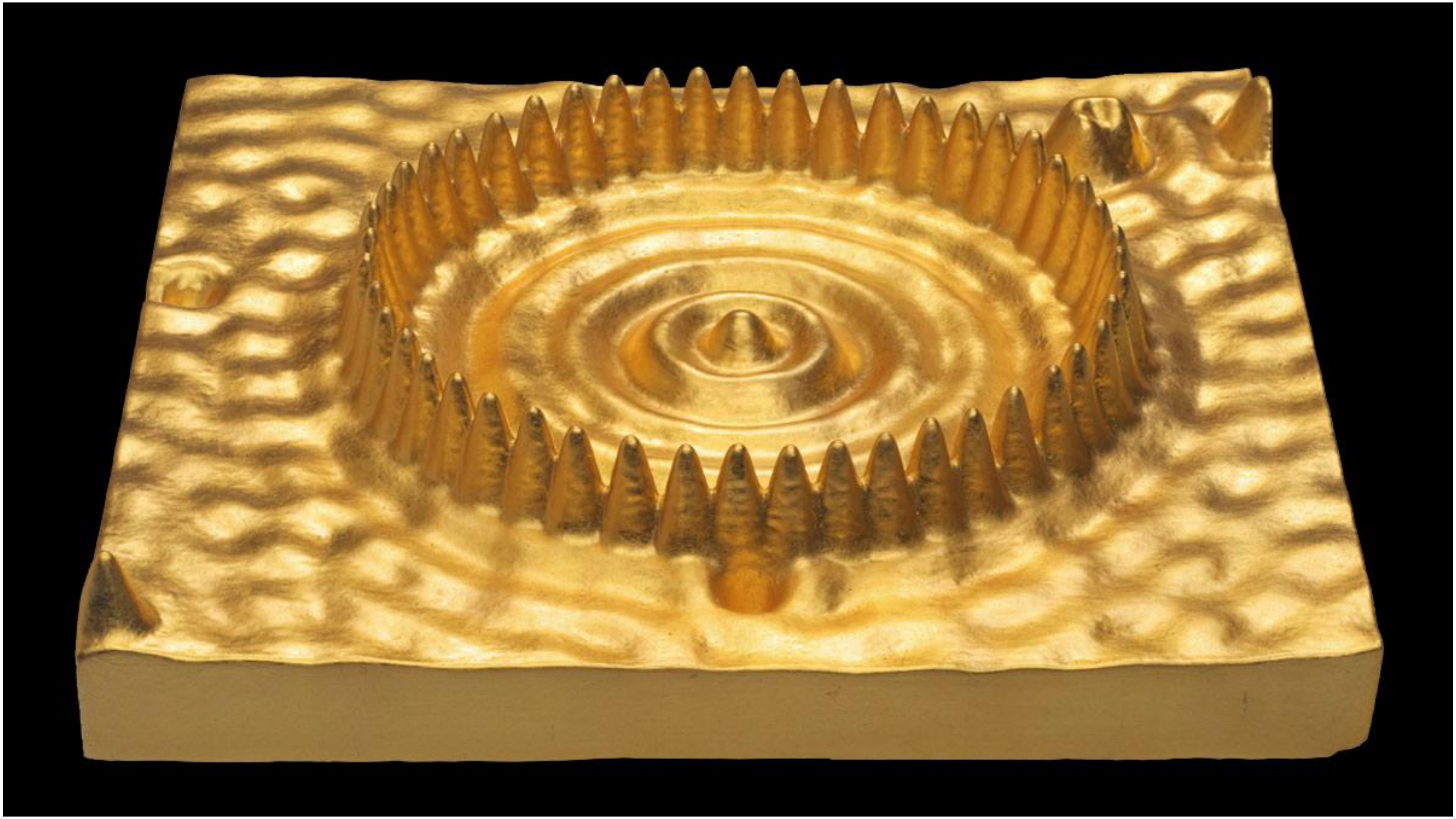

The Well (Quantum Corral) (2009) by Julian Voss-Andreae.

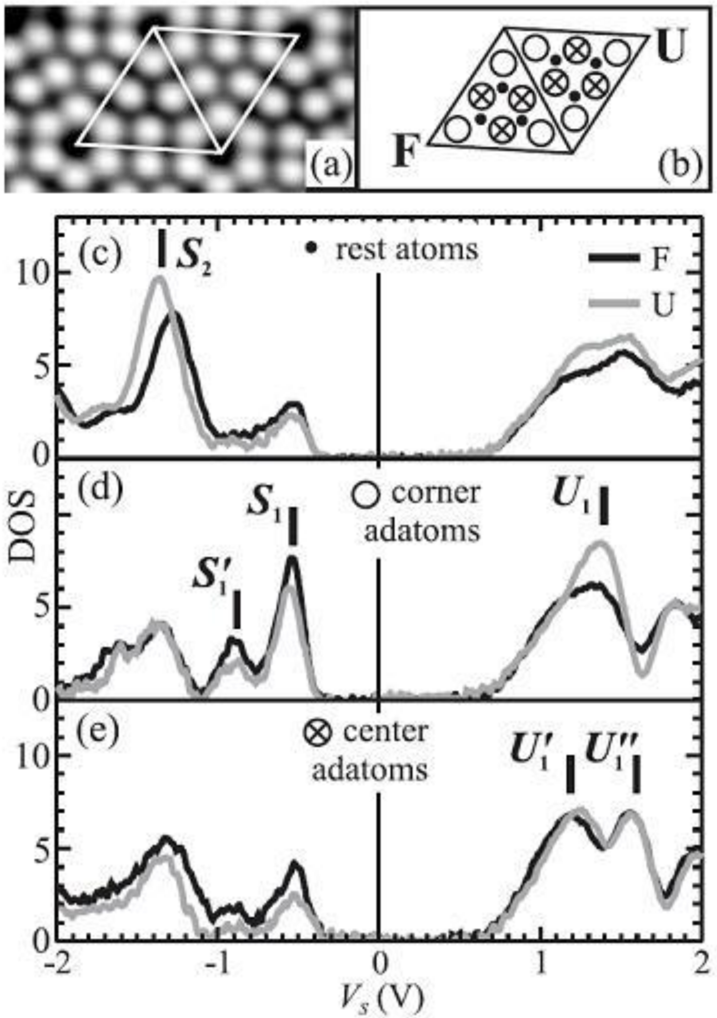
(a)
(b)
F
U
(c)
S_2
• rest atoms
F
U
(d)
S_1
S_1'
○ corner adatoms
U_1
(e)
⊗ center adatoms
U_1'
U_1''
DOS
V_s (V)
-2
-1
0
1
2
0
5
10

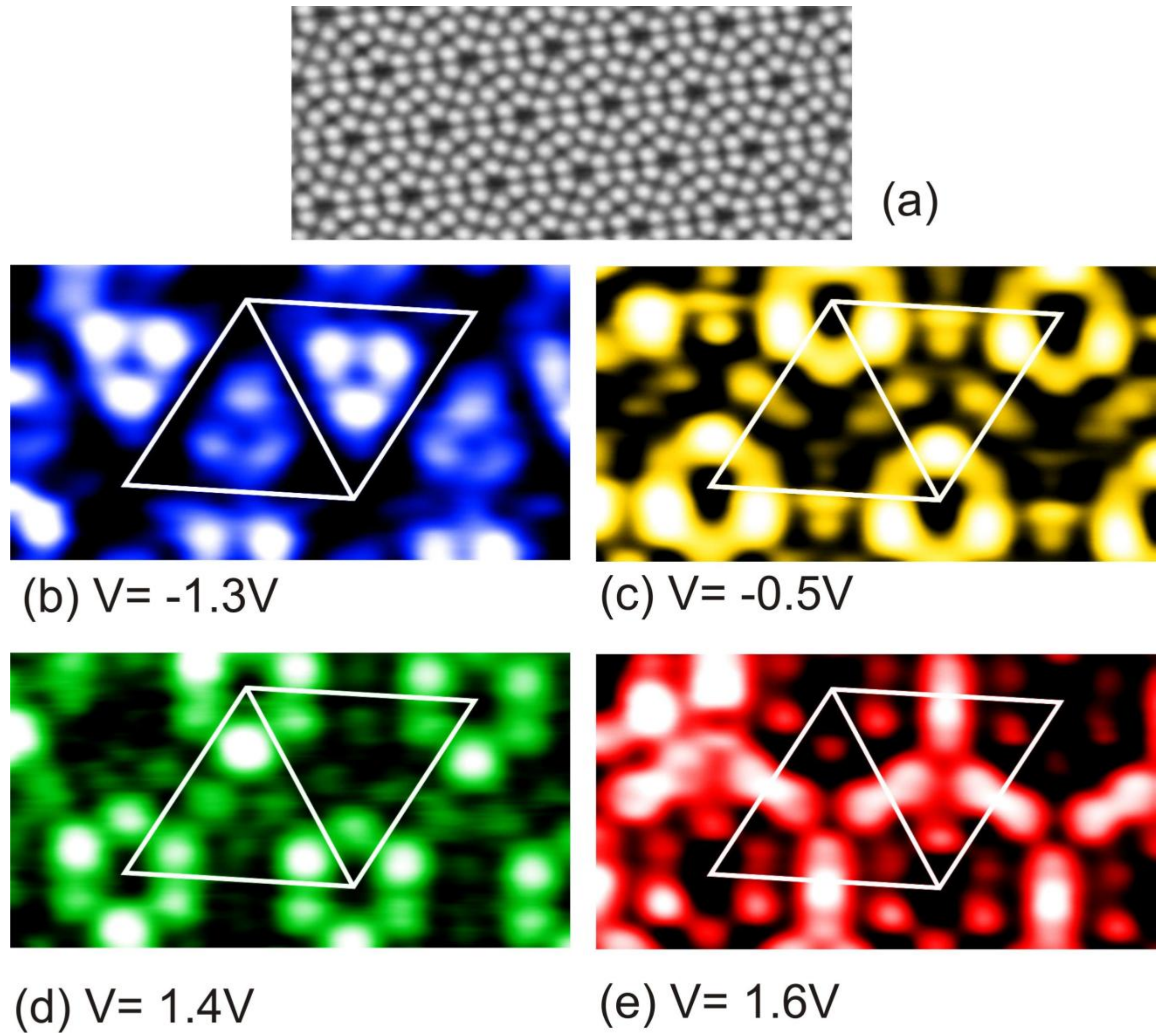
(a)
(b) V= -1.3V
(c) V= -0.5V
(d) V= 1.4V
(e) V= 1.6V

Spin-Polarized STM - Principle

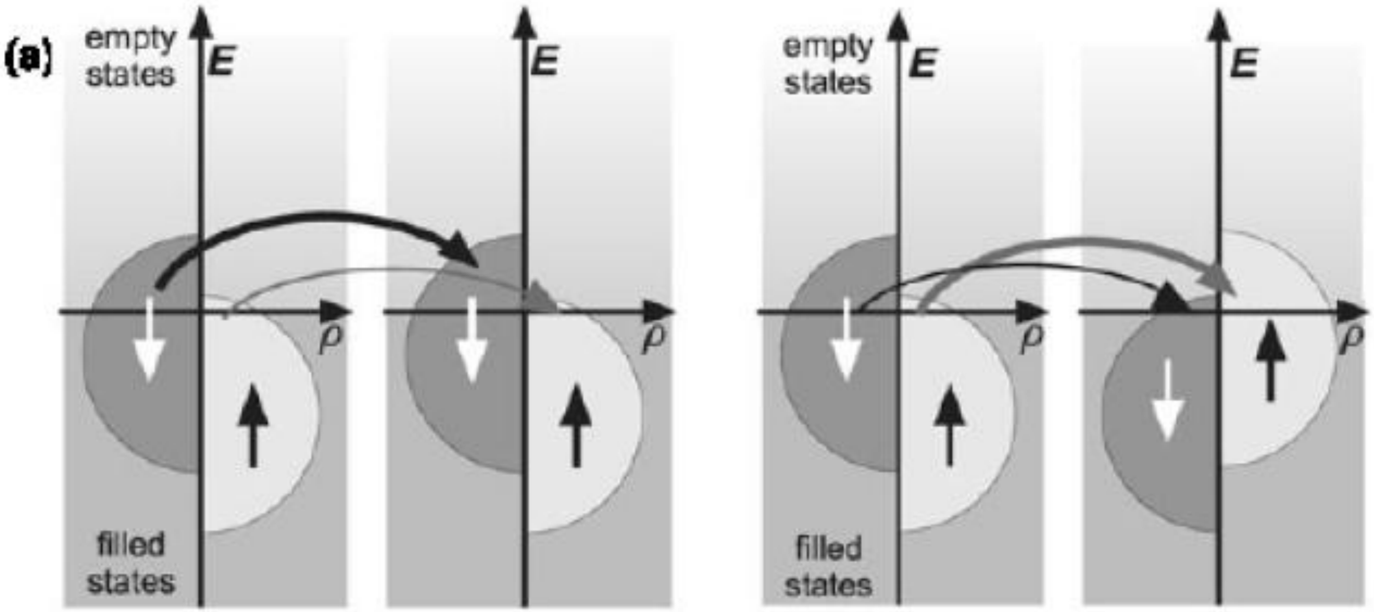

Figure 2. Principle of spin-polarized tunnelling between magnetic electrodes that exhibit (*a*) a parallel and (*b*) an antiparallel magnetization. The spin is conserved in the case of elastic electron tunnelling. Therefore, spin-up electrons that tunnel out of the occupied states of electrode A can only enter empty spin-up states of electrode B.

M.Bode, Rep. Prog. Phys. 66 (2003) 523

Fig. 28

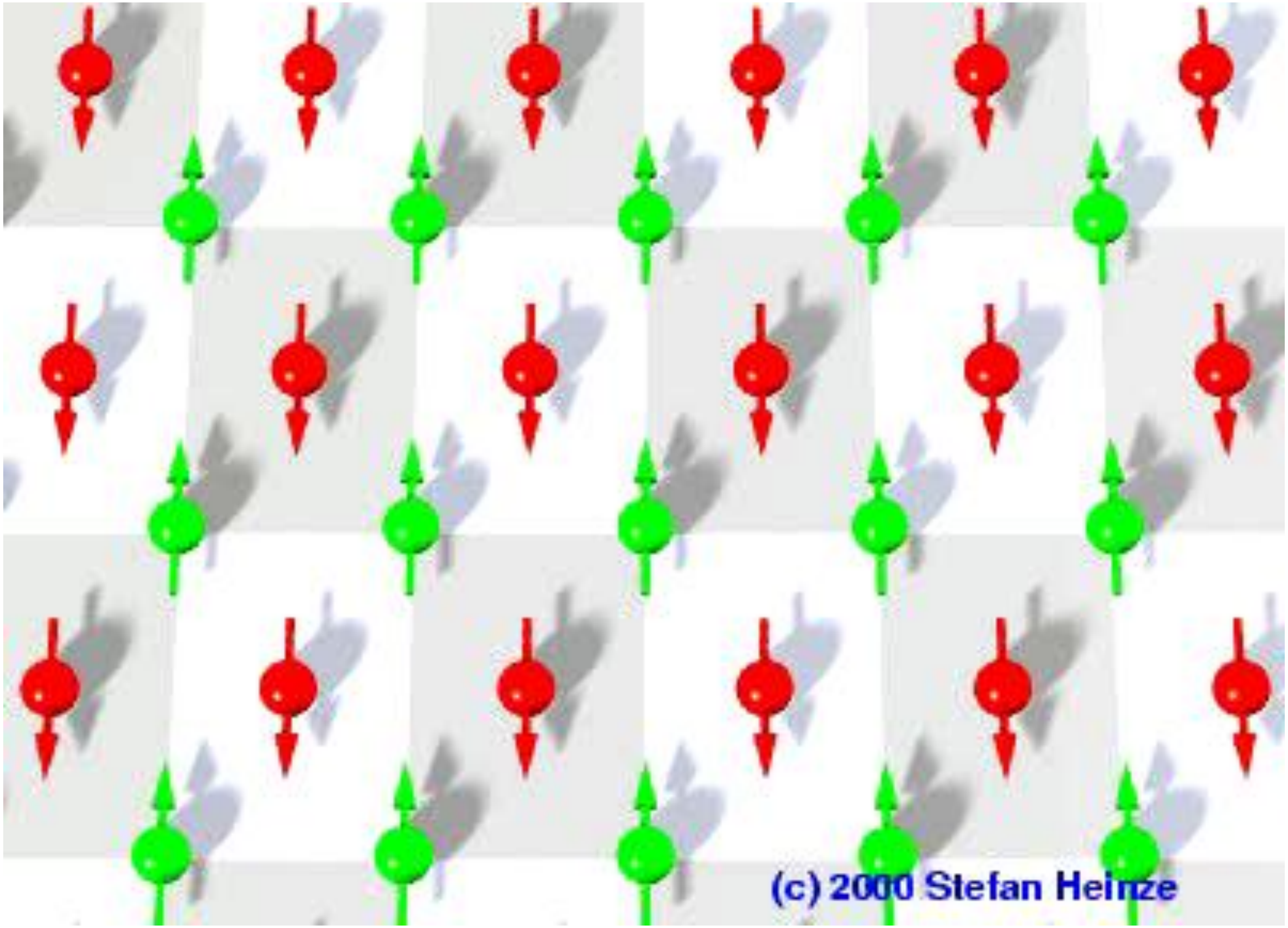
(c) 2000 Stefan Heinze

Cr(001) as a Topological Antiferromagnet

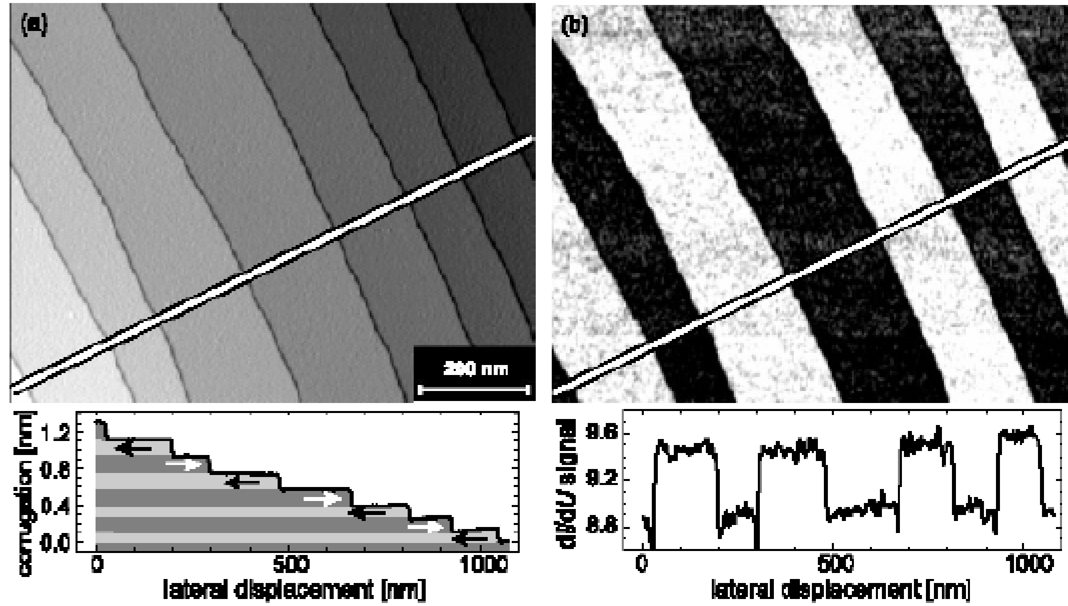

Figure 22. (*a*) Constant-current mode STM image of the Cr(001) surface. Nine te
separated by monatomic steps are visible. (*b*) Simultaneously acquired spin-resolved d
map at $U = -290$ mV sample bias. The signal changes at every step between low and hig
to antiparallel magnetization of adjacent terraces, thereby confirming the model of 'topolo
antiferromagnetism' proposed by Blügel *et al* [92].

M.Bode, Rep. Prog. Phys. 66 (2003) 52

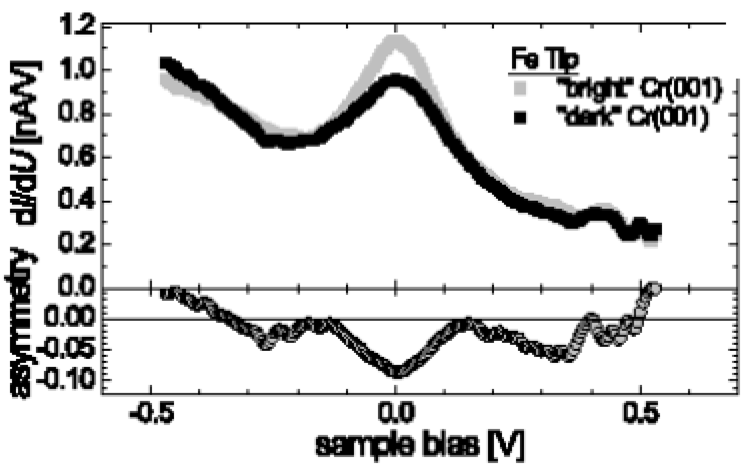

Figure 21. Tunnelling spectra and asymmetry as measured with a Fe coated probe tip above adjacent Cr(001) terraces. The spectra exhibit a peak close to the Fermi level, which is caused by a d_{z^2}-like surface state being characteristic for bcc-(001) surfaces [116]. Since the surface state is spin-polarized the intensity depends on the relative orientation of the quantization axes of tip and sample, which—due to the 'topological antiferromagnetism' of Cr(001)—changes between parallel and antiparallel for adjacent Cr terraces.

Fig. 29

Inelastic Tunneling Spectroscopy (IETS)

STM-IETS

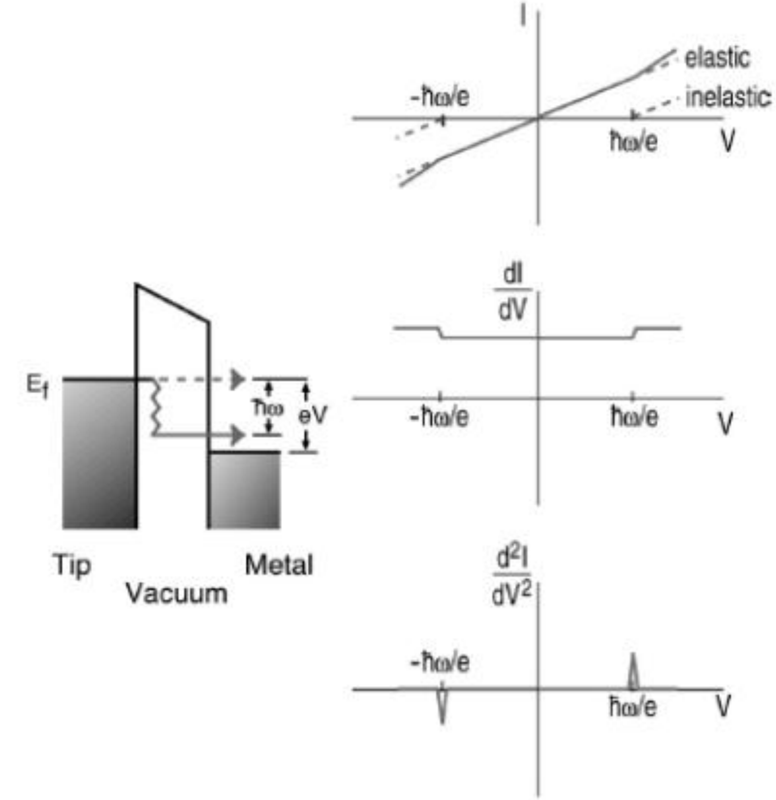

FIG. 3. Schematic showing the emergence of inelastic tunneling at the threshold for vibrational excitation. The change in the tunneling current due to vibrational excitation is too small to be measured from the $I-V$ curve. While a change in the differential conductance, dI/dV, can be seen for strong modes, more often vibrational features needs to be extracted from d^2I/dV^2. An important characteristic of vibrational inelastic electron tunneling spectroscopy (IETS) is the occurrence of a peak of the opposite sign on the negative bias side. Lacking an isotope shift analysis, the assignment of a feature to vibrational excitation needs to be confirmed by a corresponding feature with the opposite polarity at the opposite bias. This schematic depicts an increase in the conductance, associated with a positive (negative) peak for positive (negative) sample bias. In contrast, electronic spectra arise from elastic tunneling; peaks are positive and occur on either positive (unoccupied states) or negative (occupied states) sample bias.

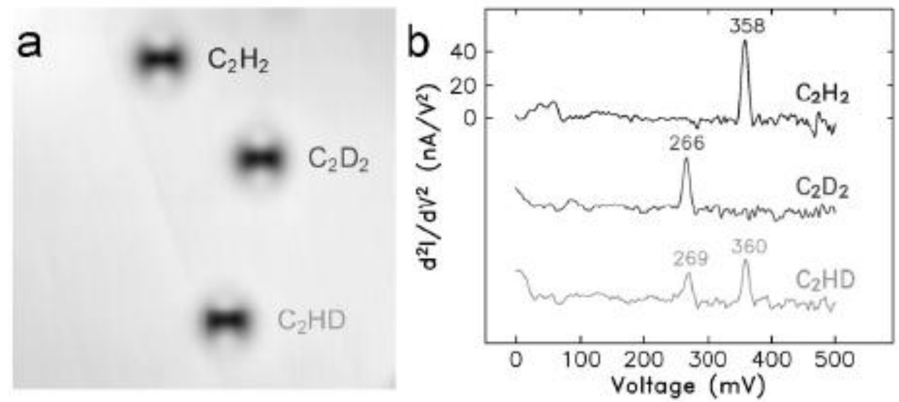

FIG. 4. (a) 56 Å×56 Å STM topographical images and (b) single-molecule vibrational spectra via STM-IETS of three acetylene isotopes on Cu(001) at 8 K. The two protrusions (bright) in the image of each isotope are due to the presence of the C–H and C–D bonds while the central depression (dark) is attributed to the C–C bond. The C–H stretch is observed at 358 meV for C_2H_2 and the C–D stretch is observed at 266 meV for C_2D_2. Small upshifts are found for the C–H and C–D stretches of C_2HD. The C_2HD spectrum demonstrated for the first time single bond sensitivity with STM-IETS.

W. Ho, J. Chem. Phys. 117, 11033 (2002

Fig. 30

Atomic Force Microscopy (AFM) :

General Components and Their Functions

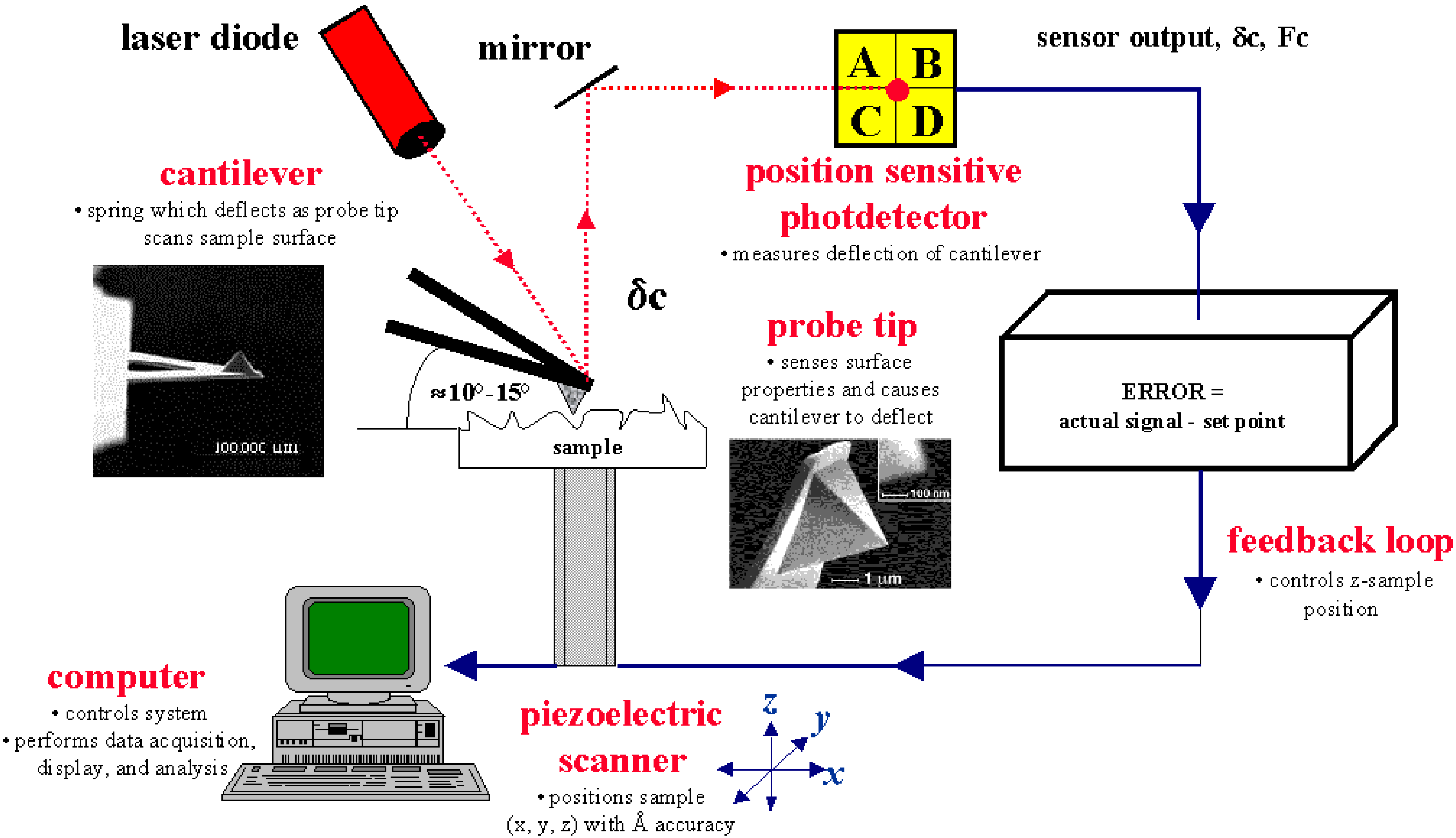

AFM: Force – distance curve, modes of operation

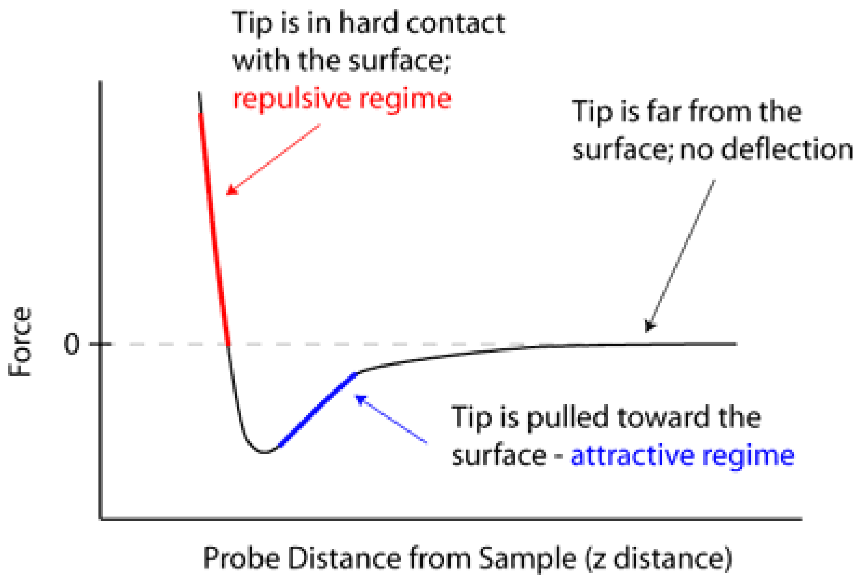

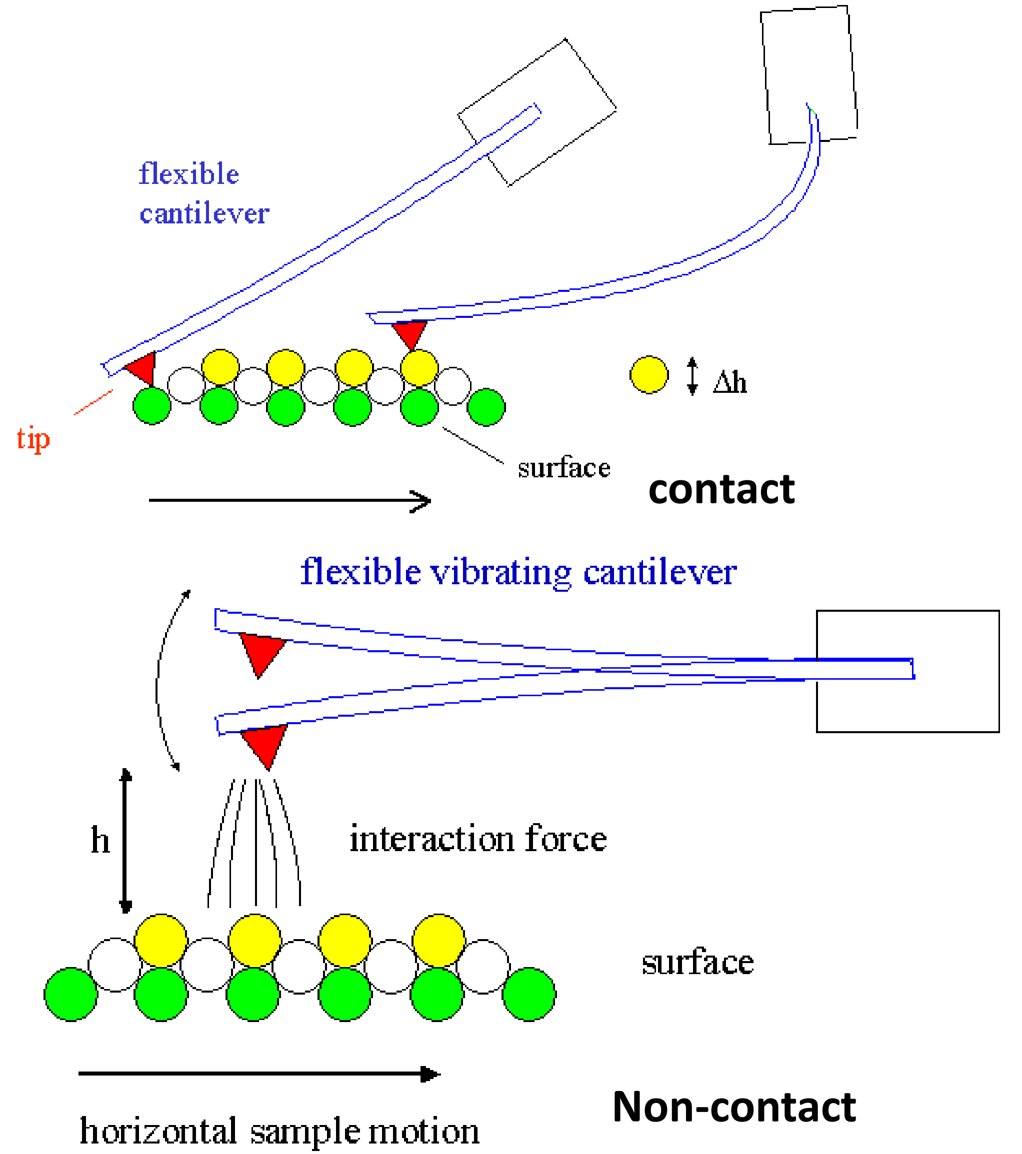

AFM: Q-Plus sensor

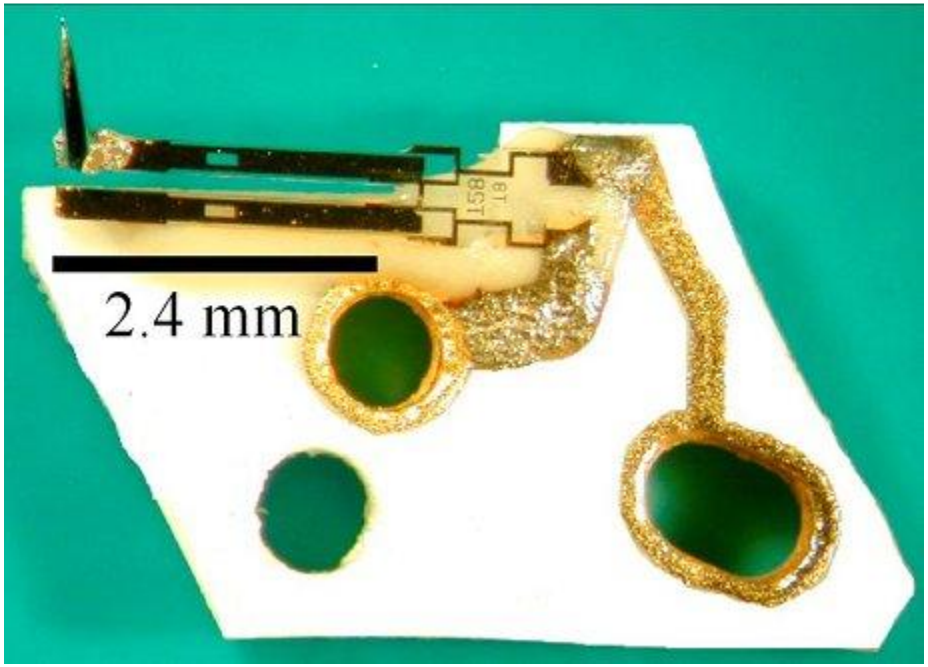

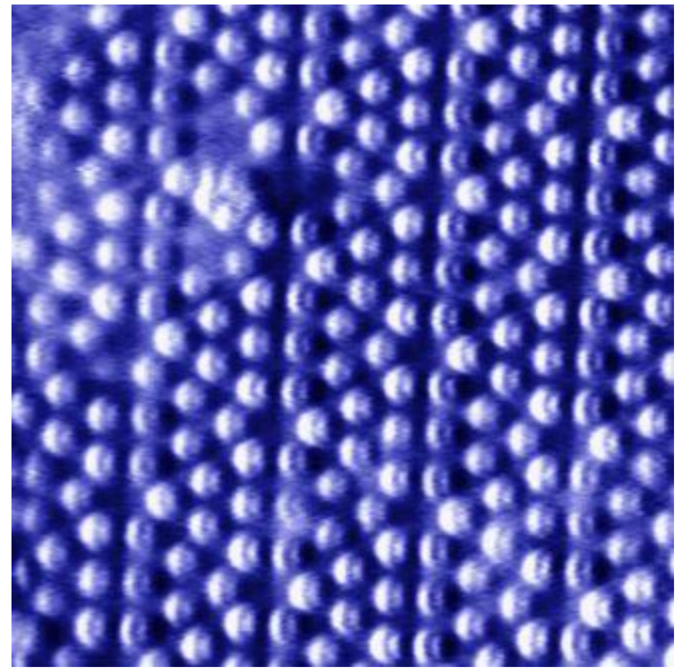

Si(111) -7x7

Can you really „see“ atoms?

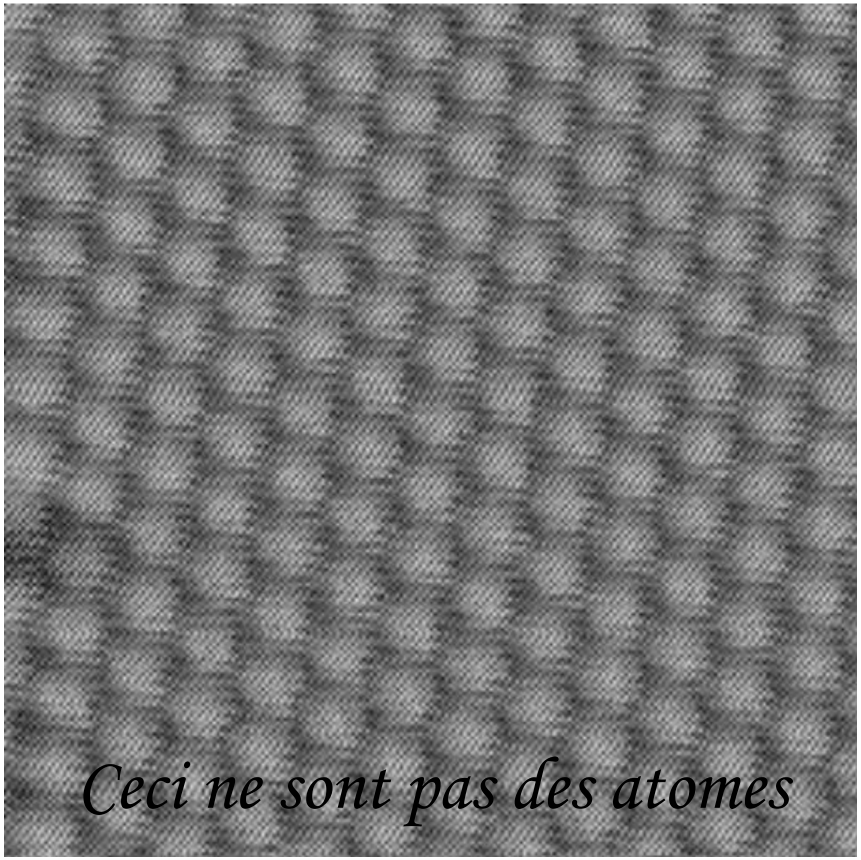

Carsten Busse, 1999 (Al(111))

René Magritte, 1923